SYNTHESIS OF SOLID ACID CATALYST FROM BIOMASS WASTE FOR GLYCEROL-FREE BIODIESEL PRODUCTION

WONG WAN YING

A project report submitted in partial fulfilment of the requirements for the award of Bachelor of Engineering (Hons.) Chemical Engineering

Lee Kong Chian Faculty of Engineering and Science
Universiti Tunku Abdul Rahman

September 2018

DECLARATION

I hereby declare that this project report is based on my original work except for citations and quotations which have been duly acknowledged. I also declare that it has not been previously and concurrently submitted for any other degree or award at UTAR or other institutions.

Signature : _____

Name : Wong Wan Ying

ID No. : 14UEB06865

Date : 18th September 2018

APPROVAL FOR SUBMISSION

I certify that this project report entitled **"SYNTHESIS OF SOLID ACID CATALYST FROM BIOMASS WASTE FOR GLYCEROL-FREE BIODIESEL PRODUCTION"** was prepared by **WONG WAN YING** has met the required standard for submission in partial fulfilment of the requirements for the award of Bachelor of Engineering (Hons.) Chemical Engineering at Universiti Tunku Abdul Rahman.

Approved by,

Signature	:	
Supervisor	:	Dr. Steven Lim
Date	:	18th September 2018

Signature	:	
Co-Supervisor	:	Dr. Pang Yean Ling
Date	:	18th September 2018

ACKNOWLEDGEMENTS

The completion of this research project would not have been a success if it was not for the participation, assistance and support of many individuals. First and foremost, I would like to express my utmost gratitude to my research supervisors, Dr. Steven Lim and Dr. Pang Yean Ling for bestowing such precious chance in allowing me to conduct my final year project under their supervisions. I am indebted to them for their invaluable advice, guidance and enormous patience throughout the development of the research.

Next, my deepest thanks to Universiti Tunku Abdul Rahman (UTAR) for providing me a great platform and learning ground to complete my final year project. Throughout the project, I was very fortunate to be blessed with the technical supports from all Assistant Laboratory Managers of Department of Chemical Engineering in Lee Kong Chian Faculty of Engineering and Science.

Last but not least, I would also like to express my greatest gratitude to my loving parents who had given me consistent support and encouragement during my venture. Not to forget all postgraduate students and course mates who had offered invaluable suggestions and assistance unconditionally.

ABSTRACT

Nowadays, homogeneous alkali-catalysed transesterification is the typical process used in biodiesel production, complicating the downstream separation processes and causing oversupply of glycerol as by-product. In the present study, glycerol-free biodiesel production via interesterification by using biomass waste derived solid acid catalyst was investigated for the first time. Triacetin, a beneficial fuel additive, was produced as by-product instead of glycerol. The aim of this study was to elucidate on the potential applicability of waste banana peels in deriving a heterogenous catalyst. The solid acid catalyst was prepared by direct sulfonation via thermal treatment with sulfuric acid and its catalytic activity was investigated for the interesterification between oleic acid and methyl acetate. Concentration of the sulfuric acid which was the sulfonating agent was varied from 2 to 13 mol/L to evaluate its effects on the resulting biodiesel yield. Catalyst characterisation was also carried out using Scanning Electron Microscopy equipped Energy-Dispersive X-ray (SEM-EDX), X-ray Diffractometer (XRD) and Fourier Transform Infrared Spectroscopy (FTIR). The interesterification of oleic acid with methyl acetate was catalysed using the synthesised catalyst under reaction conditions of methyl acetate to oleic acid molar ratio of 50:1 and catalyst loading of 12 wt.% at 60 ℃ for 8 h. The biodiesel yield increased with the concentration of sulfuric acid used to synthesise catalysts. It was found out that a yield of 43.81 % with a high acid value conversion of 83.14 % was obtained. This study proved that the biomass waste derived heterogeneous catalyst catalysed interesterification of oleic acid with methyl acetate is a promising and environmentally benign approach for production of green fuel.

TABLE OF CONTENTS

LIST OF TABLES

LIST OF FIGURES

LIST OF SYMBOLS / ABBREVIATIONS

Y	yield, %
C	conversion, %
V	volume of KOH solution used, L
B	volume of KOH solution used in blank titration, L
M	molarity of KOH solution, mol/L
MW_{KOH}	molecular weight of KOH, g/gmol
W	Weight of oleic acid, g
T_c	critical temperature, ℃
P_c	critical pressure, Pa
a^i	initial acid value of the feedstock, mg KOH/g
a^f	final acid value of the mixture after the reaction, mg KOH/g

4-BDS	4-benzenediazoniumsulfonate
BET	Brunauer-Emmett-Teller
BP	British Petroleum
CI	compression ignition
CPO	crude palm oil
DAG	diacetylglyceride
DMC	dimethyl carbonate
DMCMG	dimethyl carbonate monoglyceride
EE	energy efficiency
FAAE	fatty acid alkyl ester
FAME	fatty acid methyl ester
FFA	free fatty acid
FID	flame ionisation detector
FTIR	Fourier Transform Infrared Spectroscopy
GC	Gas Chromatography
GHG	greenhouse gases
ktoe	kilo tonnes of oil equivalent
MA	methyl acetate
MAG	monoacetylglyceride
MCDG	methyl carbonate diglyceride

mtoe	million tonnes of oil equivalent
RE	renewable energy
SCBC	sulfonated carbon-based catalysts
SEM-EDX	Scanning Electron Microscopy equipped with Energy Dispersive X-ray
TG	triglycerides
TGA	thermogravimetric analysis
TPDRO	Temperature Programmed Desorption, Reduction and Oxidation
UN	United Nations
WBPAC	waste banana peel based activated carbon
XPS	X-ray Photoelectron Spectroscopy
XRD	X-ray Diffractometer

LIST OF APPENDICES

CHAPTER 1

INTRODUCTION

1.1 Energy Consumption and Demand

Global demographic problem started to reveal recently with uncontrollable growth of population as the main concern. From the report titled World Population 2017 in 2017 by Department of Economic and Social Affairs of United Nations (UN), there would be 7.6 billion people worldwide in mid-2017. It is estimated that there is an increment of 83 million people annually. This has contributed more demand to the access of energy over the past decade. Economic growth and global industrialisation further worsen the situation.

Energy is an indispensable criterion which supports human daily lives. According to the report in 2017 by U.S. Energy Information Administration, global energy expenditure will gain 28 % between 2015 and 2040. This shocking number manifests that energy will be one of the major issues in the world. Table 1.1 shows the sources of global primary energy consumption in 2016 from the report by British Petroleum (BP) in 2017. The energy consumption is mostly dependent on fossil fuels which account for 85.52 % whereby 33.28, 24.13 and 28.11 % are contributed by crude oil, natural gas and coal, respectively whereas nuclear energy, hydroelectricity and renewable sources give rise to the remaining share of 14.48 %.

Table 1.1: Global Primary Energy Consumption in 2016 (BP, 2017)

	Million Tonnes of Oil Equivalent (mtoe)	**Share (%)**
Oil	4418.2	33.28
Natural Gas	3204.1	24.13
Coal	3732.0	28.11
Nuclear Energy	592.1	4.46
Hydroelectricity	910.3	6.86
Renewables	419.6	3.16
Total	13276.3	100.00

In Malaysia, thermal and hydro power plants are the two main types of power generating plants used to generate electricity from primary energy sources. In the aspect of thermal power plant, three major fossil fuels which are coal, natural gas and fuel oil contribute the most to the power generation, leading to unfavourable consequences for the environment. Despite their relatively easy accessibility, affordability and compatibility, they cannot be replenished after depleted, thus inviable for future generations. The burning of fossil fuels also leads to emission of greenhouse gases (GHG), triggering anthropogenic climate change issue. Over dependency on non-renewable resources for national electricity generation will jeopardise a reliable and affordable energy supply. This is due to the fact that excessive exploitation of fossil fuels can cause their reserves to deplete drastically and affect the energy security in the near future.

Malaysia is in the progress of achieving the status of developed country by 2020 via sustainable development (Mohamed, Md. and Mazlan, 2016). Sustainable energy which consists of renewable energy (RE) and energy efficiency (EE) is the major requirement for sustainable development. Malaysia is a country furnished with a variety of renewable energy resources such as solar, hydro power, biomass and ocean. To conquer the problem of environmental conservation and energy security, Malaysia started to opt for renewable energy in 2001 (Oh, et al., 2018). This had encouraged the research on alternative and renewable fuels to cater to unrelenting demand. Several new energy policies and programs have been established to support energy efficiency and provide energy sustainability.

In addition, Malaysia is well known for its agricultural production and endowed with continual supply of sunshine and rainfall all the year round. Therefore, biomass, biogas and solar are the examples of viable RE resources besides hydroelectricity. Table 1.2 shows the primary energy supply in the unit of kilo tonnes of oil equivalent (ktoe). It can be seen that, as the years go by, the roles of renewable sources are getting more important in supplying energy and as a complementary source to fossil fuels. RE is considered as environmental friendly with negligible GHG emission. For instance, biomass in RE utilises valuable organic wastes while reducing the problem of pollution and landfills. Furthermore, biogas is a mixture of gas produced from the decomposition of organic waste and it is combustible.

Table 1.2: Primary Energy Supply from Year 1996 to 2015 (Energy Commission, n.d.)

Year	Primary Energy Supply (ktoe)								
	Crude Oil	**Petroleum Products**	**Natural Gas**	**Coal and Coke**	**Hydropower**	**Biodiesel**	**Solar**	**Biomass**	**Biogas**
1996	18255	1099	15567	1677	1243				
1997	17916	3802	19041	1622	790				
1998	17133	1920	19101	1731	1113				
1999	17643	1807	21476	1940	1668				
2000	21673	-1431	26370	2486	1560				
2001	23590	-1917	25649	2970	1687				
2002	22647	-521	26101	3642	1329				
2003	25344	-1391	27257	5316	1056				
2004	25335	-37	29145	6631	1329				
2005	24339	-75	33913	6889	1313				
2006	24909	-1474	35776	7299	1568				
2007	26571	-995	36639	8848	1510				
2008	26776	-2282	39289	9782	1964				
2009	26386	96	35851	10623	1627				
2010	22487	2521	36936	14777	1577				
2011	24679	2224	35740	14772	1850	24			
2012	28053	1449	38648	15882	2150	115	11	183	4
2013	27154	5320	39973	15067	2688	188	38	297	6
2014	26765	6699	40113	15357	3038	300	63	181	12
2015	24945	4218	39365	17406	3582	389	75	189	18

1.2 Biodiesel

Biodiesel is a renewable and eco-friendly combustion fuel that composed of long chain methyl or ethyl ester of fatty acids. It is commonly derived from virgin or used agricultural oils such as vegetable oils and animal fats via a process known as transesterification (Ouda, et al., 2016). According to Malaysia Energy Statistics Handbook 2016 by Energy Commission, transportation sector occupied the largest portion of energy consumption as compared to other sectors such as agriculture and commercial. The statistical results are illustrated in Figure 1.1. Since biodiesel can be blended with petroleum-derived diesel in any proportion for compression ignition (CI) engine with little or no engine modifications, it is a potential substitute of fossil oil that can be used in its pure form in the transportation sector. The application of biodiesel in conventional diesel engines helps to remediate the global warming effect by reducing significantly the emission of carbon dioxide, CO_2 on a life cycle basis, carbon monoxide, CO, unburned hydrocarbons and particulate matters by 78, 46.7, 45.2 and 66.7 %, respectively (Ezebor, et al., 2014).

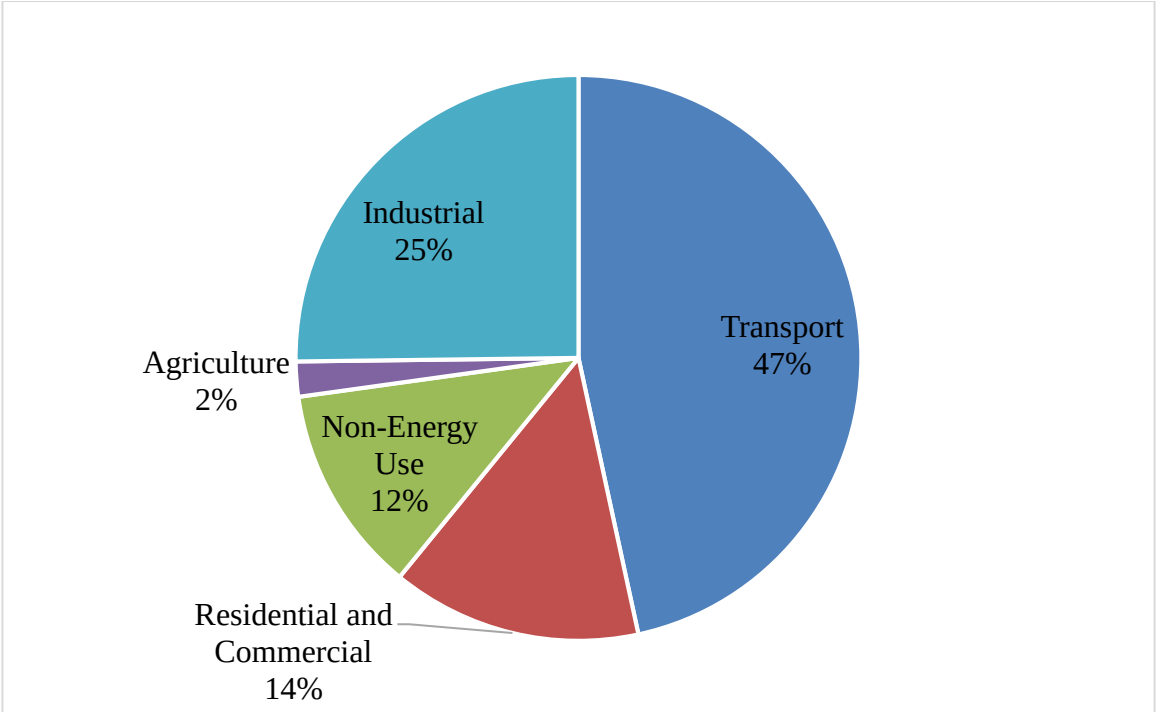

Figure 1.1: Percentage of Energy Consumption by Sectors in 2014 (Energy Commission, 2016)

There are several types of potential feedstocks for production of biodiesel which can be categorised into edible and non-edible vegetable oils or recycled oils and animal fats. For instance, the typical examples of edible oils used in the production of biodiesel are palm oil, sunflower oil and soybean oil. However, the usage of edible vegetable oils which is also known as first-generation feedstocks has created concern regarding food security. A large region of arable land is needed to grow crops for biodiesel production. Thus, second-generation feedstocks from non-edible vegetable oils has become more popular since it offers sustainable production for biodiesel. It provides a solution for the land problem since it can be grown in waste and marginal land areas. *Jatropha curcas* seed oil and waste cooking oil are the common non-edible vegetable oils. Waste cooking vegetable oils can become the feedstock for biodiesel production due to its cheaper price and the absence of disposal problem. Furthermore, with the advancement of technology, microalgae-based oils is the third-generation feedstock which provides unlimited supply at relatively lower cost as well as improved yields (Atabani, et al., 2013). As compared to petroleum, algae has remarkable energy content up to 80 %. (Chisti, 2013). They can be grown on a large scale within a short period, making them suitable to become energy crops.

Malaysia can be considered as one of the major contributors of global oil palm production and supply owing to its favourable soil conditions. To be exact, Malaysia is the second largest palm oil producer worldwide, accounting for 40 % of total international market for crude palm oil (CPO) (Johari, et al., 2015). This huge biomass feedstock is a main component used for biodiesel production. Table 1.3 shows the production of biodiesel in Malaysia over the years. From 2012 to 2014, the production amount and the consumption quantity had increased gradually. Nonetheless, biodiesel had been almost negligible in this nation compared to diesel. For instance, in year 2014, the consumption of biodiesel was 456,540 tonnes whereas the amount of diesel required was 10,161,000 tonnes of oil equivalent. Biodiesel accounted only a small portion of around 4 % of the total diesel requirement.

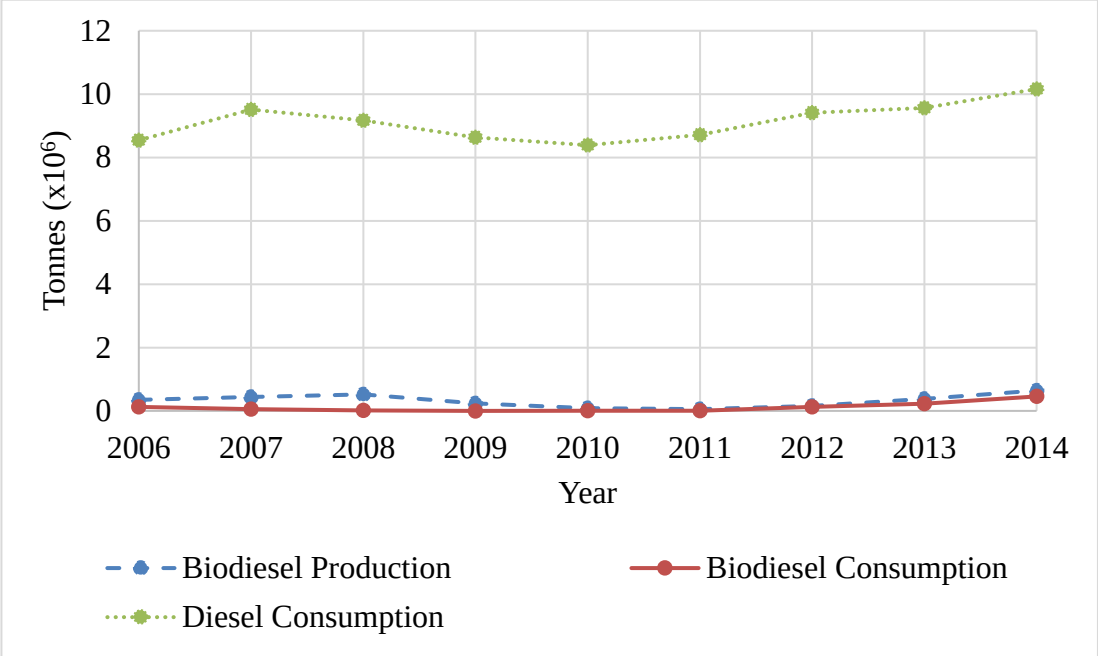

Figure 1.2: Statistics of Malaysia Biodiesel Production and Expenditure and Diesel Consumption (Johari, et al., 2015)

1.3 Problem Statement

It is vital to improve the production yield of biodiesel while keeping low cost. Thus, biodiesel is possible to substitute petroleum based diesel in the future to reduce fossil fuel dependency. Large quantity of biodiesel is needed to satisfy the present demand. The cost of biodiesel production was 1.5-3 times higher as compared to conventional diesel (Domingues, et al., 2013). Rehan, et al. (2018) reported that selection of raw material contributed up to 75 % of the overall biodiesel production cost. For example, first generation biodiesel produced from edible vegetable oils were very costly. For biodiesel to be competitive with petroleum based diesel, low costs feedstock such as used cooking oil, animal fat and algae can be used. By considering the previous literatures on interesterification involving methyl acetate, the feedstock used consists of large proportion of oleic acid, following by linoleic acid. For instance, waste cooking oil was composed of 91 % unsaturated fatty acids which were linoleic acid and oleic acids. (Maddikeri, Pandit and Gogate, 2013).

Catalytic transesterification using methanol is the typical method employed for the production of biodiesel due to the fact that methanol is relatively cheap and easily accessible. This results in huge production of glycerol as by-product, creating the problem of oversupply and declining their market price (Marx, 2016). The mixture of

unreacted methanol and glycerol exacerbates the situation since the purification of glycerol to fit the consumer market requires high temperature and low pressure distillation which is energy intensive and not cost effective. Therefore, manufacturing biodiesel via a novel glycerol-free method can be more favourable to improve the processing economics and avoid the by-production of glycerol. For instance, methyl acetate can replace the alcohol reactant in transesterification reaction and form triacetin, a higher added value by-product as compared to glycerol.

Catalyst is a crucial element in speeding up the interesterification reaction for biodiesel production. Nowadays, the commercial production of biodiesel makes use of homogeneous catalysts (Domingues, et al., 2013). This increases the overall operating cost due to downstream processes to recover the catalysts. Thus, heterogeneous catalyst is preferable. However, although heterogeneous alkaline catalyst offers high catalytic performance, its activity is affected by feedstock with high free fatty acid (FFA) content due to soap formation (Chakraborty, et al., 2016). Heterogeneous acidic catalyst is suitable to be used under the conditions of high FFA content and water without soap formation (Ezebor, et al., 2014; Konwar, Boro and Deka, 2014). Nevertheless, their synthesising process is quite complex and expensive.

However, not all biomass is suitable to be used as a support for catalyst. Study of sulfonation method and different synthesising conditions should be carried out for synthesising an effective catalyst.

1.4 Aims and Objectives

The general aim of this research project is to devise and discover potential catalyst from biomass waste for synthesis of biodiesel. Biodiesel will be produced in an alternative pathway, without the typical production of glycerol as by-product. Specifically, the objectives of the research project are:

- To synthesise solid acid catalysts from waste banana peels through direct sulfonation via thermal treatment by sulfuric acid, H_2SO_4 for biodiesel production.
- To investigate the effects of operating parameter such as concentration of sulfonating agent in the preparation of solid acid catalysts.
- To produce biodiesel through catalytic interesterification process with methyl acetate.

1.5 Scope and Limitation of the Study

The scope of the investigation focuses on the approach of synthesising solid acid catalyst. There are a wide variety of biomass suitable to be used as catalyst support after carbonisation. Therefore, it is essential to study the efficacy of different biomass supported catalysts in biodiesel synthesis in order to choose the appropriate one. Furthermore, sulfonation method plays a crucial role in determining the performance of the catalyst. In this study, banana peels are selected as the biomass candidate to go through sulfonation process involving sulfuric acid. The prepared catalyst is then applied to the production of biodiesel.

During the preparation of catalyst, the parameter to be examined is concentration of sulfuric acid. The performances and activities of catalysts will be observed and their effectiveness is measured in terms of biodiesel yield and the resulting acid value conversion. The optimum operating condition for the synthesis of catalyst is also identified. For catalyst characterisation, the physicochemical properties of the prepared catalysts such as structure and porosity are determined. The biodiesel production process is carried out via interesterification reaction with the replacement of alcohol with methyl acetate. Triacetin, instead of glycerol, is produced as by-product.

However, there are several limitations which need to be considered and can be improved in the near future. The scope of this study only covers the synthesis parameter of the catalyst. Other parameters regarding the biodiesel production such as catalyst loading, reaction time, reaction temperature and methyl acetate to oleic acid molar ratio are not being investigated.

1.6 Contribution of the Study

Majority of the related journals had discussed about the biomass-derived heterogeneous catalyst for biodiesel production. Thermal decomposition of ammonium sulfate, $(NH_4)_2SO_4$ and sulfonation by arylation using 4-benzenediazoniumsulfonate (4-BDS) are the typical sulfonation approaches. However, direct sulfonation via thermal treatment with sulfuric acid is going to be implemented in this research study.

Other than that, biodiesel is commonly produced via transesterification in the presence of alcohol with the production of glycerol as side product. Nevertheless, in this study, interesterification will be conducted to synthesise biodiesel. Methyl acetate is involved to produce triacetin as by-product. Thus, the outcome of this study may bring forward an effective production mechanism for biodiesel with the combination of interesterification and utilisation of biomass supported catalysts.

1.7 Outline of the Report

Chapter 1 manifests the brief overview and background of the research project. Problem statement, aims and objectives, deficiency and contribution of the study are also discussed. Chapter 2 highlights the detailed review of the related investigation. This includes prior empirical study of the types of biomass supported catalysts in biodiesel production, catalyst synthesis method and reaction mechanisms of biodiesel production. Next, Chapter 3 describes the research methodology and planning of synthesising the solid acid catalysts and subsequent biodiesel production. Chapter 4 elaborates the results obtained and their interpretation as well as the corresponding discussion on the performance of catalysts. Lastly, Chapter 5 concludes the study and suggests the possible recommendations.

CHAPTER 2

LITERATURE REVIEW

2.1 Reaction Mechanisms of Biodiesel Production

Vegetable oils and animal fats have high viscosities and low volatilities which hinder their direct applications in diesel engine due to the difficulties in atomization. Formation of carbon deposits and thickening are the common resulting problems. Therefore, as shown in Figure 2.1, numerous methodologies of biodiesel production can help to lower the feedstock's viscosity. However, each reaction mechanism is accompanied with their own distinct strengths and weaknesses.

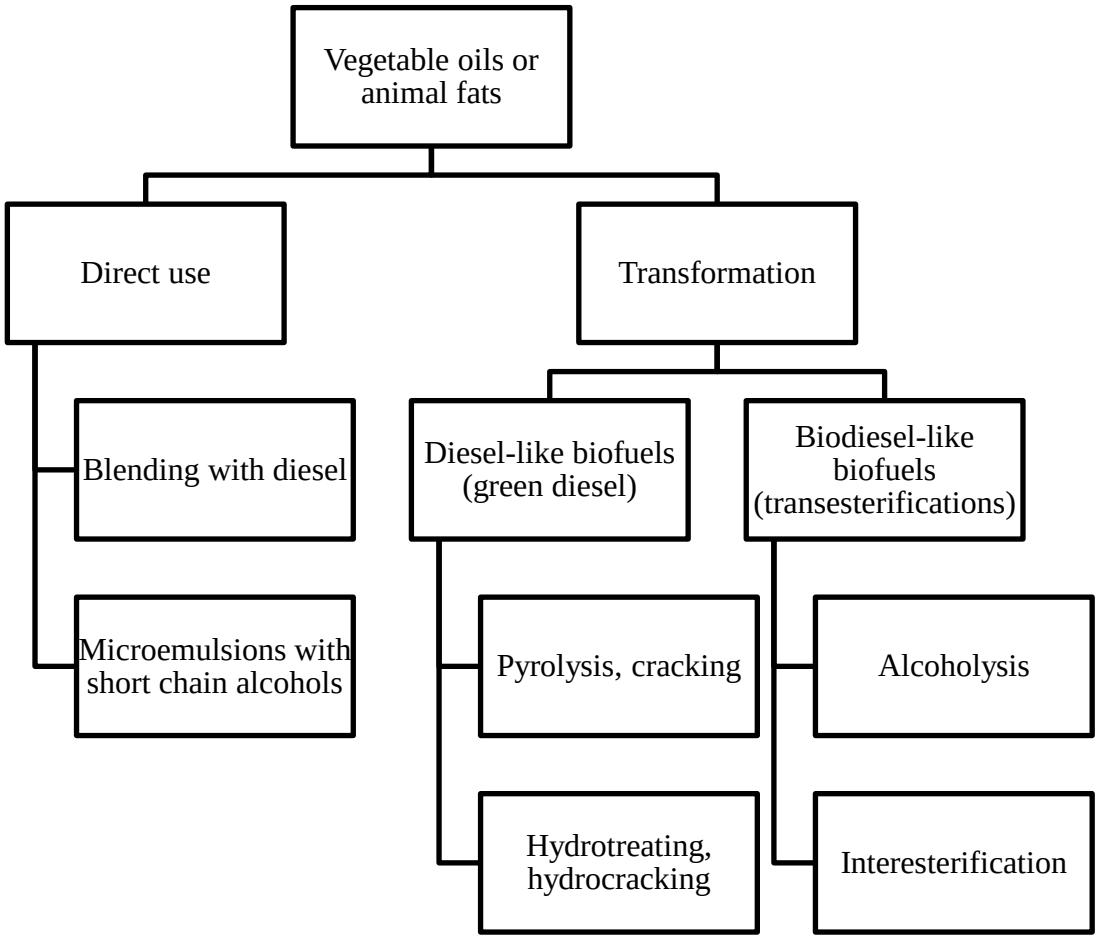

Figure 2.1: Biodiesel Production Pathways (Calero, et al., 2015)

Blending with diesel fuels helps to improve the overall fuel quality and lower fossil fuel consumption. Next, microemulsion refers to colloidal dispersion of fluid microstructures with the size ranges from 0.001 μm to 0.15 μm in solvent such as

methanol and ethanol, creating two immiscible phases. This will reduce the viscosity of oils and enhance the atomization of fuel. Eliezer, et al. (2015) claimed that the flash point, fire point and heating value of emulsified biofuels were lower as compared to diesel fuels after addition of alcohols as a co-surfactant. Furthermore, pyrolysis or thermal cracking in the absence of oxygen derives triglycerides (TG) along with other organic compounds from biomass. The complex and long molecular chain oils can then be converted into hydrocarbons with simpler structures and lower molecular weights which are suitable to be used as fuel (Rajalingam, et al., 2016). Catalysts are commonly involved to increase the rate of reaction and the process is known as catalytic cracking. Nevertheless, transesterification reaction with methanol is the most popular reaction pathway employed to obtain biodiesel that resembles petrodiesel.

2.1.1 Transesterification

Transesterification is a conventional technique employed for the production of biodiesel. It is a catalysed reversible reaction which involves a homogeneous or heterogeneous catalyst to produce biodiesel from oleaginous feedstocks with the aid of short-chain alcohol. The TG from the feedstocks are converted into fatty acid alkyl esters (FAAEs), producing glycerol as the by-product which can be separated in a decantation funnel overnight or by centrifuge (Kirubakaran and Arul Mozhi Selvan, 2018). The overall chemical equation is shown in Figure 2.2. Since this process occurs in a liquid-liquid two-phase system, its rate is constrained by the mass transfer contributed by immiscibility of oil and alcohol. Other factors such as high operating cost and energy requirements further limit its performance (Tiwari, Rajesh and Yadav, 2018).

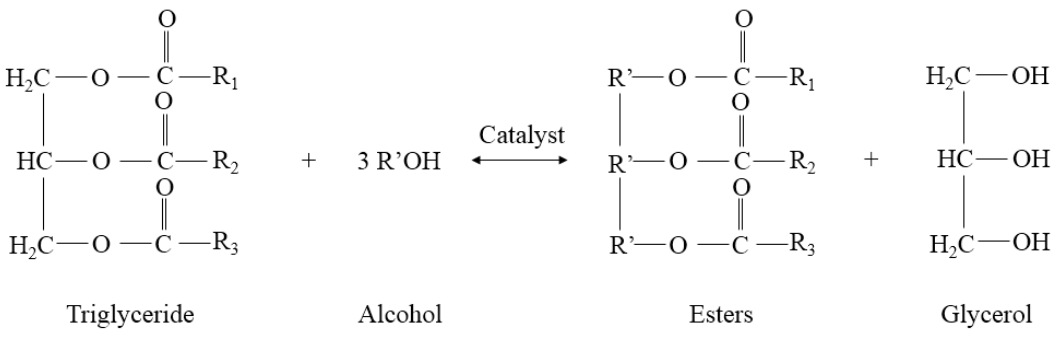

Figure 2.2: Catalytic Transesterification (Pereira, et al., 2014)

2.1.2 Interesterification

The usage of short-chain alcohol poses problems such as undesirable combination of water and FFAs. Interesterification process can be considered as a modified version of transesterification reaction with an alternative acyl acceptor to replace alcohol. It involves an interchange of acyl groups between two different ester compounds and during transesterification between fatty acid and alcohol (Ang, Tan and Lee, 2014). The potential acyl acceptors are methyl acetate (MA), ethyl acetate and dimethyl carbonate (DMC).

Interesterification with MA involves three reversible sequential reactions which is summarised as shown in Figure 2.3. TG from the feedstock reacts with one molecule of MA, yielding one molecule of monoacetylglyceride (MAG) and fatty acid methyl esters (FAMEs). Likewise, the resulting MAG then undergo the same pathway and produce diacetylglyceride (DAG). FAME is generated eventually from DAG by consuming another molecule of MA. In the presence of MA, triacetin which has a higher value will be produced instead of glycerol. For instance, triacetin can be applied as perfumery fixative (Kirubakaran and Arul Mozhi Selvan, 2018). It can also be used as a food addictive for flavouring. Triacetin can be added into diesel directly as an antiknock agent in engine as well as to improve the combustion properties of biodiesel. However, MA is considered as a weakly polar aprotic solvent, thus it offers lower reactivity as compared to methanol and DMC. Since longer reaction time is needed to complete the reaction, there is a possibility of FAME decomposition which could further decrease the yield (Ang, Tan and Lee, 2014).

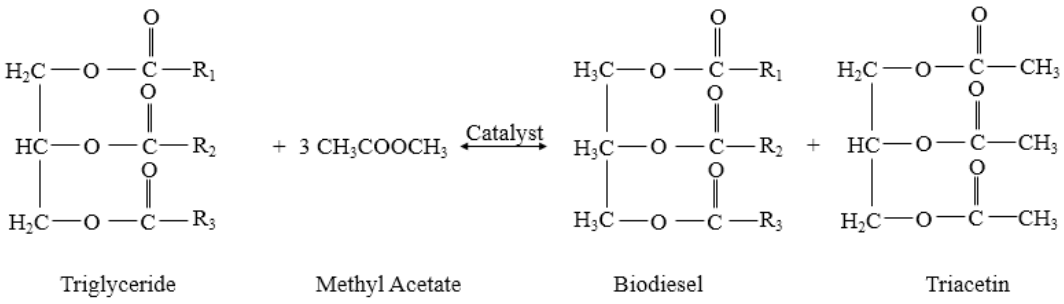

Figure 2.3: Interesterification of TG and MA

Other carboxylate esters such as ethyl acetate are promising candidates in the production of FAAEs via the reaction with TG. Producing ethyl esters is of considerable interest due to its characteristics which include safety in handling and higher flash and combustion points. Fatty acid ethyl ester biodiesel exhibits lower cloud points as compared to FAME (Leggieri, Senra and Soh, 2018). The extra carbon atom in biodiesel increases its heat content and cetane number. Nevertheless, the yield is comparatively lower due to the presence of longer alkyl chains that reduces the reactivity between TG and esters.

Furthermore, Lee, et al. (2017) reported that interesterification with DMC was more reactive as compared to conventional transesterification with methanol. The interesterification which involves DMC goes through three stages. Firstly, TG reacts with DMC to generate methyl carbonate diglyceride (MCDG) which will then react with another molecule of DMC, producing dimethyl carbonate monoglyceride (DMCMG). For the last step, DMCMG reacts with one molecule of DMC and produces FAME, glycerol carbonate and citramalic acid as the final products. This process starts with versatile and biodegradable DMC which can be easily synthesised from carbon dioxide and methanol to produce value-added by-products. Glycerol carbonate can be used to substitute petroleum derivative in the synthesis of polymers, surfactants and lubricating oils. It can also be used to produce glycidol, an epoxy compound with wide applications in plastics and textile industries. On the other hands, citramalic acid is a weak acid that has high value in pharmaceutical and cosmetic industries due to its functions in reversing the aging effects on human face, provided that high purity citramalic acid can be obtained.

2.2 Conventional Homogeneous and Heterogeneous Catalyst in Biodiesel Production

For transesterification and interesterification reactions, homogeneous or heterogeneous catalysts are generally involved to enhance the manufacturing process of biodiesel. Homogeneous catalysts are mainly found in the technology of biodiesel production due to their characteristics of higher solubility in oil, more reactive and lower costs. However, the cost of biodiesel production increases due to non-reusability of catalyst and lower FAME recovery (Boon-anuwat, et al., 2015). Large amount of waste water is also produced due to the downstream neutralisation and purification procedures.

Heterogeneous catalytic system poses a solution for the aforementioned problem. Their relatively easy recovery, using filtration or centrifugation, makes them favourable to be utilised. Several heterogeneous catalysts are capable to undergo reaction for several cycles without regeneration. However, due to heterogeneous phase reaction, the mass transfer between oils, acyl acceptor and catalyst phases is the main limiting step which must be improved. Korkut and Bayramoglu (2018) suggested that intense mixing and agitation could be carried out to increase the resulting biodiesel yield.

As shown in Figure 2.4, these catalysts can be further categorised into acidic or basic types. Moreover, enzyme-catalysed reaction and non-catalytic supercritical reaction conditions are also the feasible alternatives for biodiesel production.

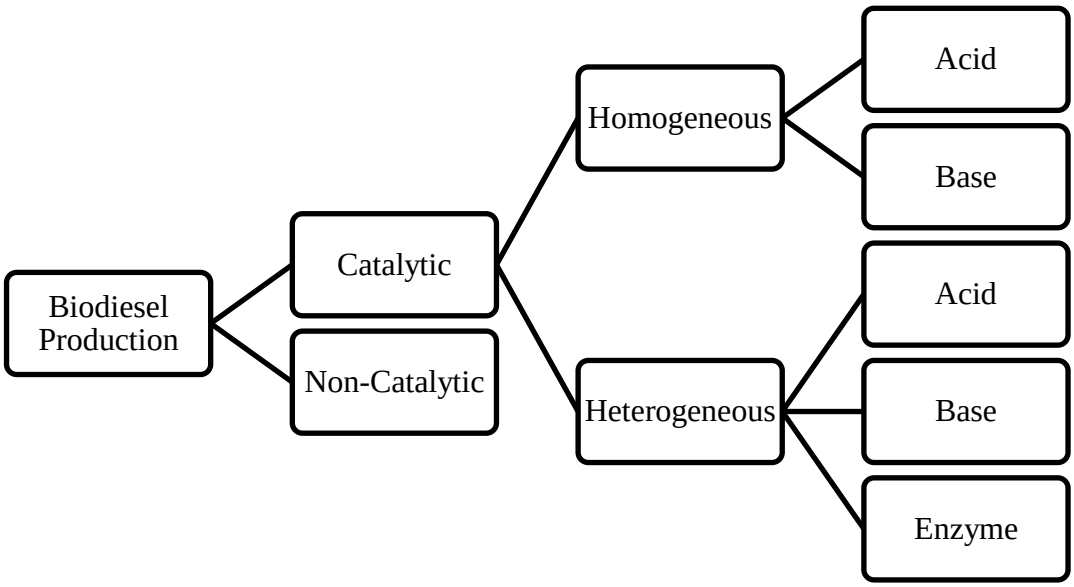

Figure 2.4: Biodiesel Production Classification (Nomanbhay and Ong, 2017)

2.2.1 Alkaline Catalyst

Transesterification reaction between TG and methanol with the aid of homogeneous alkaline catalysts such as potassium hydroxide, KOH, sodium hydroxide, NaOH and methoxide, CH_3O- is the typical pathway employed in industrial-scale biodiesel production (Ehsan and Chowdhury, 2015). This is because alkaline catalyst offers higher reaction rate, around 4000 times faster as compared to acidic catalysts (Nomanbhay and Ong, 2017). Hence, the reaction can be performed at milder condition with high biodiesel yield as supported by the data shown in Table 2.1. These alkaline catalysts can be obtained at low cost since they are widely available.

Table 2.1: Transesterification Reaction with Alkaline Catalysts

Catalyst	Catalyst Reusability (no. of cycles)	Feedstock	Reaction Conditions					References
			Temperature (˚C)	Time (h)	Methanol to Oil Molar Ratio	Yield [*Y*] / Conversion [*C*] (%)	Catalyst	
Homogeneous								
Sodium hydroxide	-	Citrullus vulgaris (watermelon)	60	2	5:1	*Y*= 70	0.13 g	(Efavi, et al., 2018)
Tetramethyl ammonium hydroxide	-	Sunflower oil	60	2	6:1	*Y*= 97.33	1.76 wt.%	(Sánchez, et al., 2013)
Potassium hydroxide	-	Refined cotton seed oil	55	1	6:1	*Y*= 96	0.6 % in concentration basis	(Onukwuli, et al., 2017)
Heterogeneous								
Calcium Oxide	-	Vegetable oil	65	1.25	6:1	*C*= 100	3 wt.%	(Colombo, Ender and Barros, 2017)
CaO-MgO mixed oxide	3	*Jatropha curcas* oil	-	0.067	18:1	*C*= 95	4 wt.%	(Buasri, et al., 2015)

The bottleneck of alkaline process is its high sensitivity to FFA level (>0.5 wt.%) and water content (>0.06 wt.%) in oils, leading to soap formation via saponification which complicates the downstream separation, neutralisation and purification processes (Ashton Acton, 2013). The catalyst efficiency and overall biodiesel yield are thus reduced. Therefore, extra pre-treatment step is necessary to be carried out to lower the FFA level in feedstock. The production plant must also possess facilities to treat the alkaline waste water before releasing it to the environment (Ang, Tan and Lee, 2014). Despite all the beneficial properties of alkaline catalysts, additional problems such as catalyst deactivation due to exposure to the surrounding air and contamination of product due to catalyst active sites arise when heterogeneous phase catalyst is employed.

2.2.2 Acidic Catalyst

The application of acidic catalysts diminishes inherent problems associated with FFA level and moisture in substrates as the catalysts' performance is not severely affected. They can catalyse both transesterification and FFA esterification simultaneously with no soap formation (Atadashi, et al., 2013). Nevertheless, they have comparatively lower reaction rate, thus requiring longer reaction times (≤ 96 h) and higher alcohol to oil molar ratios (≤ 150:1) as shown in Table 2.2. In the occasion where higher reaction temperature is needed, the biodiesel production process becomes energy intensive. Corrosive feature of acidic catalyst can damage the reaction vessels, thus restricting their industrial applications (Meher, et al., 2013). Heterogeneous acidic catalysts likewise encounter the problem of active sites leaching.

Table 2.2: Transesterification Reaction with Acidic Catalysts

Catalyst	Catalyst Reusability (no. of cycles)	Feedstock	Reaction Conditions					References
			Temperature (˚C)	Time (h)	Alcohol to Oil Molar Ratio	Yield [*Y*] / Conversion [*C*] (%)	Catalyst	
Homogeneous								
Hydrochloric acid	-	Highly wet microalgae	95	2	10 ml/g	*Y* > 90	0.1-1.5 ml	(Kim, Im and Lee, 2015)
Sulfuric acid	-	Soybean oil	65	51	30:1 (1-butanol)	*C*= 99	1 mol%	(Bharathiraja, et al., 2014)
Heterogeneous								
Tungstated zirconia WO_3/ZrO_2	3	Microalgal lipids	100	3	12:1 (methanol)	*C*= 94.58	15 wt.%	(Guldhe, et al., 2017)
Sulfonic acid-functionalized platelet SBA-15 mesoporous silica	1	Crude *Jatropha* oil	150	75	23:1 (methanol)	*Y*= 75-78	15 wt.%	(Chen, et al., 2014)

2.2.3 Enzymatic Catalyst

The application of enzymes such as lipases as biocatalyst offers several environmental and economic advantages over conventional chemical catalysts. Enzymatic catalysts provide good selectivity and biodiesel production can be conducted under more gentle conditions, thus more energy efficient. From Table 2.3, the operating temperature of enzyme catalysed transesterification varies from 35-40 ℃ which is considerably moderate. The ease of enzyme recycling and separation simplifies the production process. Enzymatic catalysts are appropriate for biodiesel synthesis from a variety of TG substrates which comprise fats and waste oils with high levels of FFA. Biodiesel production using enzymatic catalysts can be considered as environmentally benign since there is no requirement of waste water treatment facilities (Nomanbhay and Ong, 2017).

Nevertheless, their implementation is restricted owing to the high costs of enzymes, low reaction rate and large reaction volumes (Calero, et al., 2015). Other than that, the utilisation of short-chain alcohols deactivates the lipase and inhibits its activity, causing the enzymes to have short lifespan. More enzymes are needed to achieve the desired biodiesel yield and eventually raising the costs. Other acyl acceptors like MA, DMC and ethyl acetate may act as a promising substitute to replace alcohol.

Table 2.3: Transesterification Reaction with Enzymatic Catalysts

Catalyst	Feedstock	Reaction Conditions					References
		Temperature (˚C)	Time (h)	Methanol to Oil Molar Ratio	Yield (%)	Enzyme (wt.%)	
Eversa Transform (L)	Castor oil	35	8	6:1	94.2	5	(Andrade, Errico and Christensen, 2017)
Candida rugosa lipase (l)	Tallow kernel oil	40	24	4:1	95.4	10	(Su, et al., 2016)
Candida antarctica lipase B	Waste tallow	-	0.333	4:1	85.6	6	(Adewale, Dumont and Ngadi, 2015)
Callera Trans L	Rapeseed oils	35	24	4.5:1	95.3	0.5	(Nordblad, et al., 2014)

2.2.4 Non-Catalytic Supercritical Process

Non-catalytic supercritical transesterification process offers high conversion and reaction rate which produces large yield in a short period of time. Simpler separation and purification procedures are involved since there is no catalyst present. Supercritical biodiesel production is not affected by the presence of FFA and water content in oils or fats. Pre-treatment step to reduce the water content in oils is not needed.

However, according to Sakdasri, Sawangkeaw and Ngamprasertsith (2018), supercritical transesterification demanded high alcohol to oil molar ratio up to 42:1. Despite faster reaction and promising yield, the installation costs for industrial plant are very expensive. Furthermore, the operating temperature and pressure of supercritical reaction typically varies in the range of 200-400 ℃ and 10-25 MPa, respectively. This is because the temperature and pressure must be above the critical values of alcohol for it to be more soluble in oils (Nomanbhay and Ong, 2017). Several examples of transesterification in supercritical methanol are listed in Table 2.4. It can be seen that the operating temperatures and pressures of the reaction are higher than the critical temperature (T_c) and pressure (P_c) of methanol which are 239 ℃ and 8.09 MPa, respectively (Micic, et al., 2016). These operating conditions consume large amount of energy, thus making biodiesel production economically unfavourable and restraining it from striding into industrial level. (Pourzolfaghar, et al., 2016).

Table 2.4: Supercritical Transesterification Reaction

Feedstock	Reaction Conditions					References
	Temperature (˚C)	Pressure (MPa)	Time (h)	Methanol to Oil Molar Ratio	Yield [*Y*] / Conversion [*C*] (%)	
Waste vegetable oil	271.1	23.1	0.34	33.8:1	*Y*= 95.27	(Ghoreishi and Moein, 2013)
Refined and used palm olein oil	400	15	0.333	12:1	*C*= 99	(Sakdasri, Sawangkeaw and Ngamprasertsith, 2015)
Krating oil	260	16	0.167	40:1	*Y*= 90.4	(Samniang, Tipachan and Kajorncheappun-ngam, 2014)
Jatropha oil	320	15	0.0833	40:1	*Y*= 84.6	(Samniang, Tipachan and Kajorncheappun-ngam, 2014)
Karanja oil	300	26	1.5	43:1	*Y*= 81.15	(Ortiz-Martínez, et al., 2016)
Jatropha oil	325	35	1.5	42:1	*C*= 100 *Y*= 99.5	(Salar-García, et al., 2016)

2.3 Biomass Derived Carbon-Based Solid Acid Catalyst

Despite the benefits of commercial heterogeneous acid catalysts, their derivation procedure involves high-priced chemical reagents, raising the overall production costs. It is very essential that the catalysts can be prepared at lower cost with satisfactory activity, stability and reusability. Therefore, reutilisation of various biomass waste as support material in synthesising effective catalysts is a promising pathway for biodiesel production. Nowadays, biomass has gained its popularity in catalysis other than becoming feedstock for biofuel manufacturing. One of the major components of transesterification is the oil content in feedstock. After extraction, the biomass residue will form waste which is made up mainly by large organic hydrocarbon compound, creating disposal problem.

Application of biomass residue as carbon precursor for solid acid catalyst is favourable since it is readily available from many sources and environmentally benign. The biomass residue must be first cleaned and gone through the calcination process to produce biochar which will be discussed particularly in the Section 2.4. Next, the biochar will undergo sulfonation process. A flowchart of the catalyst synthesis procedure is depicted in Figure 2.5. The sulfonated carbon-based catalysts (SCBC) carry three functional groups, namely sulfonic acid, -SO_3H, carboxylic acid, -COOH and phenolic acid, -OH after appropriate sulfonation process to alter the surface chemical properties (Abdullah, et al., 2017). As comparison, the conventional solid acid catalysts have only one functional group. These acid sites contribute to the catalytic activity of the catalysts collaboratively. For instance, sulfonic acid sites play the main role in catalysis with the other two acid sites help to enhance the accessibility of reactants to the catalyst surface by raising its hydrophilic properties. Table 2.5 outlines the application of different types of biomass waste as the solid acid catalyst for producing biodiesel.

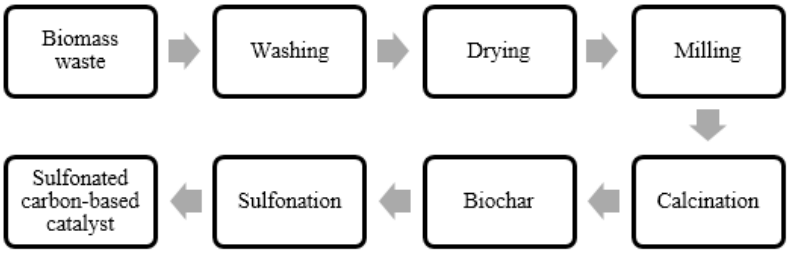

Figure 2.5: Preparation of Sulfonated Carbon-Based Catalyst (SCBC) (Abdullah, et al., 2017)

Table 2.5: Literature Survey on Biomass-Derived Solid Acid Catalyst for Biodiesel Production

Biomass	Surface Area (m^2/g)	Strength (mmol/g)	Catalyst Reusability (no. of batches)	Feedstock for Biodiesel Production	Reaction Conditions		Yield [*Y*]/ Conversion [*C*] (%)	References
					Methanol to Oil Molar Ratio	Time (h)		
Calophyllum inophyllum	0.2-3.4	0.6-4.2	4	Non-edible oil	30:1	5	*C*= 99	(Dawodu, et al., 2014)
Douglas fir wood chips	3.51	1.37	10	Fast-refined microalgal oil	5:1–30:1	0.167-1.5	*Y*= 99	(Dong, et al., 2015)
Corn straw	-	2.64	-	Oleic Acid	7:1	4	*Y*= 98	(Liu, et al., 2013)
Bagasse	-	-	8	Waste cooking oil	18:1	5-6	*C*= 94.4	(Zhang, et al., 2014)
Rice husk char	4	2.46	5	Waste cooking oil	20:1	15	*Y*= 87.57	(Li, et al., 2014)

2.4 Carbonisation and Pre-Treatment of Biomass

To prepare a biomass-derived catalyst, several pre-treatment steps must be carried out in order to ease the subsequent carbonisation process. Firstly, the biomass must be cleaned and washed with distilled water to remove any impurity. It will then undergo size reduction with grinder and dry with oven to remove all moisture. The carbon precursor is carbonised in a muffle furnace at a specific temperature for a certain period of time to convert the organic biomass into carbon residue. Continuous flow of nitrogen gas is used to create an inert environment in the furnace, maintaining the homogeneity (Bora, et al., 2018). Touhami, et al. (2017) suggested that carbonisation could also be done by pyrolysis using a tube furnace with continuous flow of nitrogen. Calcination is a process similar to carbonisation where it focuses to eliminate volatile compounds and oxidise the biomass. During combustion, calcium carbonate, $CaCO_3$ in the organic compound decomposes into calcium oxide, CaO and liberates a portion of carbon dioxide, CO_2 gas. Both processes are typically carried out in the temperature range of 300-1000 ℃, depending on the types of feedstock (Abdullah, et al., 2017). Table 2.6 summarises the carbonisation temperature and time for different biomass wastes.

Table 2.6: Carbonisation Conditions for Various Biomass Wastes

Biomass Waste	**Calcination Conditions**		**References**
	Temperature (℃)	**Time (h)**	
Coconut shell	422	4	(Endut, et al., 2017)
Waste shell of Mesua ferrea Linn seeds	500	1.5	(Bora, et al., 2018)
Rice husk	400	4	(Touhami, et al., 2017)
De-oiled *Jatropha* curcas seeds	350	4	(Mardhiah, et al., 2017)
Pomelo peel	600	2	(Zhao, et al., 2018)

Carbonisation and calcination temperatures play a significant role in controlling the performance of the fabricated catalyst by manipulating its surface morphology. It affects the formation of calcium oxide as the presence of calcium oxide

provides extra void on the carbon structure, resulting in larger total pore volume and pore diameter. Excessive temperature will cause the disintegration of carbon skeleton and breakdown of macromolecules. The organic portions might be removed too. Micropores may grow to reduce the pore volume, leading to low amount of accessible active site on the catalyst surface.

Other than that, calcination time is another important factor to be considered as it affects the development of calcium oxide. Inadequate holding time might cause the calcium oxide to be underdeveloped, thus the resulting catalytic activity is not promising. On the other hand, prolonged calcination time will result in sintering which causes the catalyst grains to shrink and decreases the total effective surface area. Therefore, it is essential to synthesise the catalyst with optimum calcination time so that to ensure complete conversion of calcium carbonate.

Last but not least, grounding of the carbonised sample can be conducted eventually to produce fine powder of about 0.5 to 1 mm in particle size (Endut, et al., 2017).

2.5 Sulfonation of Activated Carbon

Sulfonation is the major process for synthesising a carbon acid catalyst where the carbon precursor is equipped with active sulfonic acid group, $-SO_3H$. There are various sulfonation techniques available to graft the active site onto the structural support, providing catalysts with different catalytic activities. Sulfonated carbon catalyst was stated to be the most proficient and cost-effective catalyst for the biodiesel production from high FFA content feedstock (Bora, et al., 2018). It is important to utilise a suitable sulfonation method, so that it can perform well in a reaction.

Endut, et al., (2017) conducted the sulfonation of activated carbon by using sulfuric acid, H_2SO_4. 10 g of carbon catalyst was mixed with 100 ml sulfuric acid in a 250 ml conical flask. Excess acid was discarded after 15 minutes. Next, the wet solids residual was transferred to a ceramic crucible and heated in a muffle furnace. The optimum sulfonation time and temperature were found out to be 15 h and 100 ℃, respectively. The sulfonated carbon catalyst was cleaned with excess distilled water after it was cooled to room temperature. The washing process continued until the wash water achieved neutral pH. The synthesised catalyst was then dried with air-drying

oven at 105 ℃ for 10 h, followed by storing in a sealed container to avoid contamination.

Direct sulfonation via thermal treatment with concentrated sulfuric acid manufactures sulfonated carbons with comparatively lower specific surface area and acid density. They are also vulnerable to leaching of sulfonic acid groups which results in low reusability. Konwar, et al. (2014) carried out sulfonation using covalent anchoring of 4-benzenediazoniumsulfonate radicals via two methods. The biomass derived activated carbon was maintained at a temperature of 3-5 ℃ and stirred with 100 mL of 20-32 % hypophosphorous acid, H_3PO_2 for 30 min. After that, another 50 mL hypophosphorous acid was added and the mixture was hold for 1 h with periodical stirring. Next the mixture was filtered and washed with acetone and water extensively, followed by drying overnight in vacuum. The second method was using hydrochloric acid instead of hypophosphorous acid with similar washing procedure. The obtained catalyst was dried at 110 ℃ in an oven. The mixture was hold for 12 h at 5 ℃. Sulfonation using 4-benzenediazoniumsulfonate helps to maintain structural stability of the carbon surface and presence of high strength C-SO_3H bonds leads to improved reusability.

Tamborini, et al. (2015) mixed 0.2 g nanoporous carbon with 10 mL fuming sulfuric acid, producing a suspension which was then heated at a temperature of 80 ℃ for 8 h under reflux. They were then cooled to ambient temperature and washed with distilled water until no sulfate ions were found in the wash water via barium chloride test. Next, upon drying at 70 ℃ for 12 h, centrifugation was used to separate black precipitate from the reaction mix. The application of fuming sulfuric acid is not recommended as it causes safety and operation problem as compared to other methods (Kang, Ye and Chang, 2013). Tamborini, et al. (2015) also reported another method using a mixture of chlorosulfuric acid, $HClSO_3$ and sulfuric acid in a molar ratio of 2:10 instead of fuming sulfuric acid. The subsequent mixture was heated at the same conditions with previous but with additional constant stirring. Similar filtration and washing procedure were carried out too.

Negm, et al. (2017) enumerated the procedure to prepare a super acidic sulfonated modified mica catalyst (Mica-Ph-SO_3H). Phenyl grafted mica was distributed in 1,2-dichloroethane and excess chlorosulfonic acid was added at 0 ℃. This mixture was stirred vigorously for 12 h and subsequently warmed at 50 ℃. The

precipitate was washed thoroughly with 1,2-dichloroethane, followed by drying at 50 ℃ under vacuum.

Niu, et al. (2018) proposed the arylation of sulfanilic acid to synthesise heterogeneous acid catalyst. Mixture of sulfanilic acid and bamboo activated carbon at a molar ratio of 1 was vigorously stirred to attach the Ph-SO_3H active sites to the carbon structure. Sodium hydroxide, NaOH was used to control the pH of this mixture emulsion at around 7-8. Sodium nitrite, $NaNO_2$ was added to terminate the sulfonation process and it dissolved completely by adding deionized water. 25 wt.% hydrochloric acid was added drop by drop to prevent spontaneous rise of reaction temperature. Next, filtration was carried out under vacuum and washing step was done by using de-ionized water until neutral pH. The slurry residual was cleaned by purging acetone to remove any impurities before drying in an oven. The optimum sulfonation temperature and time were at 50 ℃ and 10 minutes, respectively.

Wu, et al. (2014) suggested the method of wet impregnation of ammonium persulfate, $(NH_4)_2S_2O_8$ into the dried precipitate of ZrO_2-TiO_2-Fe_3O_4 at different Zr to Ti molar ratio. They were mixed with a solution to solid ratio of 15 mL/g and stirred for 1 h at 500 rpm. Filtration was carried out to remove the precipitated solid, followed by drying at 110 ℃ for 12 h. This method was a bit different from others. Calcination was only done next for 3 h in air. It was stated that Zr to Ti molar ratio of 3:1 and calcination temperature of 550 ℃ gave the best activity due to highest acidity.

Tang, et al. (2017) proposed the thermal decomposition of ammonium sulfate, $(NH_4)_2SO_4$ as a sulfonation method. Different concentrations of ammonium sulfate was mixed with biochar. The mixture was ultrasonicated with water bath for 10 minutes with the aid of an ultrasonicator and subsequently heated to 235 ℃ in a furnace for 15-90 min. Prior to washing with distilled water and filtration, the reaction mixture was allowed to cool. The filtered precipitate was dried in an oven at 80 ℃ overnight. The optimum sulfonation conditions were 10.0 w/v% of ammonium sulfate and 30 minutes of heating period.

2.6 Characterisation and Screening of Synthesised Catalyst

Characterisation of fabricated catalysts is essential to study and understand the intrinsic and extrinsic properties of the catalysts. This is aided by various analytical instruments which generate information about surface morphology, thermal stability,

acid density and identity of the attached functional groups. The valuable outcomes will justify the efficacy of the catalyst preparation methods. Examples of the instrument involved are thermogravimetric analysis (TGA), Scanning Electron Microscopy equipped with Energy Dispersive X-ray (SEM-EDX), Brunauer-Emmett-Teller (BET), Fourier Transform Infrared Spectroscopy (FTIR) and Temperature Programmed Desorption, Reduction and Oxidation (TPDRO).

Ayodele and Dawodu (2014) reported the usage of TGA for evaluating the thermal stability and decomposition of prepared catalysts where the original mass of the sample was measured by using an external weighing balance. The proposed operating condition of TGA by Correia, et al. (2014) was heating rate of 10 ℃/min with temperature range of 25-1000 ℃.

Furthermore, the images obtained from SEM-EDX provide structural information, sulfur content and surface morphologies of the synthesised catalysts. The SEM was operating under a vacuum of 1.33×10^{6} mbar with a 20 kV accelerating voltage (Correia, et al., 2014). Sputter coater was used at first to cover the samples with a thin layer of gold of about 10 nm.

On the other hand, TPDRO generates information about activation energy, single point BET, acid sites concentration on surface with high precision, accuracy and reliability in a short period of time (Fadoni and Lucarelli, n.d.). Surface area, pore volume and size can be evaluated according to BET methods.

FTIR absorption or transmittance spectrum provides information about organic compounds found in the synthesised catalysts. Zhang, et al. (2014) suggested that FTIR analysis can be carried out in the wavenumber range of 600-4000 cm^{-1}. The sample was mixed with potassium bromide, KBr, forming a pellet for the subsequent analysis. The functional groups present in the catalysts can be identified by careful inspection of the spectrum.

Besides, titration method can be employed to determine the acid density of the catalysts. A detailed procedure was enumerated by Konwar, et al. (2014). 0.04 g of the prepared catalyst was mixed with 20 mL of 0.01 M sodium hydroxide aqueous solution. The mixture was stirred uniformly for 4 h at room temperature with the aid of a magnetic stirrer. The resulting solution was then titrated with 0.01 M hydrochloric acid, HCl aqueous solution with phenolphthalein as an indicator. Centrifugal separation can be used to eliminate any undissolved catalysts.

2.7 Characterisation of Feedstock and Products

For feedstock with high FFA content, it is advisable to use acid catalyst for higher yield. Therefore, it is necessary to carry out an investigation of the feedstock's chemical composition and their respective amount prior to the biodiesel production process. The fatty acids that are attached to glycerol in a TG molecule can be saturated or unsaturated, depending on the presence of carbon-carbon double bond. Taking linoleic acid as an example, it can be described as C 18:2 which means that it is a hydrocarbon chain with 18 carbon atoms and two carbon-carbon double bonds. Table 2.7 shows a list of fatty acids which are commonly found in oils.

Table 2.7: Examples of Fatty Acids

Fatty acid	Notation
Palmitic acid	C 16:0
Stearic acid	C 18:0
Oleic acid	C 18:1
Linoleic acid	C 18:2
Linolenic acid	C 18:3

Santos Ribeiro, et al. (2017) carried out an interesterification reaction between macaw oil and MA. A Gas Chromatography (GC) equipped with flame ionisation detector (FID) and RTX-Wax capillary column (30 m × 0.25 mm × 0.25 μm) was used. The fatty acids were first converted into methyl esters and the resulting retention time was compared with that of FAME standards to find out the identity of the fatty acids. Oleic acid and palmitic acid were found to be the major fatty acids in macaw oil with a composition of 74.18 wt.% and 13.05 wt.%, respectively.

Casas, Ramos and Pérez (2011b) conducted another interesterification using sunflower oil and MA as reactants. It was stated that the refined sunflower oil consisted of 63 % linoleic acid, 25.2 % oleic acid, with palmitic acid, steric acid and linolenic acid at minimal quantity.

Maddikeri, Pandit and Gogate (2013) claimed that the waste cooking oil used in the interesterification with MA made up mainly by unsaturated fatty acids such as linoleic and oleic acids. This was further supported by their similar research in 2014.

In another interesterification reaction carried out by Sustere, Murnieks and Kampars (2016) using rapeseed oil with different types of alkyl acetates, the feedstock was determined to contain 62.5 % oleic acid and 21.7 % linoleic acid.

The yield of FAME and the corresponding conversion are crucial parameters which must be determined in order to verify the potency of the reaction pathway and catalysts used. Casas, Ramos and Pérez (2013) claimed that the quantitative analysis of FAME was conducted according to EN 14103 standard. The compositions of other components such as triacetin, diacetin, monoacetin, glycerol, diacetinmonoglyceride, monoacetindiglyceride and triglyceride were deduced based on method EN 14105. All these analyses can be done using GC.

A sample of 150 mg was diluted in 10 ml of n-heptane which acted as a carrier. 1 ml of the mixture and 500 μL of internal standard which was 10,000 ppm methyl heptadecanoate with pyridine as solvent was transferred to an analysis vial. 1 μL of the final solution was injected and travelled through capillary column (15 m × 0.32 mm × 0.10 μm). By comparing the retention time of a peak in the sample with that in the standard, the FAME and triacetin peaks could be identified. The integrated area of the peak representing FAME would give an indication value of the yield. The total yield of FAME in unit of percentage can be expressed in Equation 2.1 (Santos Ribeiro, et al., 2017).

$$FAME\ Yield\ (\%) = \frac{measured\ FAME\ amount\ in\ the\ sample\ (g)}{theoretical\ amount\ from\ initial\ oil\ content\ on\ basis\ of\ its\ fatty\ acid\ composition\ (g)} \times 100 \quad (2.1)$$

The total percentage yield of FAME can also be obtained from the FAME calibration curve using external standard methods. Moreover, the conversion of FFA can be evaluated by titration with potassium hydroxide, KOH. Potassium hydroxide acts to neutralise the acids present. Titration results signify the initial acid value of the feedstock (a^i) and final acid value of the mixture after the reaction (a^f). The acid value is a number expressed in the unit of milligrams of potassium hydroxide needed to neutralise 1 g of FAME (Casas, Ramos and Pérez, 2011). The resulting conversion can be calculated based on Equation 2.2 (Ayodele and Dawodu, 2014).

$$FFA\ conversion\ (\%) = \frac{a^i - a^f}{a^i} \times 100 \quad (2.2)$$

2.8 Interesterification for Biodiesel Production

A detailed procedure of ultrasound aided interesterification was emphasised by Maddikeri, Pandit and Gogate (2013). A 100 mL three-neck batch reactor was initially filled with MA and waste cooking oil with a MA to oil molar ratio of 12:1. Three openings were used to fit condenser, ultrasonic horn and temperature sensor. Condenser worked to liquefy the vaporised methyl acetate while temperature sensor was used to monitor the temperature change during the reaction. This experimental set up can be switched to conventional interesterification by replacing the ultrasonic horn with a stirrer. The mixture was heated to 40 ℃. The 1 % catalysts in concentration basis was then added into the reactor before reaction was started. Several samples were withdrawn at a designated interval of time. Stoichiometric amount of ortho-phosphoric acid was used to quench the collected samples immediately to inhibit the continual progress of the reaction. Next the sample was washed to remove the catalyst by using water. A 3Å molecular sieve was put in to eliminate the trace amount of moisture. The samples were then refrigerated until further analysis.

Chemical interesterification reaction between rapeseed oil and MA was carried out by Sustere, Murnieks and Kampars (2016). The mixture of rapeseed oil and methyl acetate in MA to oil molar ratio of 18:1 was heated up to 55 ℃ in a three-neck flask. Next, reaction was started once catalyst in catalyst to oil molar ratio of 0.16:1 was added and progressed for 60 min. Phosphoric acid in equimolar amount was added and emerged salts were eliminated by filtration. Repetition of experiment was carried out to calculate the average value.

Wu, et al. (2014) proposed a novel interesterification of cottonseeds and methyl acetate to be carried out by *in situ* reactive extraction. A mixture of 20 g cottonseeds and varying volumes of MA was charged into a round-bottom flask accommodated with water-cooled condenser and magnetic stirrer. The mixture was then heated to a temperature of 50 ℃. Once the catalyst was added, the reaction was initiated with mechanical stirring at around 300 rpm for a reaction period of 10.8 h. The mixture was then cooled and filtered to remove any solid residue. The discussed interesterification reactions are summarised in Table 2.8.

Table 2.8: Interesterification of Biodiesel Production

Feedstock	Reaction Time (h)	Reaction Temperature (℃)	Methyl Acetate to Oil Molar Ratio	Catalyst Amount	Yield (%)	References
Waste cooking oil	-	40	12:1	1% in concentration basis	90.0	(Maddikeri, Pandit and Gogate, 2013)
Cottonseed oil	10.8	50	13.8 mL/g	21.3 wt.%	98.5	(Wu, et al., 2014)
Rapeseed oil	1	55	18:1	Catalyst to oil molar ratio= 0.16:1	82.7	(Sustere, Murnieks and Kampars, 2016)

2.8.1 Optimisation Study

The preparation procedures suggested in Sections 2.4 and 2.5 are sufficient to fabricate a feasible catalyst for biodiesel production. The determination of optimum conditions for the fabrication process is crucial to maximise the performance of catalyst in reaction. Various parameters involved such as calcination temperature and time can be manipulated to obtain the highest biodiesel yield or conversion.

Meng, et al. (2013) reported an investigation on calcination temperature of a solid Ca/Al composite oxide-based alkaline catalyst prepared via chemical synthesis and thermal activation with the aid of sodium aluminate solution and calcium hydroxide emulsion. Calcination temperature has great influence on the catalytic activity. Since the fabricated catalyst consisted of $Ca_{12}Al_{14}O_{33}$ and CaO, development of the $Ca_{12}Al_{14}O_{33}$ phase at higher calcination temperature resulted in larger surface area as shown in Figure 2.6. The optimum calcination temperature was found to be 600 ℃ with the highest biodiesel yield of more than 94 % (Reaction conditions: methanol/rapeseed oil molar ratio 15:1, catalyst amount 6 wt.%, reaction temperature 65 ℃ and reaction time 3 h).

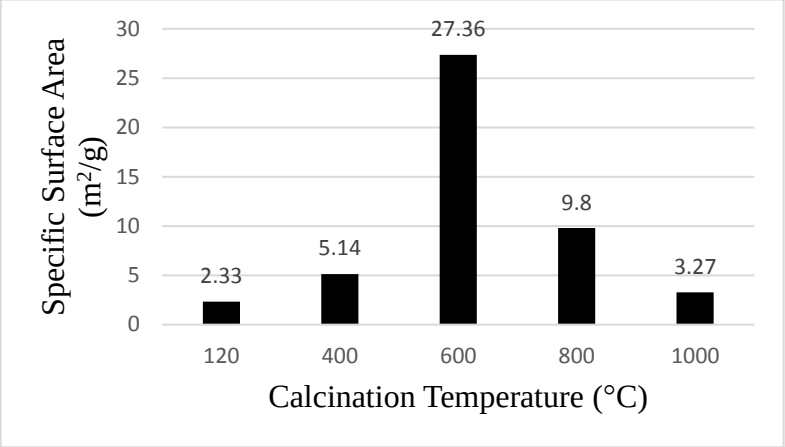

Figure 2.6: Specific Surface Area of Ca/Al Composite Oxide Catalysts at Different Calcination Temperatures (Meng, et al., 2013)

The effect of sulfonation temperature on performance of catalyst in esterification reaction was discussed by Yu, et al. (2017). Sulfonation temperature regulates the quantity and location of -SO_3H groups as well as the firmness of their attachment to the carbon-based structure. It was proven that the increment in sulfonation temperature from 90 to 105 ℃ resulted in an increase of oleic acid conversion with a maximum value of 95.7 %. However, further rising of sulfonation temperature gave adverse outcome. Therefore, it can be concluded that 105 ℃ was the optimum sulphonation temperature for this case.

Beside calcination temperature, the performance of catalyst is strongly impacted by calcination time. Aguilar-Garnica, et al. (2013) conducted the sulfonation of recycled poly(styrene-co-butadiene) via fuming sulfuric acid. The sulfonation process was conducted using varying times and temperatures. Three sulfonating times of 1, 3 and 5 h were applied to each of the temperature (30, 70 and 110 ℃). This 3 × 3 experimental design was used to set up a mathematical model in order to obtain the sulfonation data at 95 % confidence. The achieved optimum condition was 2.5 h and 75 ℃ with maximum number of acid sites attached to the polymer. The prepared catalysts were proven to be able to work with the feedstock with high FFA content.

2.8.2 Stability and Regeneration Test

To transform the biodiesel production into a sustainable process, the synthesis and utilisation of solid catalysts for consecutive cycles without considerable drop in activity is an important parameter to be considered. Stability test can be conducted to

evaluate the reusability of the prepared catalyst, thus deciding whether it is suitable to be used for practical applications. After each experimental run, the active site grafted on catalyst may leach to the reaction solution, influencing the catalytic performance. Regeneration can be performed to restore the catalytic activity.

Mardhiah, et al. (2017) conducted an esterification reaction using carbon-based solid acid catalyst derived from de-oiled *Jatropha curcas* seeds. The catalyst was prepared via sulphonation by heat treatment with concentrated sulfuric acid. Once the reaction was completed, the catalyst was gathered and cleansed thoroughly with hot distilled water at 80 ℃ and n-hexane to eliminate any impurities, followed by drying. The catalyst was then re-used for a series of the same esterification reaction under the optimum operating conditions. The product from each cycle was tested for acid value and conversion yield which indicated the catalyst effectiveness on each cycle. Moreover, the presence of sulfate groups, $-SO_3$ in the filtered methanol was tested using barium chloride to verify the occurrence of leaching. Titration method was also used to monitor the changes in the acid capacity of the catalyst after each cycle. Figure 2.7 shows that there was a slight decline in conversion yield until the fourth cycle. Drop in catalytic activity is due to the decline in catalyst's acid capacity. Nevertheless, there was no sulfate leaching since the barium chloride testing gave a negative result.

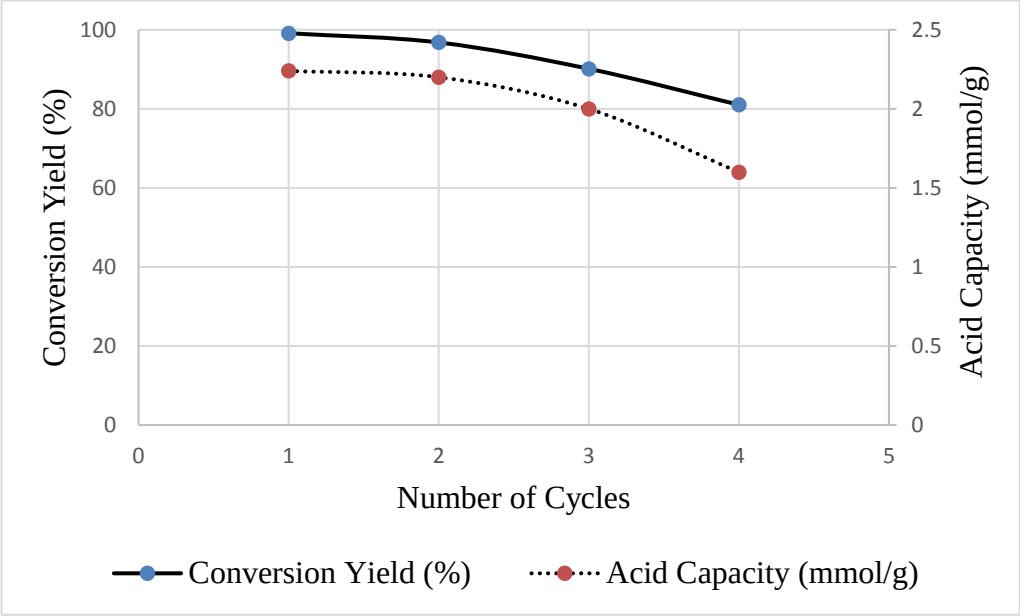

Figure 2.7: Reusability of Carbon-Based Acid Catalysts (Reaction conditions: methanol/oil ratio 12:1, catalyst amount 7.5 wt.%, reaction temperature 60 ℃, reaction time 1h and stirring rate 350 rpm) (Mardhiah, et al., 2017)

Asikainen, Munter and Linnekoski (2015) made use of seven different types of solid acid catalysts to catalyse the production of FAME from palmitic acid derivatives. Deactivation studies of Nafion NR50 were studied by conducting five successive reaction cycles of 24 h on mixture of algae oil model compounds. The reaction was carried out with 0.05 mmol of model compound, 5 mL of methanol and 80 mg of catalyst at temperature of 65 ℃ and stirring rate of 450 rpm. The experimental results obtained for 5 cycles were 35 ±5 %, signifying that no catalyst deactivation took place. For Nafion or silica composite catalyst, deactivation may take place due to blockage caused by large molecular weight hydrophobic products.

Wu, et al. (2014) had investigated the usage of magnetic solid acid catalysts for biodiesel production from cottonseeds. Same reaction was repeated consecutively under optimum conditions to determine the stability and reusability of $S_2O_8^{2-}/ZrO_2$-TiO_2-Fe_3O_4 with Zr/Ti molar ratios of 3/1 (SZTF-3-1) catalyst. The catalytic activity remained high with minimal decrement after eight cycles. A drastic drop in catalytic activity was discovered after being reused for nine times. This was further supported by the declining trend in biodiesel yield. X-ray Photoelectron Spectroscopy (XPS) was used to determine the chemical state of sulfur in the fabricated catalyst after each experimental run. The corresponding results are depicted in Figure 2.8 and it conformed with that of biodiesel yield over the recycled catalyst. This is because the sulfur present on the sulfated oxide catalyst contributes to acidity which in turn imposes a great impact on the catalytic activity. Nevertheless, the regeneration of the catalyst can be easily done by treatment with $S_2O_8^{2-}$ again.

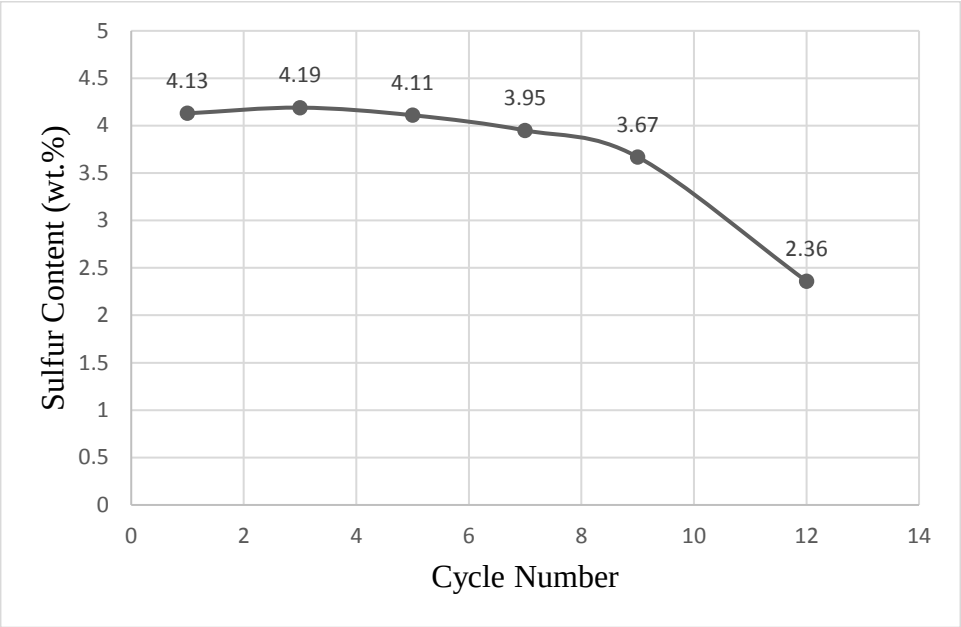

Figure 2.8: Sulfur Content of SZTF-3-1 catalyst (Reaction conditions: methyl acetate/seed ratio 13.8 mL/g, catalyst amount 21.3 wt.%, reaction temperature 50 ℃ and reaction time 10.8 h) (Wu, et al., 2014)

CHAPTER 3

METHODOLOGY AND WORK PLAN

3.1 Prerequisite Requirements

The required raw materials, chemicals and equipment for the research project are clearly stated in the following sections. The raw materials and chemicals must be well prepared prior to the experiment whereas the apparatus and instrument are used to perform the experiment and evaluate the characteristics of the experimental products, respectively.

3.1.1 Raw Materials

In this project, biomass waste of banana peels was chosen as the carbon precursor for synthesising the solid acid catalysts. Waste banana peels was obtained from a local hawker at Negeri Sembilan, Malaysia.

3.1.2 Chemicals

Table 3.1 lists out the chemicals that were involved in catalyst preparation, biodiesel production reaction and analytical procedures. Their respective sources, purities and the approximate amounts are clearly stated too.

Table 3.1: List of Chemicals Required

Chemicals	Source	Purity	Estimated Quantity	Purpose
2-Propanol	Merck	≥99.8 %	200 mL	Solvent for biodiesel
Cooking oil	Lam Soon Edible Oils	100 %	10 mL	Reactant for interesterification

Table 3.1 (Continued)

Chemicals	Source	Purity	Estimated Quantity	Purpose
Distilled water	UTAR	100 %	Excess	Preparation of sulfuric acid, hydrochloric acid, potassium hydroxide and sodium hydroxide aqueous solutions and washing of solid acid catalyst
Hydrochloric acid	Fisher Chemical	37 %	100 mL	Titrant for measurement of acid density of synthesised catalyst
Methanol	Merck	≥99.8 %	100 mL	Reactant for transesterification
Methyl acetate	Alfa Aesar	99 %	3 L	Reactant for interesterification
Methyl heptadecanoate	Sigma-Aldrich	4 g/L	100 mL	Internal standard for Gas Chromatography (GC)
n-Hexane	Merck	≥99 %	1 L	Solvent for biodiesel product in GC analysis
Oleic acid	Fisher Chemical	85-92 %	2.5 L	Reactant for interesterification
ortho-Phosphoric acid	Merck	85 %	2.5 L	Chemical activation of waste banana peels
Palmitic acid	Merck	≥98 %	50 g	Reactant for interesterification

Table 3.1 (Continued)

Chemicals	Source	Purity	Estimated Quantity	Purpose
Phenolphthalein	R & M Chemicals	1 g/L	100 mL	pH indicator
Potassium hydroxide pellets	Merck	≥99 %	50 g	Titrant for measurement of acid values of feedstock and product
Sodium hydroxide pellets	Merck	≥85 %	50 g	Measurement of acid density of synthesised catalyst
Stearic acid	Merck	≥97 %	50 g	Reactant for interesterification
Sulfuric acid	Fisher Chemical	98 %	2.5 L	Sulfonating agent

3.1.3 Apparatus, Instruments and Equipment

Throughout the research, different apparatus and equipment were involved to offer various applications. Table 3.2 shows the apparatus and equipment employed in synthesis of solid acid catalyst and interesterification while Table 3.3 displays the instruments utilised in the analysis of feedstock, products and fabricated solid acid catalysts.

Table 3.2: List of Apparatus and Equipment

Apparatus/ Equipment	Specification	Purpose
Blender	Berjaya	Size reduction of biomass waste
Condenser column	Coil Type	Condensing vapour methyl acetate during reaction

Table 3.2 (Continued)

Apparatus/ Equipment	Specification	Purpose
Furnace	Muffle	Carbonisation of biomass waste into biochar
Heating mantle	Mtops	Maintaining the desired operating temperature of interesterification
Mortar and pestle	-	Size reduction of biochar
Oven	Memmert	Drying of biomass waste, biochar and solid acid catalyst
Separating funnel	500 mL	Separation of biodiesel from the remaining reactants
Sieve	PRADA (300 and 850 micron)	Sieving of biomass waste and biochar
Three-neck round bottom flask	500 mL	Interesterification flask

Table 3.3: List of Instruments

Instrument	Specification	Purpose
Fourier Transform Infrared Spectroscopy (FTIR)	Nicolet iS10 FTIR	Identification of adsorbed species and chemisorption of the solid catalyst from the functional groups present
Gas Chromatography (GC)	GC-FID Perkin Elmer Clarus 500	Determination of biodiesel yield
Scanning Electron Microscopy Equipped with Energy Dispersive X-ray (SEM-EDX)	Hitachi Model S-3400N	Determination of surface morphology and chemical elements such as sulfur present in the fabricated catalyst

Table 3.3 (Continued)

Instrument	Specification	Purpose
X-ray Diffractometer (XRD)	Shimadzu XRD-6000 |	Identification of crystalline phase and chemical composition in the synthesised catalyst

3.2 Overall Research Methodology and Flow Diagram

The research process comprises of a series of methodology with the main purpose of synthesising a carbon based solid acid catalyst for biodiesel production. The overall research plan can be divided into various successive components and the project was carried out according to the flow diagram illustrated in Figure 3.1.

3.3 Experimental Procedures

The experimental works that need to be carried out are mainly the synthesis of catalyst and production of biodiesel via interesterification. Repetition of experiment is necessary to optimise the catalytic performance of the produced catalyst.

3.3.1 Catalyst Preparation

The collected waste banana peels were washed and any unwanted part was removed. They were then cut into smaller pieces and placed evenly on a metal tray. Preliminary cutting was required to increase the surface area for drying. Drying was carried out using an oven at 80 ℃ overnight to eliminate moisture. This moderate temperature was used to prevent decomposition of biomass waste at high temperature. Further size reduction was carried out using a blender to make the fully dried banana peels into powder form as fine particles size facilitated the sulfonation procedures. Next, a test sieve with 850 μm mesh was used to control the particle size distribution of the powder. Extra samples of waste banana peels were kept in reserve in the fridge for use when needed.

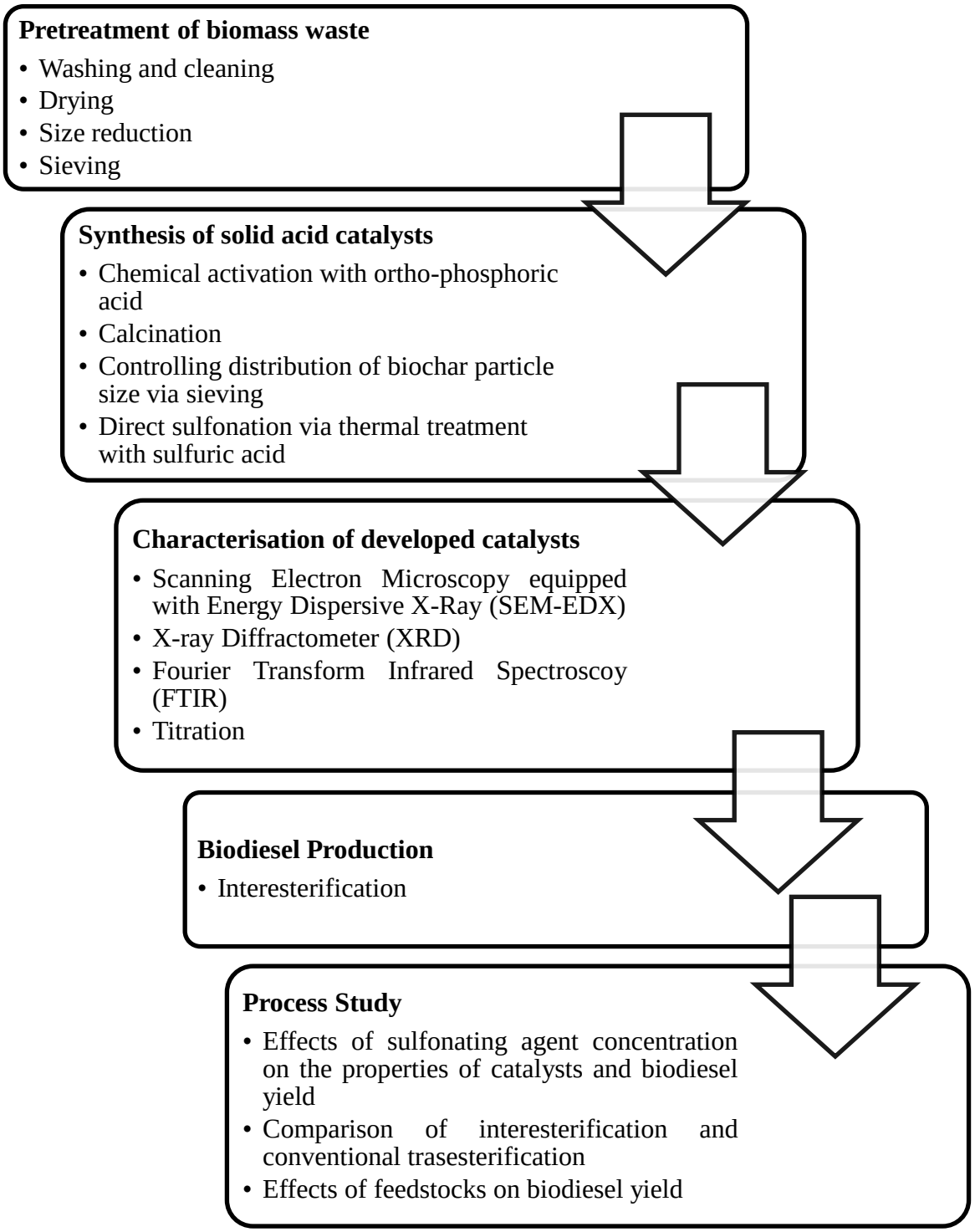

Figure 3.1: Flow Diagram of Research Methodology

3.3.2 Calcination of Biomass and Sulfonation

Powder formed was mixed with 30 v/v% ortho-phosphoric acid in acid to solid mass ratio of 7:1 and impregnated for 24 h (Ee, et al., 2017). This was to increase the porosity of the biomass waste particles and cause fragmentation of lignocellulosic materials. Washing of chemical impregnated biomass waste was done with distilled water and this step was repeated for three times prior to drying at 80 ℃ overnight. After drying, the solid was subjected to 3 h calcination in air at 600 ℃ (Viena, Elvitriana and Wardani, 2018). The calcination process was carried out in a programmable furnace with heating rate of 5 ℃/min. Appendix A shows the illustration of waste banana peel based activated carbon (WBPAC) that appeared in black powder form. Biochar produced was sieved under the size of 300 micron. Catalysts used for biodiesel production were prepared via direct sulfonation with different concentrations of sulfuric acid while maintaining all the other parameters. All sulfonations were performed by immersing 25 g of WBPAC in 250 mL of sulfuric acid at 80 ℃ (Tamborini, et al., 2015). The mixture was stirred drastically at 500 rpm for 6 h. The resulting precipitated solid was filtered out and dried at 80 ℃ overnight. Table 3.4 depicts the catalyst annotation and the corresponding preparation conditions. Appendix A also shows the sulfonated catalyst which all presented as black powder.

Table 3.4: Catalyst Synthesis Parameter and Nomenclature

Catalyst Sample	Concentration of Sulfuric Acid (mol/L)
Cat-2	2
Cat-3	3
Cat-8	8
Cat-13	13

3.3.3 Biodiesel Production

The synthesised solid acid catalysts were used to produce biodiesel via interesterification. Their catalytic performances would be evaluated based on the resulting biodiesel yield and conversion. Oleic acid was chosen as the feedstock to react with methyl acetate in this research project. Interesterification was conducted in a 500 mL three-neck round bottom flask equipped with a coil condenser, a thermometer, magnetic stirrer and heating mantle. Capacity of 500 mL was selected

since the reaction mixture did not exceed 200 mL. Coil condenser was used to condense the evaporated methyl acetate, preventing them from escaping. A thermometer was dipped inside the reaction mixture to monitor the reaction temperature.

10 mL of oleic acid was added to form a reaction mixture which consisted of methyl acetate and oleic acid at a molar ratio of 50:1. 12 wt.% of developed catalyst was also added into the mixture. The reaction was performed for 8 h excluding the temperature build-up period with rotational speed of 600 rpm provided by a magnetic stirrer. Stirring was to ensure uniform temperature and well mixing of the reaction mixture. At the end of the reaction, excess methyl acetate was eliminated through evaporation and the catalyst was filtered after the product was cooled to room temperature. Each set of experiment conducted using synthesised catalysts was repeated twice.

In addition, the synthesised solid acid catalyst with optimum chemical and physical properties from the interesterification process was used to produce biodiesel via conventional transesterification under the same reaction conditions. To evaluate the effectiveness of applying interesterification in producing biodiesel, other feedstocks such as palmitic acid, stearic acid and cooking oil were employed with concentrated sulfuric acid as homogeneous catalyst.

3.4 Feedstock Characterisation: Acid Value

Titration method was employed to evaluate the acid value of the feedstock. 1 g of oleic acid was mixed with of 5 mL 2-propanol which was the solvent in a conical flask, forming the analyte while 0.1 M potassium hydroxide, KOH aqueous solution was the titrant. Few drops of phenolphthalein were added too to serve as pH indicator. Titration process continued until a pink colour appeared which signified the end point. Blank titration was also carried out to eliminate the influence of solvent on the results. Acid value of the oleic acid can be calculated using Equation 3.1 as stated below. Acid value of other feedstocks that were palmitic acid, stearic acid and cooking oil were evaluated too.

$$Acid\ value\ of\ oleic\ acid\left(\frac{mg\ KOH}{g}\right) = \frac{(V-B)\times M\times MW_{KOH}}{W}\times\frac{1000\ mg}{1\ g} \quad (3.1)$$

where

V = Volume of KOH solution used (L)

B = Volume of KOH solution used in blank titration (L)

M = Molarity of KOH solution= 0.1 M

MW_{KOH} = Molecular weight of KOH= 56.11 g/gmol

W = Weight of oleic acid= 1 g

3.5 Catalyst Characterisation and Screening

Numerous characterisation techniques were carried out on all the developed solid acid catalysts before and after sulfonation. The purpose of doing so is to study the effect of synthesis parameter on the chemical and physical characteristics of the catalysts. This can be done by using high performance analytical instruments such as Scanning Electron Microscope equipped with Energy-Dispersive X-ray (SEM-EDX), Fourier Transform Infrared Spectroscopy (FTIR) and X-ray Diffractometer (XRD). Conventional titration method was also used to determine the acid density of the catalyst.

3.5.1 Scanning Electron Microscopy Equipped with Energy Dispersive X-ray (SEM-EDX)

SEM-EDX was utilised to obtain information about surface morphology of the synthesised solid acid catalysts. In order to carry out analysis using SEM, the test sample must be conductive. This could be done by using a sputter-coater machine to cover a thin layer of palladium or gold on the surface of the catalyst. Catalyst was observed under the magnifications of 700X and 1000X with SEM-EDX which was operated at an accelerating voltage of 15 kV. The acquired images were used to evaluate the pore diameter of the catalysts via manual measurement. The actual pore size could be calculated by referring to the scale of each micrograph. Since SEM was

furnished with EDX, the elemental and chemical information of the developed catalysts were also generated. The attachment of certain elements on the catalysts surface such as sulfur and their corresponding composition were also known.

3.5.2 X-ray Diffractometer (XRD)

XRD was applied to locate the precise arrangements of atoms in a crystal structure and to identify the crystalline phase present and composition of the synthesised catalysts. X-rays were generated in a cathode ray tube and filtered to produce monochromatic radiation. Sample was finely ground and pressed on a steel plate to ensure a uniform, homogenise and smooth surface. During the analytical test, the sample was oriented and scanned from 10 ° to 80 ° with a scanning speed of 2 °/min in order to obtain a diffractogram which was presented as a function of intensity in terms of the angle 2 theta/theta.

3.5.3 Fourier Transform Infrared Spectroscopy (FTIR)

FTIR was used to study the chemisorption of functional groups anchored on the catalysts. It was a qualitative analysis used to validate the presence of the sulfonic groups, $-SO_3H$. An infrared radiation with wavenumber ranging from 400 to 4000 cm^{-1} was passed through a sample which is placed atop of the diamond crystal. The sample was maintained at fixed position with the aid of the pressure tower and compression tip. Energy of radiation was absorbed by the sample molecules to vibrate and rotate. However, only radiation of a specific wavelength could be absorbed by the samples molecules to vibrate at specific frequencies due to their distinct molecular structure. These frequencies could be associated with particular bond types. The results were presented in transmittance spectra. An infrared background data from cleaned diamond crystal was collected every time before conducting FTIR scanning for catalyst samples.

3.5.4 Acid Density

Back titration technique could be used to determine the acid density of the synthesised solid acid catalyst. 0.1 g of catalyst was mixed with 60 mL of 0.01 M sodium hydroxide, NaOH aqueous solution. The mixture was agitated uniformly at room temperature and 300 rpm for 30 minutes by using magnetic stirrer. After filtration, the filtrate was titrated with 0.01 M hydrochloric acid, HCl in the presence of phenolphthalein. The

titration process stopped when the solution changes from pink to colourless. The chemical reaction between sodium hydroxide and hydrochloric acid is described by Equation 3.2. It is known from the stoichiometry ratio that 1 mol of sodium hydroxide reacted with 1 mol of hydrochloric acid. The volume of hydrochloric acid added was used to evaluate the acid density of the catalyst as shown in Equations 3.3, 3.4 and 3.5.

$$NaOH + HCl \rightarrow NaCl + H_2O \tag{3.2}$$

$$\begin{aligned} &Mole\ of\ HCl \\ &= Volume\ of\ HCl\ added\ (mL) \times 0.01 \frac{mol}{L} \times \frac{1\ L}{1000\ mL} \end{aligned} \tag{3.3}$$

$$Mole\ of\ NaOH\ neutralised\ by\ HCl = \ Mole\ of\ HCl$$

$$\begin{aligned} &Mole\ of\ NaOH\ neutralised\ by\ acid\ sites\ on\ catalyst \\ &= Initial\ mole\ of\ NaOH - Mole\ of\ NaOH\ neutralised\ by\ HCl \end{aligned} \tag{3.4}$$

$$\begin{aligned} &Acid\ density\ \left(\frac{mmol\ NaOH}{g}\right) \\ &= \frac{Mole\ of\ NaOH\ neutralised\ by\ acid\ sites\ on\ catalyst}{0.1} \\ &\quad \times \frac{1000\ mmol}{1\ mol} \end{aligned} \tag{3.5}$$

3.6 Biodiesel Characterisation

Biodiesel produced via interesterification between oleic acid and methyl acetate in the presence of synthesised catalyst was analysed using gas chromatography (GC) to determine the resulting yield. Titration was also performed to obtain conversion via determination of the products' acid values.

3.6.1 Gas Chromatography (GC)

Samples of the interesterification product were withdrawn for GC analysis. Product samples were diluted with n-hexane according to a specific dilution factor. A constant

amount of methyl heptadecanoate was also added as an internal standard. After appropriate dilution and preparation, 1 µL of test sample was injected into GC and instantly vaporised.

Helium gas acted as a carrier gas to bring the samples to flow along the fused silica capillary column (30 m x 0.53 mm x 0.5µm). Table 3.5 depicts the setting of the GC for quantitative analysis of biodiesel content in the product. Separation of the sample mixture into its constituent components was due to different travelling speeds and retention times. GC was equipped with a flame ionisation detector (FID) which sensed the individual components while recorder analysed the results, producing a chromatogram. Peaks of the spectrum related to the amount of biodiesel present in the sample.

Table 3.5: Gas Chromatography Specifications for Biodiesel Samples

Specifications	**Set Value**
Injector temperature (℃)	200
Detector temperature (℃)	220
Carrier gas flowrate (mL/min)	3
Oven initial temperature (℃)	110
Oven maximum temperature (℃)	220
Heating rate (℃/min)	10

Since external standard was employed as the analysis method to determine the biodiesel yield, a standard methyl oleate calibration curve, that was a plot of peak area ratio against concentration of methyl oleate, needed to be generated beforehand. In this case, methyl oleate was diluted with n-hexane before conducting the GC analysis. Various dilution factors were used to generate test samples at different concentrations. A line equation that was obtained from the calibration curve was used to estimate the biodiesel concentration in the product. The concentration data could be used to calculate the respective biodiesel yield as shown in Equation 3.6.

$$Yield(\%) = \frac{\frac{Concentration\ of\ methyl\ oleate\ \left(\frac{g}{L}\right)}{Dilution\ factor} \times Volume(L)}{10\ mL\ oleic\ acid \times Density\ of\ oleic\ acid\ \left(\frac{g}{mL}\right)} \times 100\% \quad (3.6)$$

3.6.2 Acid Value

Acid value determination method that was discussed in Section 3.4 was applied for product analysis. The analyte was replaced by product obtained from interesterification reaction. Titration result gave the final acid value after the reaction. Conversion of the reaction can be calculated based on the initial and final acid values as shown in Equation 3.7.

$$Acid\ Value\ Conversion\ (\%) = \frac{a^i - a^f}{a^i} \times 100\% \quad (3.7)$$

where

$a^i = initial\ acid\ value\ of\ oleic\ acid\ (\frac{mg\ KOH}{g})$

$a^f = final\ acid\ value\ of\ product\ (\frac{mg\ KOH}{g})$

CHAPTER 4

RESULTS AND DISCUSSION

4.1 Catalyst Characterisation

Since the catalysts used in this study were sulfonated with different concentrations of sulfuric acid as sulfonating agent, characterisation of catalyst was conducted to study their differences in chemical and physical aspects. This was done by utilising four types of analytical instruments, namely Scanning Electron Microscope equipped with Energy Dispersive X-ray (SEM-EDX), X-ray Diffractometer (XRD) and Fourier Transform Infrared Spectroscopy (FTIR). The catalytic performance of different types of catalyst on biodiesel production were investigated too. Biodiesel production was carried out through interesterification at 60 ℃ with methyl acetate to oleic acid molar ratio of 50, 12 wt.% catalyst loading and stirring speed of 600 rpm for a period of 8 h.

4.1.1 Scanning Electron Microscope (SEM)

SEM was used to study the topography, surface morphology and structural properties of untreated and pretreated waste banana peels, WBPAC and synthesised catalysts at the magnification of 700X and 1000X non-destructively. Figure 4.1 shows the SEM images of the waste banana peels, chemically activated banana peels, WBPAC and the synthesised catalyst Cat-13. Cat-13 was chosen as the representative among all the synthesised catalysts to compare with samples at different stages of synthesising procedures because it was the best performed catalyst in interesterification reaction.

It can be seen that a naturally smooth and irregular morphology was observed in waste banana peel. Less cracks and crevices were available for the acidic site to anchor. After undergoing chemical treatment of activation, modification in structure and textural properties were revealed. More cracks and defects with rough texture surface were noticed. This proves that activation process helps in porosity development which in turn largely affects the surface area (Prachpreecha, Pipatpanyanugoon and Sawangwong, 2016).

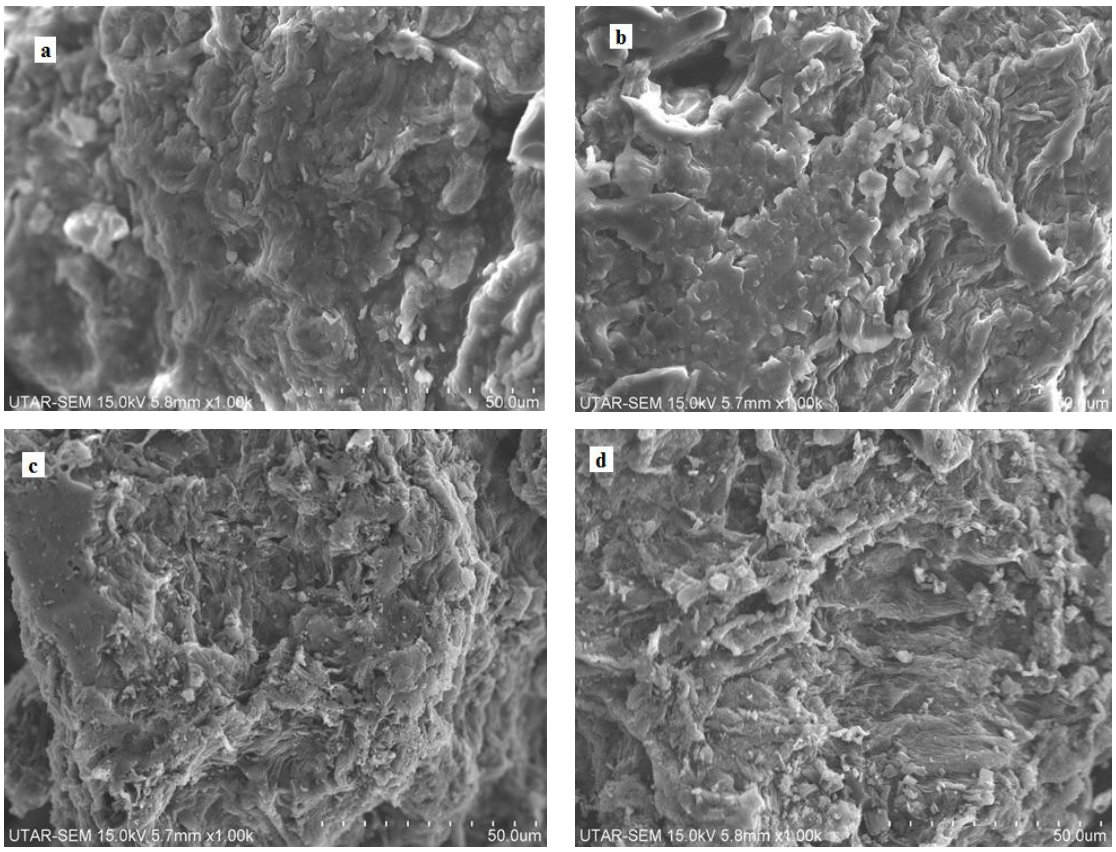

Figure 4.1: SEM Images of Waste Banana Peels, Chemically Activated Banana Peels, WBPAC and Synthesised Catalyst Cat-13 at the Magnification of 1000X, (a) Waste Banana Peels, (b) Chemically Activated Banana Peels, (c) WBPAC and (d) Cat-13

Surface roughness was increased in a large extent where uneven and unorganised surfaces, small particles and pores were visible after carbonisation, thus making WBPAC a promising catalyst support. According to Viena, Elvitriana and Wardani (2018), high temperature of thermal activation resulted in hollower pores on the carbon due to release of some volatile compounds. The pore size of WBPAC was estimated to be around 3 μm from the microscopy image. These small perforations present increase the specific surface area and act as a site for the attachment of sulfonic groups. However, the surface morphology had not much difference between before and after sulfonation process.

Besides, Figure 4.2 illustrates the SEM images of various catalysts at different concentration of sulfonating agent. As the catalyst were prepared using higher concentration of sulfuric acid, the surfaces became rougher and the porosity were increased. Mao, et al. (2018) claimed that usage of high concentration of sulfuric acid in sulfonation process will result in better carbon frame structures. Less pores were

observed on the surface of Cat-2 compared to Cat-13. Surfaces of Cat-2 and Cat-3 were smoother than others. On the other hand, Cat-13 was high in porosity with numerous black holes on the surface. There was no noticeable change on the surface morphology between Cat-8 and Cat-13.

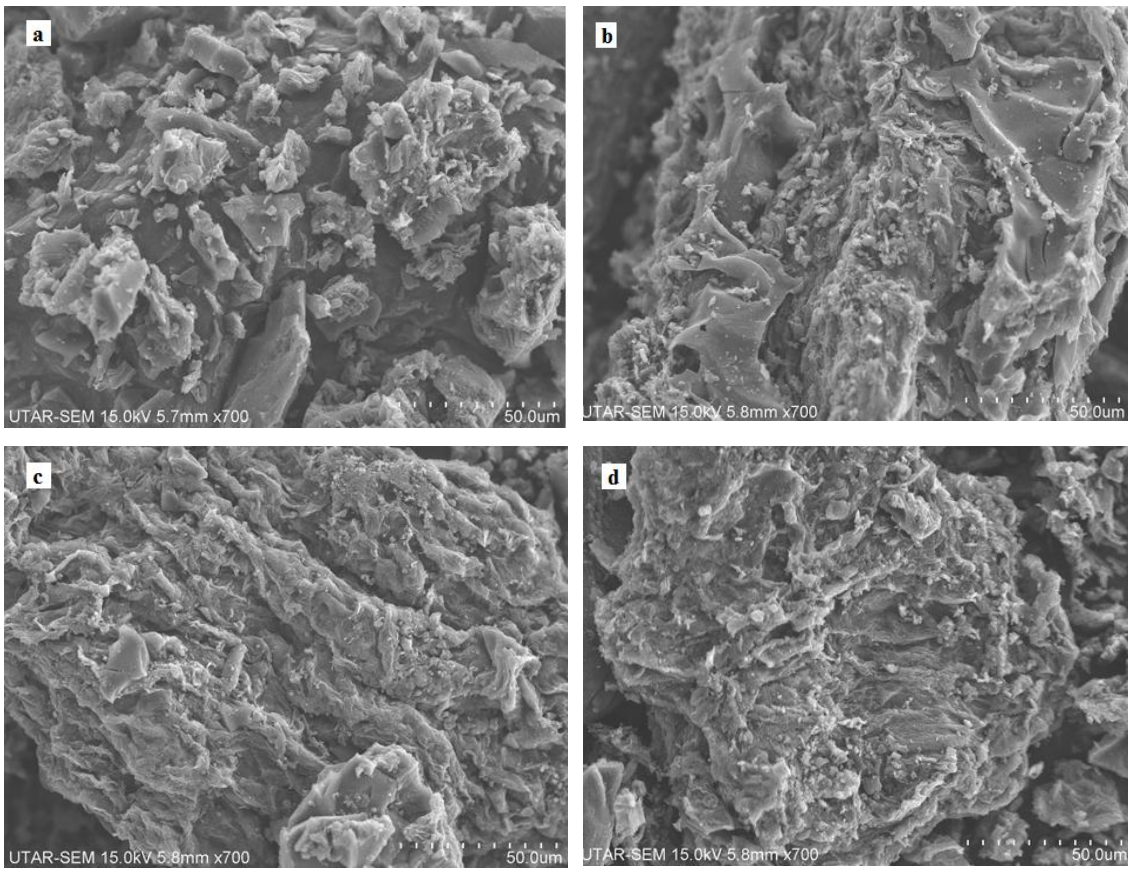

Figure 4.2: SEM Images of Synthesised Catalysts at the Magnification of 700X, (a) Cat-2, (b) Cat-3, (c) Cat-8 and (d) Cat-13

4.1.2 Energy Dispersive X-ray Spectrometer (EDX)

EDX is a surface characterisation technique that reveals the identity of the chemical elements present at the surface. In the analytical test, data were collected at four different spots for each sample to obtain an average and more accurate information. Atomic percentage is preferred over weight percentage in result presentation because the former only depends on the number of atom whereas the latter is influenced by the atomic mass of the element itself. In other words, if an element has a large value of atomic mass, this contributes to a larger weight percentage. The detailed elemental compositions of carbon, C, oxygen, O, silicon, Si, phosphorus, P, sulfur, S and indium,

In in atomic percentage for untreated and pretreated waste banana peels, WBPAC and synthesised catalysts are summarised in Table 4.1.

Table 4.1: Surface Elemental Composition in Atomic Percentage

Sample	Elemental Composition (at.%)					
	C	**O**	**Si**	**P**	**S**	**In**
Waste banana peels	57.27	37.91	0.62	0.39	0.24	3.57
Chemically activated banana peels	67.85	30.50	0.31	0.99	0.26	0.09
WBPAC	82.17	13.91	1.35	2.33	0.09	0.15
Cat-2	88.05	9.35	0.91	1.02	0.63	0.04
Cat-3	86.14	10.67	1.39	0.97	0.78	0.05
Cat-8	84.96	11.43	0.84	1.39	1.28	0.10
Cat-13	81.13	16.11	0.67	0.59	1.39	0.11

Waste banana peels mainly consist of carbon and oxygen, supplementing by minor elements such as silicon, phosphorus, sulfur and indium. The carbon content must surpass others since it is the building block of life. The atomic percentage of the carbon increased from 57.27 % to 82.17 % as it transformed from waste banana peels to activated carbon. However, the atomic percentage of carbon did not vary much after the sulfonation process. On the other hand, the significant oxygen content is contributed by the rich sources of carbohydrates and fibres in the samples (Palma, et al., 2010).

The elemental compositions of silicon and phosphorus fluctuated below 2.50 at.%. Leaching of silicon from the ceramic crucible might be the factor that causes the atomic fraction of silicon to increase after thermal activation. Moreover, phosphorus content increased from 0.39 to 0.99 at.%. This is because phosphoric acid was used to

pretreat the waste banana peels and the increment might due to the retainment of phosphoric acid resulting from insufficient washing. The presence of high atomic percentage of indium in the waste banana peels might originate from the agricultural soil. Ladenberger, et al. (2015) reported that the indium had a median value of 0.0176 mg/kg in agricultural soil. Nonetheless, indium had been successfully reduced through the chemical treatment of phosphoric acid, washing and carbonisation.

Sulfur is the chief active element responsible for the catalytic activities of the synthesised catalysts and it can be assumed that all sulfur atoms were present as sulfonic acid sites on the catalyst surface (Ngaosuwan, Goodwin and Prasertdham, 2016). Activated carbon prior to sulfonation had negligible sulfur content that was 0.09 at.% but this was increased noticeably after sulfonation, indicating successful attachment of active sites on the catalyst support. As depicted in Figure 4.3, as the concentration of sulfonating agent increased, the sulfur content of the resulting catalyst increased too with the highest sulfur content in Cat-13. This was attributed to that higher sulfuric acid concentration could stimulate more H_2SO_4 molecules to form a connection with carbon layer, giving more sulfonic group attachment and yielding higher acid capacity. Large specific surface area with mesopores in activated carbon further increased the accessibility of sulfuric acid to the catalyst support. As a result, Cat-13 gave the highest biodiesel yield when it was implemented in the interesterification reaction. Figure 4.4 depicts the EDX analysis spectrum at one of the spot of Cat-13. A complete EDX analysis report for all the samples tested are attached in Appendix B.

Nevertheless, carbon, oxygen, silicon, phosphorus and indium contents of the catalysts were inconsistent. Some elements exist both on the surface and inside the pore. EDX works only for surface elemental analysis and does not represent the bulk composition. Hence, those element inside the pore may not be discovered completely by using EDX.

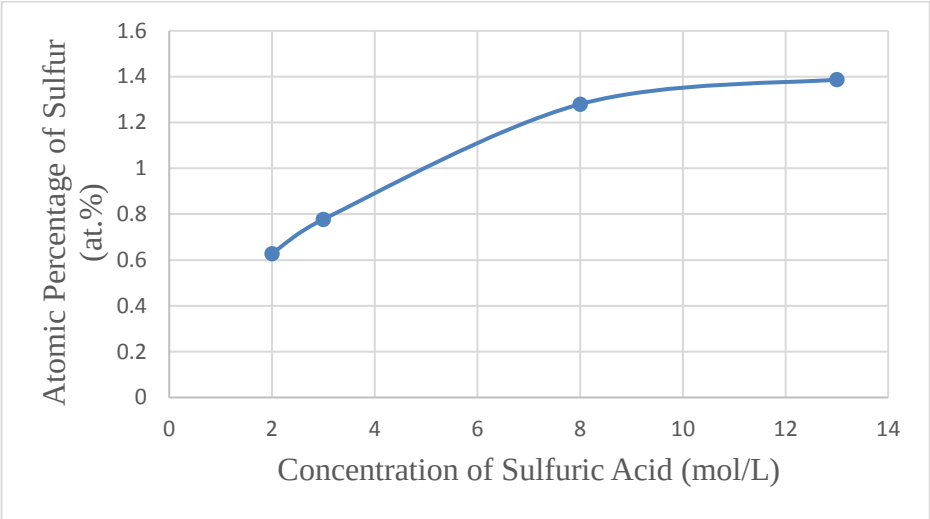

Figure 4.3: Sulfur Content of Synthesised Catalysts

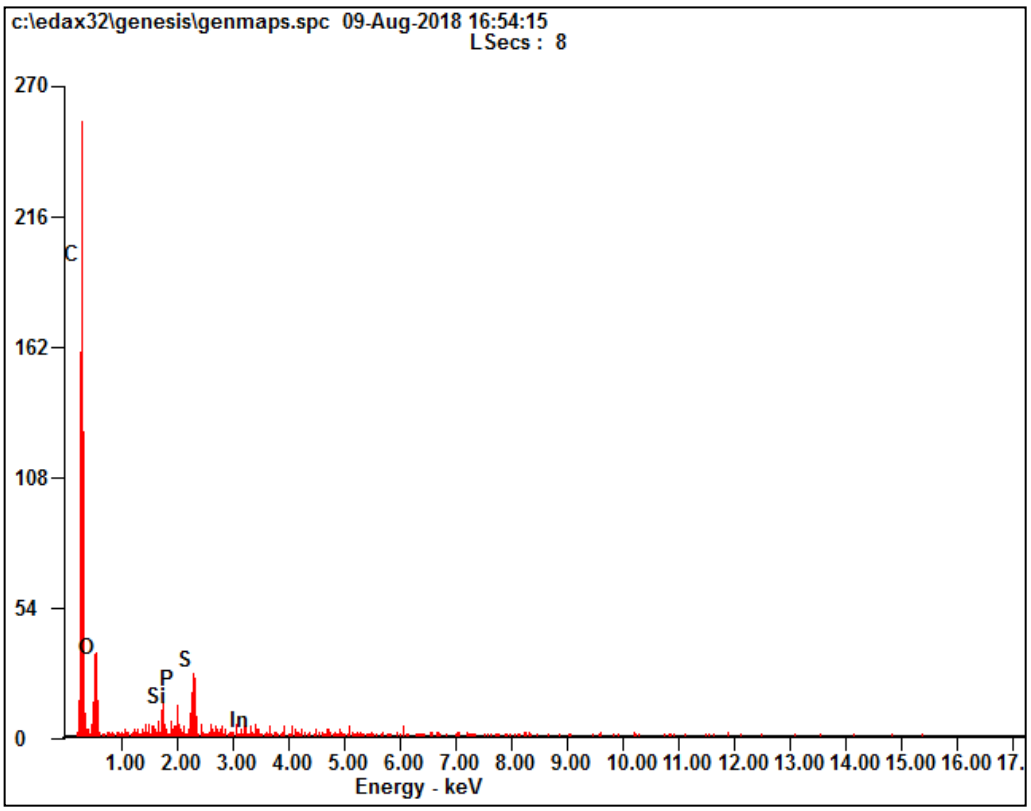

Figure 4.4: EDX Analysis Spectrum of Cat-13

4.1.3 X-ray Diffractometer (XRD)

XRD is an analytical technique used to identify the composition, crystalline phase and crystallite size from the constructive interference of monochromatic X-rays and a crystalline sample. Only a solid with crystalline structure can diffract the beams of X-ray. This is due to the fact that unlike amorphous materials, the atoms of crystalline

structure are arranged in a periodic array. The XRD patterns of the untreated and pretreated waste banana peels, WBPAC and Cat-13 are shown in Figure 4.5. It can be seen that all the samples tested were semicrystalline since only a few crystalline phases were detected. Chellappan, et al. (2018a) claimed that the broad diffraction peak at 2Θ ranging from 20 ° to 30 ° in each sample corresponded to C (0 0 2). This was induced by the presence of amorphous carbon structure which consisted of randomly oriented aromatic carbon sheets. However, this broad peak became narrower from waste banana peels to Cat-13 due to the formation of stable carbonaceous material that is ordered graphitic structure in the fabricated catalyst.

The XRD patterns of the activated banana peels and WBPAC were not the same, indicating that there is a change of crystal structure during thermal treatment. The XRD pattern of Cat-13 was almost identical to that one of the WBPAC which means the direct sulfonation method has negligible impact on the mirostructure of the carbon materials. Nevertheless, the intensity of diffraction peak C (0 0 2) decreased, suggesting the attachment of sulfonic group on the surface of the catalyst support which leads to increment in the degree of randomness among the carbon sheets (Chellappan, et al., 2018a).

Figure 4.6 depicts the XRD diffraction peaks of catalysts that were synthesised under different sulfonating conditions. Similar peaks were found at 2Θ of around 38.5°, 44.7 °, 65 ° and 78.2 ° which correspond to Al (1 1 1), (2 0 0), (2 2 0) and (3 1 1) (Hu, et al., 2018). These peaks were contributed by the sample holder which is made out of aluminium. On the other hand, Zhao, et al. (2018) emphasised that the main characteristics reflection of sulfur crystal happens at 2Θ of 23.16° which corresponds to S (2 2 2). However, it is difficult to observe any information regarding sulfur from the diffraction peak pattern since S (2 2 2) overlaps with C (0 0 2). Contrarily, intensities of diffraction peak at 2Θ of 23.16° for the synthesised catalysts are tabulated in Table 4.2. As the concentration of the sulfonating agent increased, the diffraction peak intensified, signifying that more sulfur phase was present.

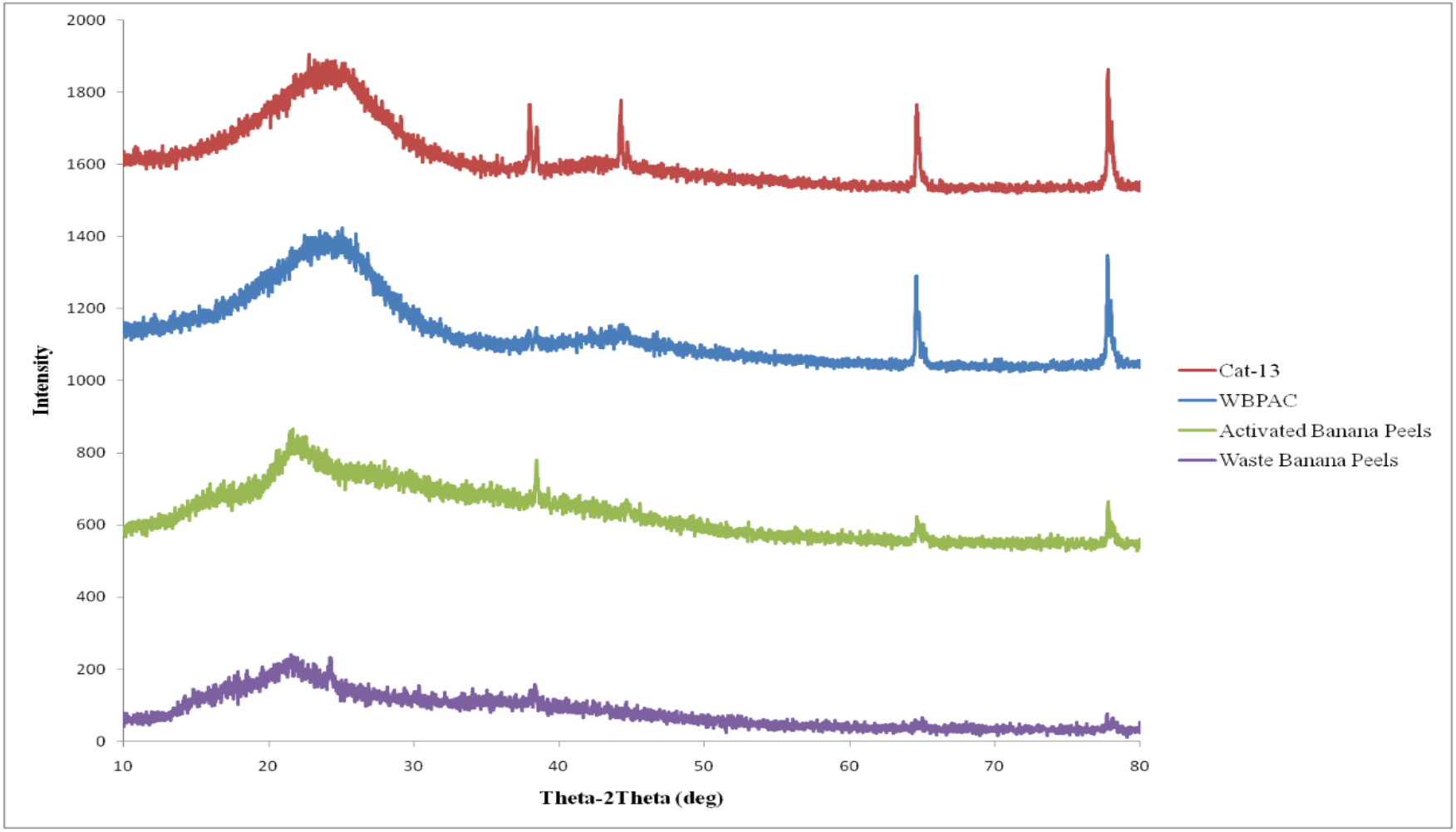

Figure 4.5: XRD Patterns of Waste Banana Peels, Chemically Activated Banana Peels, WBPAC and Synthesised Catalyst Cat-13

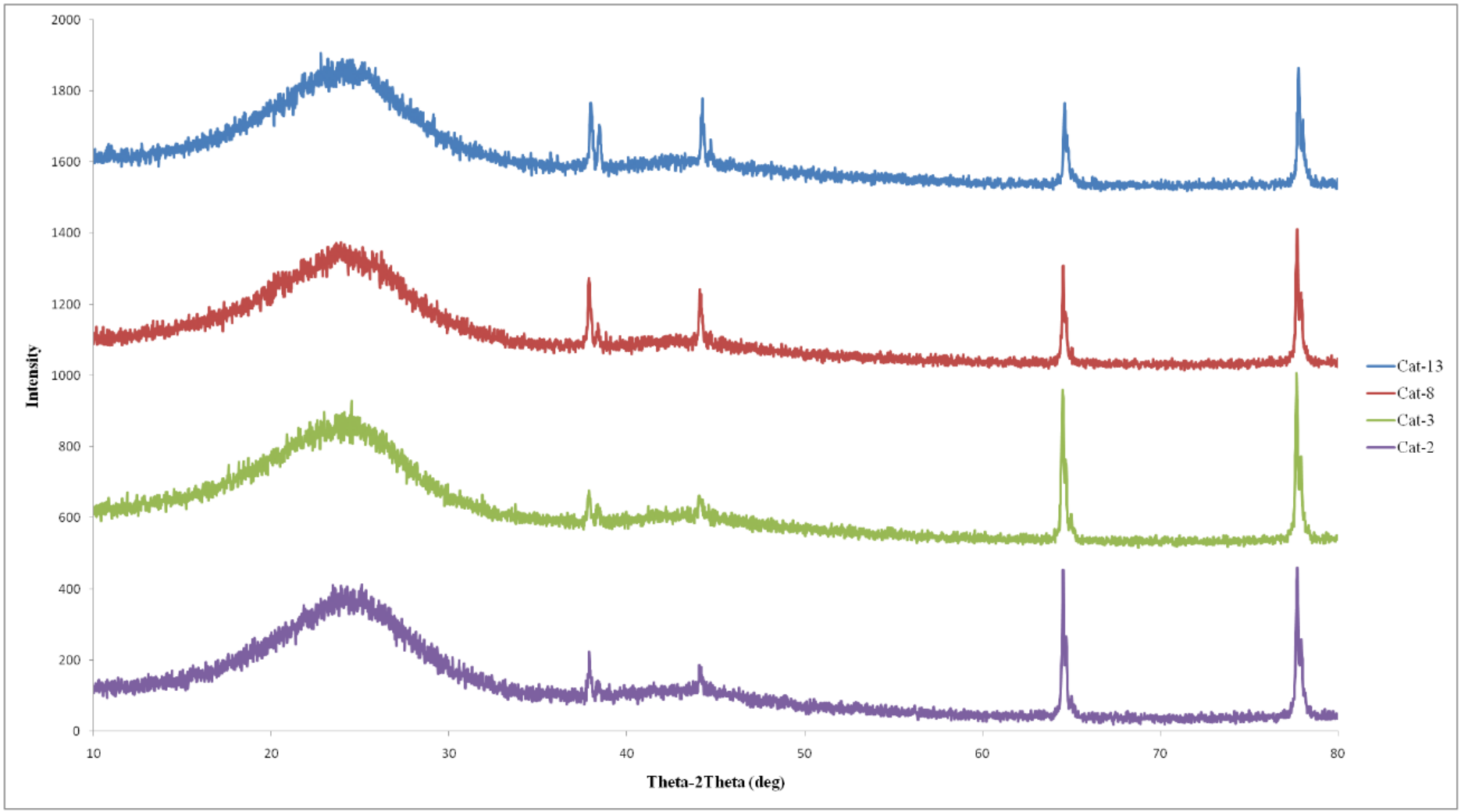

Figure 4.6: XRD Patterns of Synthesised Catalysts

Table 4.2: Data of Diffraction Peaks at 2Θ of 23.16°

Sample	Intensity
Cat-2	336
Cat-3	354
Cat-8	360
Cat-13	390

4.1.4 Fourier Transform Infrared Spectroscopy (FTIR)

FTIR analysis was performed with the wavenumber range of 400 to 4000 cm^{-1} to identify the functional group present on the surface of the catalysts. This is a critical analytical test to verify the presence of the acidic group which is the active site in catalysing the interesterification reaction and leading to biodiesel production. According to Chellappan, et al. (2018a), a solid acid catalyst must possess hydroxyl, -OH, carboxylic acid, -COOH and sulfonic acid, $-SO_3H$ functional groups for it to be efficient. Table 4.3 lists out the common stretching vibrations in catalysts and their corresponding frequencies.

Table 4.3: Infrared Stretching Frequencies (Thushari and Babel, 2018; Coates, 2006; Niu, et al., 2018)

Vibration	Frequency Range (cm^{-1})
O-H stretch	2800-3600
C=O stretch	1500-1800
C=C stretch	1600
O=S=O stretch	1100-1200
$-SO_3H$ stretch	1296
C-S stretch	670-715

As shown in Figure 4.7, well defined discrepancies were detected from the comparison of WBPAC and the synthesised solid acid catalyst Cat-13, revealing the effect of direct sulfonation method on the catalyst support. A deep band ranging from 1100 to 1200 cm^{-1} appeared in the FTIR spectrum of Cat-13, indicating the stretching vibration of O=S=O in symmetrical and asymmetrical forms. Bands at around 1296 cm^{-1} and 670 to 715 cm^{-1} demonstrated the existence of sulfonic group and its

successful incorporation onto the carbon matrix of WBPAC. Since concentrated sulfuric acid was used as the sulfonating agent, aliphatic groups of CH_2 or CH_3 can be oxidised to carboxylic acid groups, enhancing the total acid density of the fabricated catalysts (Sandouqa, Al-Hamamre and Asfar, 2018). This was supported by the presence of vibration bands around 1500 to 1800 cm^{-1} which signified the C=O stretching of the carbonyl or carboxylic acid functional groups at the surface of the solid acid catalyst. However, catalyst support was suspected to have carbonyl or carboxylic region prior to sulfonation since the relevant peak was also present in the FTIR spectrum of WBPAC. The stretching mode of conjugated C=C bond at 1600 cm^{-1} was attributable to the aromatic ring formed as a result of incomplete carbonisation of carbonaceous materials. Therefore, a more rigid carbon material was formed. The stretching vibration of hydroxyl group was not obvious in both samples but its presence would enhance the catalytic performance of the synthesised catalysts (Shuit and Tan, 2014).

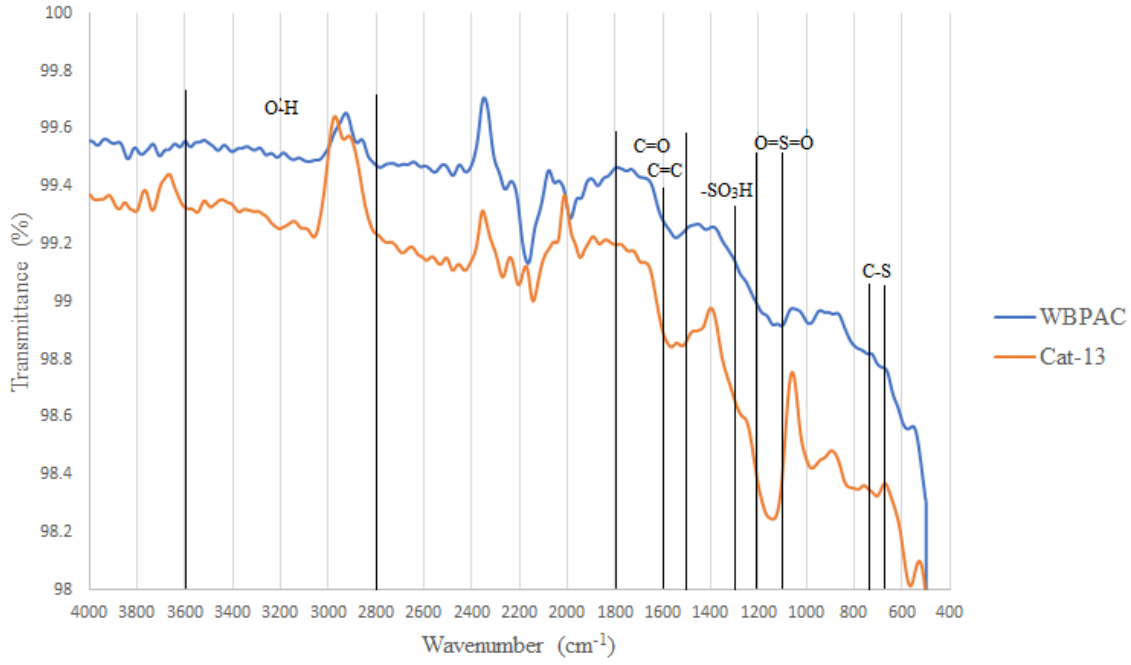

Figure 4.7: Comparison of FTIR Spectra of WBPAC and Cat-13

FTIR spectra of various synthesised solid acid catalysts were compared in Figure 4.8 and analysis was done to notify any variation. The observed transmittance peaks at 1296 cm^{-1}, 1100 to 1200 cm^{-1} and 670 to 715 cm^{-1} were attributed to the O=S=O stretching, $-SO_3H$ stretching and C-S stretching, respectively. This proved that

the active sites were well established on the surface of the sulfonated solid acid catalysts. Sulfonic acid group was the most prominent functional group since the O=S=O and -SO_3H stretching peaks were more significant compared to others. The weak and broad peak at wavenumber ranging from 2800 to 3600 cm^{-1} was assigned to the stretching mode of O-H in the alcoholic or phenolic group in the samples. All the catalysts produced showed a clear characteristic peak of incompletely carbonised materials at band of 1600 cm^{-1}. A more defined EDX spectrum for each sample is attached in Appendix C.

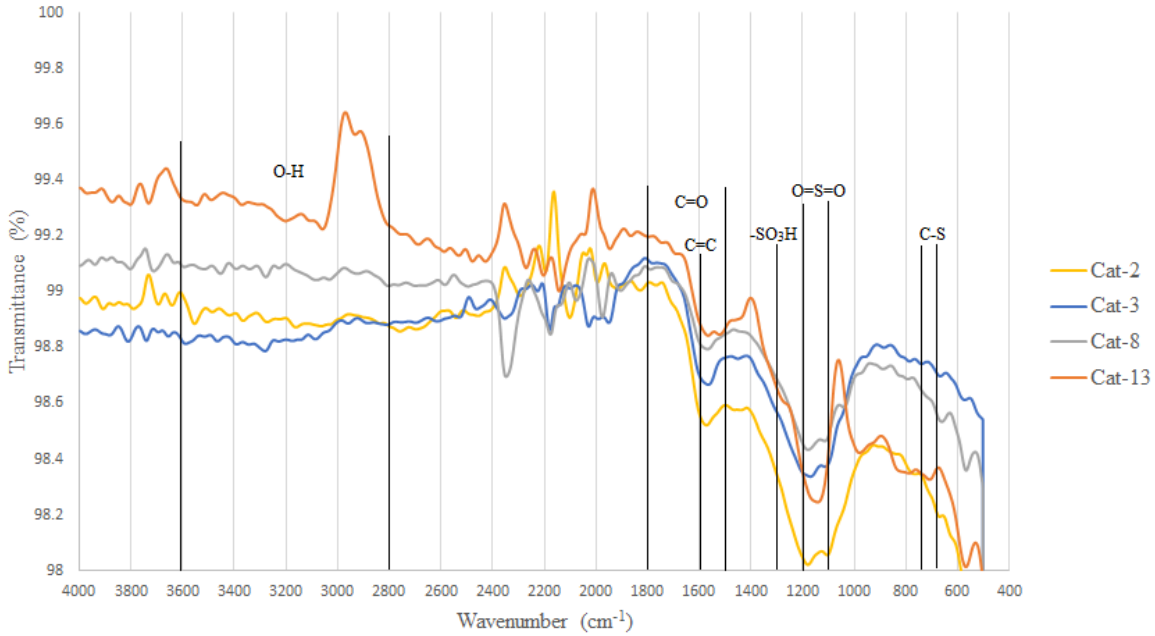

Figure 4.8: Comparison of FTIR Spectra of All Catalysts

4.1.5 Total Acid Density

Back titration was conducted to evaluate the total acid density of catalyst that contributed mainly by the sulfonic acid group and enhanced by the weak hydroxyl or phenolic and carboxylic acid groups (Abdullah, et al., 2017). The total acid densities of all catalysts produced under different concentrations of sulfuric acid are tabulated in Table 4.4 whereas the corresponding trend is clearly depicted in Figure 4.9. All fabricated catalysts showed excellent acidic site concentration. Chellappan, et al. (2018a) stated that strong hydrogen bonding to sulfonic groups caused mutual electron-withdrawal which subsequently resulted in high acid density. The total acid density of the synthesised catalyst increased with the concentration of sulfonating

agent used. As the concentration of sulfuric acid increased, higher sulfur content will allow more acidic site to anchor on the catalyst support and thus resulting in higher distribution of acidity (Abdullah, et al., 2017).

Table 4.4: Total Acid Density of Synthesised Catalysts at Different Concentrations of Sulfonating Agent

Catalyst Sample	Concentration of Sulfuric Acid (mol/L)	Total Acid Density (mmol NaOH/g)
Cat-2	2	0.70
Cat-3	3	0.87
Cat-8	8	1.02
Cat-13	13	1.74

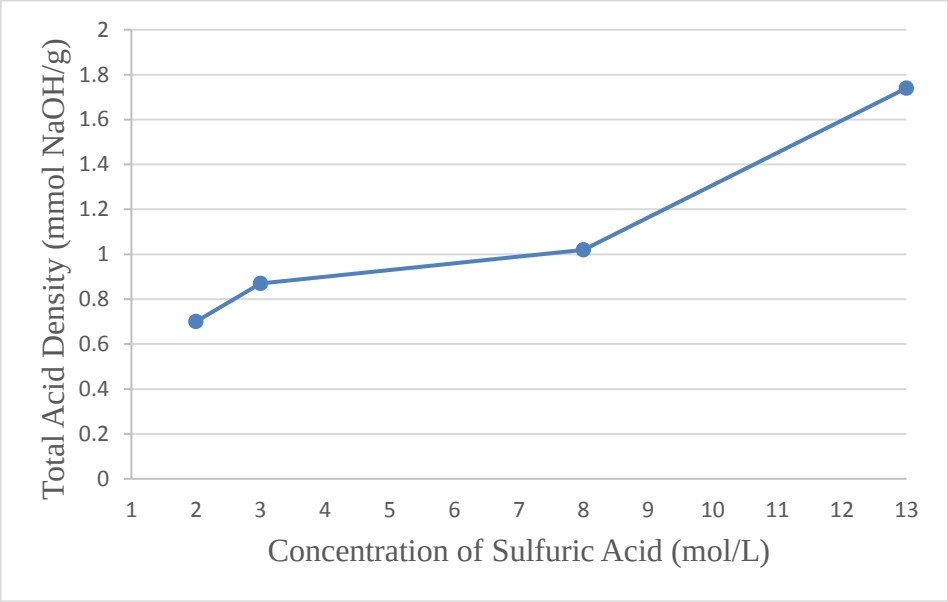

Figure 4.9: Total Acid Density of Synthesised Catalysts at Different Concentrations of Sulfonating Agent

Cat-13 that was sulfonated using the highest concentration of sulfuric acid possessed the strongest acidity of 1.74 mmol/g. This result was supported by the preceding EDX analysis whereby the highest sulfur content was determined in Cat-13. This is also supported by the microstructure of Cat-13 since it was rougher as compared to others, having larger specific surface area. Hence, more surface acidic sites were exposed directly to the sodium hydroxide solution. Chellappan, et al. (2018b)

also applied direct sulfonation method with concentrated sulfuric acid and obtained a comparable total acid density of 1.71 mmol/g for the wood sawdust biochar based catalyst. However, for Cat-2, the total acid density was only 0.70 mmol NaOH/g because the loaded sulfonic acid groups were insufficient, resulting in low catalytic efficiency.

4.2 Feedstock Characterisation: Acid Value

Oleic acid was the main feedstock that reacted with methyl acetate in the presence of synthesised catalysts to produce methyl oleate as the desired product of biodiesel and triacetin as the by-product. In addition to oleic acid, other feedstocks such as palmitic acid, stearic acid and cooking oil were also used to produce biodiesel in the presence of concentrated sulfuric acid as homogeneous catalyst. This was to compare the effectiveness of interesterification reaction with that of conventional transesterification in producing biodiesel.

The acid values of all the feedstocks involved were determined using conventional titration method involving potassium hydroxide solution and all the relevant results are tabulated in Table 4.5. Since the purchased stearic and palmitic acids are in pellet forms, they were subjected to melting prior to titration. Nevertheless, the acid number of stearic acid could not be detected since solid was formed during the titration process. The solid nature of the stearic acid is contributed by the presence of long chain saturated fatty acids and thus it is only slightly soluble in the form of potassium salts (Kanicky and Shah, 2002). In addition, the melting points of fatty acids such as palmitic and stearic acids lie within the range of 30 to 65 ℃ but the titration process carried out at room temperature. Contrarily, as compared to palmitic acid, stearic acid has higher melting point and is easier to solidify due to its longer carbon chain (Mondal, 2011). However, an acid value range for stearic acid is obtained from a report in 2016 by The United States Pharmacopeial Convention. All the detected acid values will be used in the Sections 4.3.2, 4.4 and 4.5 to calculate the acid value conversion in interesterification reaction.

Table 4.5: Acid Values of Feedstocks

Sample	Volume of KOH used (ml)	Acid Value (mg KOH/g)
Oleic Acid	42.7	239.59
Palmitic Acid	44.6	241.83
Stearic Acid	-	194-212
Cooking Oil	0.2	1.12

4.3 Biodiesel Characterisation

In this study, all the synthesised catalysts were employed in the interesterification reaction at 60 ℃ for 8 h with 12 wt.% catalyst loading and methyl acetate to oleic acid molar ratio of 50:1 to yield methyl oleate. The interesterification reaction conditions were remained unchanged for all the experimental run to study the efficiency and effectiveness of the catalysts used. The methyl oleate yield as well as the acid value conversion will be used as indicators to discover the catalyst that exhibits the best catalytic activity. The optimum sulfonation condition that produces the best performed catalyst will be identified too. An illustration of the product of interesterification reaction is shown in Appendix A.

4.3.1 Gas Chromatography (GC)

GC was used to verify the presence of methyl oleate and its area under the chromatogram can be used to evaluate the resulting biodiesel yield. Figure 4.10 depicts a standard calibration curve with ratio of methyl oleate area to internal standard area (MO/IS) against the concentration of methyl oleate. The line equation shown can be used to determine the corresponding methyl oleate concentration in product. Retention time of methyl oleate is about 15 min and the product of the interesterification reaction was assumed to consist of methyl oleate only, neglecting the presence of by-product. Figure 4.11 shows a chromatogram including methyl oleate produced in the interesterification reaction.

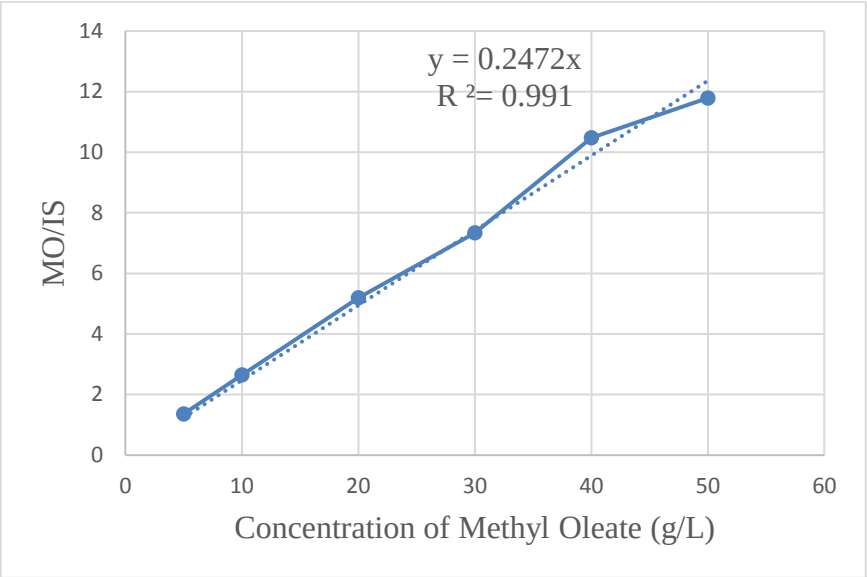

Figure 4.10: Methyl Oleate Standard Calibration Curve

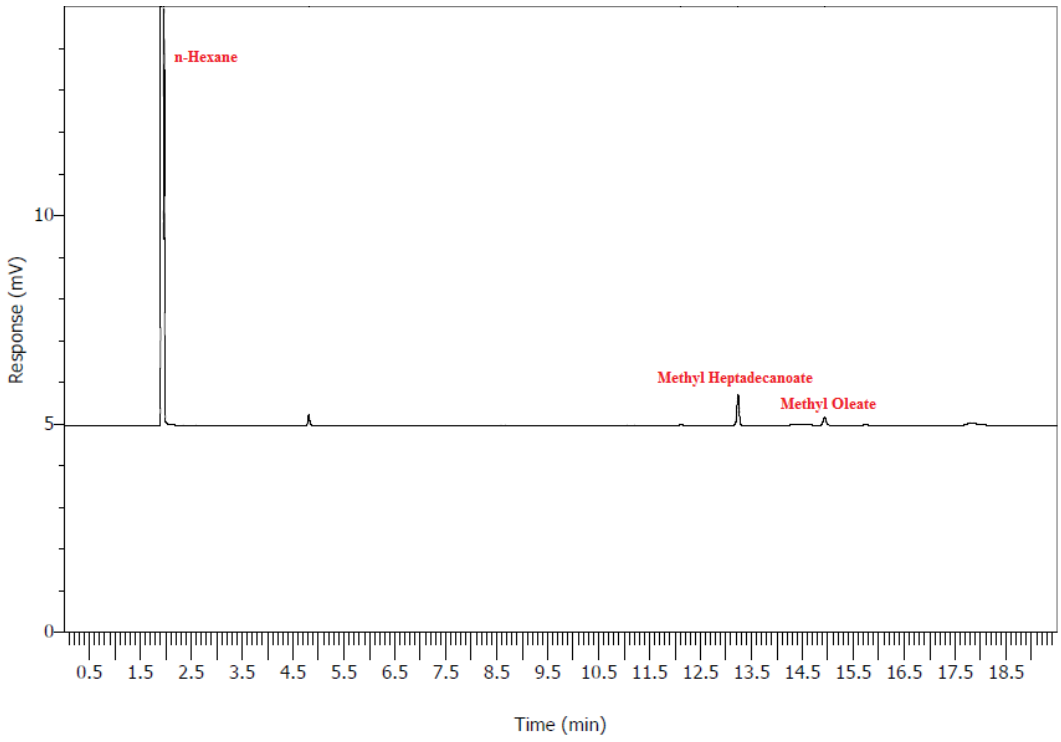

Figure 4.11: Chromatogram of Interesterification of Oleic Acid with Methyl Acetate

Table 4.6 shows the concentrations of methyl oleate produced using different synthesised catalysts and the respective calculated yield. Looking into the pattern of Figure 4.12, as the concentration of sulfuric acid increased, the biodiesel yield increased. This shows a similar trend to that of the sulfur content and acid density of the synthesised catalysts. Cat-13 which underwent sulfonation using 13 mol/L sulfuric

acid gave the highest yield of 43.81 %. The results of gas chromatography analysis are conformed to the observation of microstructure from SEM analysis which showed that Cat-13 had high specific surface area with mesopores. Other than that, it also possessed the highest sulfur content and acidity from the outcomes of EDX analysis and acid density test, respectively. Catalyst that is sulfonated under more concentrated sulfonating agent will have more sulfonic acid groups attached on its surface giving it to have higher total acid density and subsequently offer better catalytic activity. All these evidences explain the combined effect of high acid density and large surface area of Cat-13 in producing the highest methyl oleate yield. The gas chromatography reports for all catalysts are attached in Appendix D as reference.

Table 4.6: Methyl Oleate Yield with Different Catalysts Used

Catalyst	Methyl Oleate Concentration (g/L)	Yield (%)
Cat-2	0	0
Cat-3	0.96	1.89
Cat-8	4.68	11.17
Cat-13	18.90	43.81

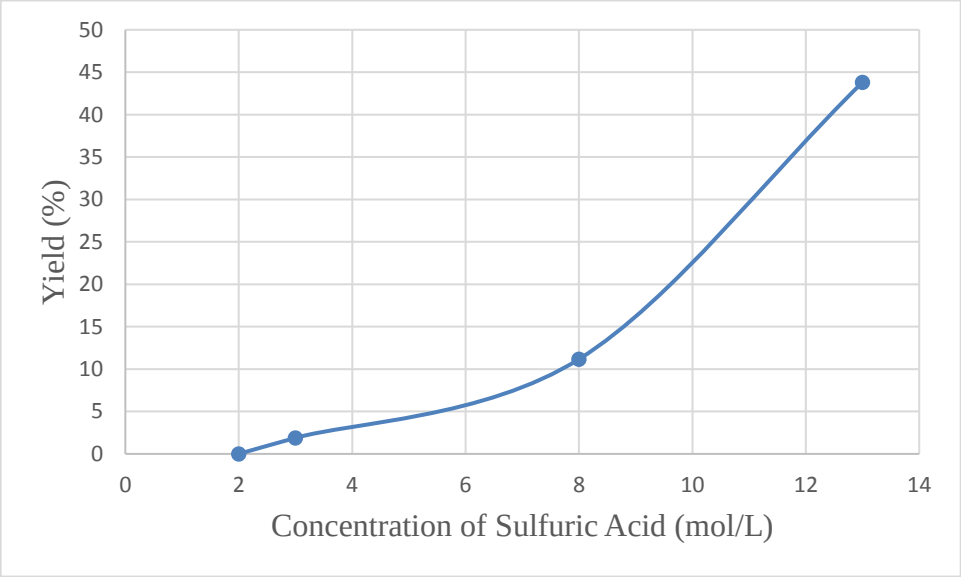

Figure 4.12: Effect of Concentration of Sulfonating Agent on the Methyl Oleate Yield

One repetitive interesterification reaction was conducted using catalysts sulfonated with concentrated sulfuric acid and produced negative result. This is because concentrated sulfuric acid has high viscosity and cause adverse effect by limiting the dispersion of WBPAC in the sulfonating agent. The motion of WBPAC might be constrained and resulting in the formation of lump as well as decreasing the total specific surface area that can be exposed for the attachment of sulfonic acid groups. Other than that, concentrated sulfuric acid may oversaturate the surface of catalyst support with sulfonic acid groups and render it to become highly negatively charged. Therefore, lone-pair electron of the oleic acid carbonyl group is hard to reach the hydroxyl group of the sulfonic acidic site (Shuit, Ng and Tan, 2015).

The overall yield was not satisfied due to the fact that the acid density might probably attributable to weak acid groups such as hydroxyl or phenolic and carboxylic groups which had poor catalytic performance in the interesterification reaction. Wu, et al. (2014) reported a biodiesel yield of 98.5 % using magnetic solid acid catalyst of $S_2O_8^{2-}/ZrO_2$-TiO_2-Fe_3O_4 that was prepared via sulfonation with ammonium persulfate. Interesterification was carried out at 50 ℃ for 10.8 h with 21.3 wt.% of catalyst loading and methyl acetate to seed ratio of 13.8 mL/g. This result obtained was much higher as compared to this study which was using biomass derived solid acid catalyst. The difference maybe contributed by different sulfonating agent and conditions of interesterification reaction.

Interesterification reaction using Cat-13 was repeated by adding in 5 wt.% concentrated sulfuric acid as auxiliary homogeneous catalyst, giving a comparable yield of 42.74 %. This showed that the concentrated sulfuric acid did not improve the overall biodiesel yield. Another experimental run was conducted by using 5 wt.% concentrated sulfuric acid and WBPAC in the absence of any synthesised catalyst. In this case, WBPAC acted as a medium for the interesterification reaction to take place. A higher yield of 56.38 % was obtained which challenged the effectiveness of the fabricated catalysts. All these investigations were performed to find the most efficient and affordable reaction pathway for biodiesel production from acidic oil.

4.3.2 Acid Value Conversion

At the end of the interesterification reaction, excess methyl acetate was removed by evaporation and the remaining product was tested to determine the final acidity. Table 4.7 enumerates the final acid value of the products whereas Figure 4.13 depicts the calculated acid value conversions. All synthesised catalysts brought about acid value reduction from an initial acid number of 239.59 mg KOH/g, excluding Cat-2. As the concentration of sulfonating agent increased, the final acid value of the reaction mixture decreased in a larger extent. For instance, Cat-3 successfully reduced the acid value of the reaction mixture from 239.59 to 230.61 mg KOH/g whereas the acid value dropped to 189.09 mg KOH/g for Cat-8 which was sulfonated using higher concentration of sulfuric acid.

In the case of Cat-2, yield obtained from GC analysis is zero which means that the acid value should remain constant throughout the reaction. Leaching of acidic active site into the reaction mixture was probably happened and contributed to the increment in acid value. Talha and Sulaiman (2016) claimed that heterogeneous acid catalyst had an intrinsic drawback that is leaching of catalyst active sites to contaminate the product. To eliminate the problem of leaching, catalysts can be fabricated in larger molecular size (Emrani and Shahbazi, 2012). Acid value for interesterified oleic acid in the presence of Cat-13 was 40.40 mg KOH/g which corresponded to a conversion of 83.14 %. This proves that the interesterification reaction was performed well and oleic acid was successfully converted into products. The results of acid value conversion are accord with the those yields determined by using GC.

Table 4.7: Acid Values of Biodiesel Products

Catalyst	Volume of KOH used (ml)	Acid Value (mg KOH/g)	Acid Value Conversion (%)
Cat-2	45.8	256.42	-
Cat-3	41.1	230.61	3.75
Cat-8	33.7	189.09	21.08
Cat-13	7.2	40.40	83.14

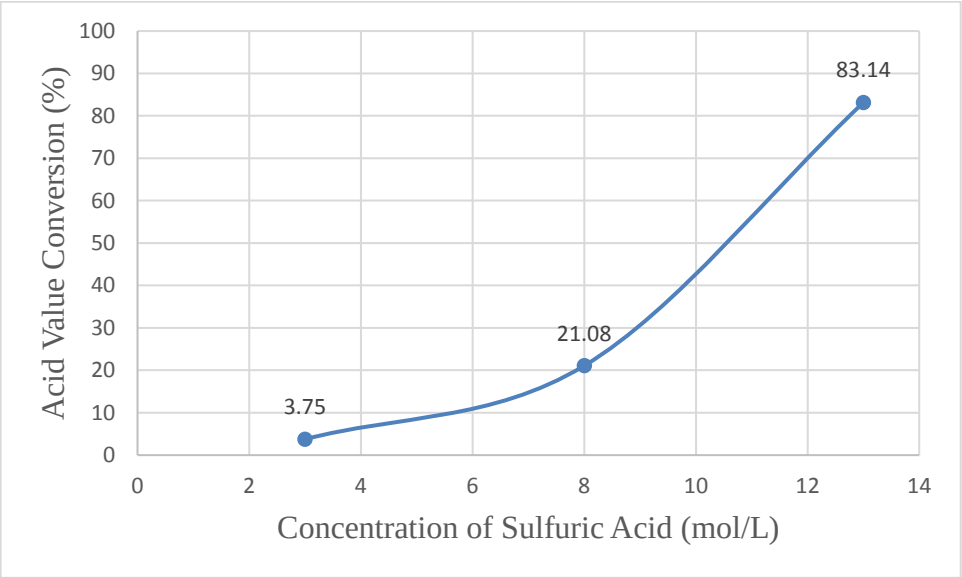

Figure 4.13: Effect of Concentration of Sulfonating Agent on the Acid Value Conversion

4.4 Comparison with Conventional Transesterification Method

The synthesised catalysts did not achieve outstanding yield in the biodiesel production as interesterification reaction involving methyl acetate is more preferable to be carried out under non-catalytic supercritical reaction conditions (Marx, 2016). To verify the effectiveness of the synthesised catalysts, Cat-13 which attained the highest yield of 43.81 % was applied in the conventional transesterification reaction.

Transesterification reaction was carried out by using methanol instead of methyl acetate under the same molar ratio of reactants, catalysts loading, temperature, stirring rate and reaction time. A methyl oleate yield of 72.66 % accompanied by an acid value conversion of 87.82 % was obtained. The resulting methyl oleate yield was much higher than that obtained from using methyl acetate. This proved that the fabricated catalysts had promising catalytic activity in producing biodiesel. Furthermore, in comparison with interesterification utilising methyl acetate, transesterification with methanol was more readily to take place. Tian, et al. (2018) stated that interesterification between triglycerides and methyl acetate had slower kinetics, influencing the energy consumption throughout the process. Casas, Ramos and Pérez (2011a) reported the same theory that is transesterification reaction between triglycerides and methanol took place at a faster rate than the interesterification reaction involving methyl acetate. Conversion of DAG to triacetin is the rate-limiting

step in interesterification. Therefore, rate of interesterification reaction is low, resulting in unsatisfied biodiesel yield.

4.5 Interesterification with Different Types of Feedstocks

Due to the reason that the synthesised catalysts could not give a favourable biodiesel yield, interesterification was repeated using pure concentrated sulfuric acid as homogeneous catalyst with other reaction conditions remained. 5 wt.% of concentrated sulfuric acid was used to replace the biomass derived solid acid catalysts (Fernandes, et al., 2014). Additional experimental runs were conducted by utilising other kinds of feedstock such as palmitic acid, stearic acid and cooking oil instead of oleic acid. At the end of the reaction, separating funnel was used to separate the spent concentrated sulfuric acid from the desired product. The respective outcomes were tabulated in Table 4.8.

Table 4.8: Biodiesel Yields and Acid Values of Different Feedstocks

Sample	Yield (%)	Initial Acid Value (mg KOH/g)	Final Acid Value (mg KOH/g)
Oleic Acid	67.17	239.59	56.11
Palmitic Acid	0.08	241.83	54.99
Stearic Acid	0.06	194-212	-
Cooking Oil	28.23	1.12	132.42

As referring to the previous data of the best performed catalyst, Cat-13, the biodiesel yield of oleic acid increased a lot from 43.81 to 67.17 % by applying pure concentrated sulfuric acid. High acid value conversion of 76.58 % was also obtained, corresponding to the final acidity of 56.11 mg KOH/g. Other feedstocks showed comparatively lower yields. For instance, palmitic and stearic acids produced yields of 0.08 and 0.06 %, respectively. Due to the high melting point of palmitic acid, accumulation might occur during the progress of reaction and caused heterogeneity between palmitic acid and other reactants (Wu, et al., 2017). This mass transfer limitation leaded to low biodiesel production. The situation was even worse for the case of stearic acid since it has higher melting point as compared to palmitic acid. The

final acid value in the interesterification with stearic acid could not be detected due to formation of solid.

Cooking oil consists of a mixture of four types of fatty acids, namely oleic acid, palmitic acid, stearic acid and linoleic acid. Thus, the product formed not only composed of methyl oleate but with methyl palmitate, methyl stearate and methyl linoleate. It resulted in higher yield as compared to palmitic and stearic acids but still lower than that of oleic acid. However, the increment of acid value after the reaction was due to the contamination of product by the spent concentrated sulfuric acid.

CHAPTER 5

CONCLUSIONS AND RECOMMENDATIONS

5.1 Conclusions

The present work focused on synthesising solid acid catalyst from biomass waste of banana peels for glycerol-free biodiesel production. Several characterisation techniques such as SEM-EDX, XRD and FTIR were carried out on the synthesised catalysts. SEM micrographs showed that the catalysts produced had rough and porous surface. EDX analysis showed an increasing trend of sulfur content with the concentration of the sulfonating agent used. On the other hand, based on the results of FTIR analysis, the presence of sulfonic acid group vibration band proved its successful attachment on the catalyst support. It was identified that an increase in the concentration of sulfuric acid favoured the formation of high specific surface area, acid densities and sulfur content in the synthesised solid acid catalyst. The catalyst produced by biochar sulfonated with 13 M sulfuric acid exhibited the highest total acid density and sulfur content of 1.74 mmol NaOH/g and 1.39 at.%, respectively.

The synthesised catalysts were then used to catalyse the interesterification of oleic acid with operating conditions as methyl acetate to oleic acid molar ratio of 50:1 and catalyst loading of 12 wt.%. The main finding of this work showed an improvement in reaction yields using a catalyst synthesised under more concentrated sulfonating agent. This novel approach of biomass derived solid acid catalyst catalysed interesterification demonstrated a biodiesel yield of 43.81 % and reduction of the acid value from 239.59 to 40.40 mg KOH/g for the best performed catalyst which is Cat-13. The superiority of the synthesised catalyst was established with an increase of biodiesel yield to 72.66 % in the case of conventional transesterification. This indicated the potential of waste banana peel as a promising biomass waste to synthesise catalyst.

In addition, the current work established the effects of feedstock on the biodiesel production with the aid of concentrated sulfuric acid as homogeneous catalyst. Other typical fatty acids such as palmitic acid and stearic acid as well as cooking oil were tested. For the case of oleic acid, the biodiesel yield obtained using concentrated sulfuric acid was higher than that of the synthesised catalyst as

homogeneous catalyst did not have the problem of mass transfer limitation. The collected results indicated the potential for interesterification to produce methyl oleate and triacetin while eliminating the production of glycerol. It also proved that methyl as an efficient acyl acceptor.

Overall, all the planned objectives were fulfilled. The presented results were very important as they emphasised on one of the cheaper synthesis route of catalyst which considerably useful in biodiesel production. It can be concluded that the low cost of biomass waste derived solid acid catalyst compared to alternative catalyst such as enzymes or non-catalytic supercritical reaction conditions, combined with promising biodiesel yield assures further exploration into this scheme.

5.2 Recommendations for Future Work

Experimental work was conducted according to the scope of study but aberration occurred in the results caused consumption of time to perform more repetition of laboratory work, restricting the exploration of the study. The discrepancies in the results might due to differences in every batch of samples collected or catalyst produced. Several improvements can be made in the future related research work in order to ameliorate the precision, consistency and reliability of the experimental data. Various recommendations related to the study are listed in the following.

i. Mass production of sample that is demanded for the experimental procedure is more preferable to be done in one batch. This is to eliminate the deviation of sample properties found in different batches of production.
ii. The equipment used such as hot plate and magnetic stirrer in every step of the procedures must be consistent to maintain the uniformity of the experimental environment.
iii. Beside concentration of sulfuric acid, more parameter studies on the synthesis of catalyst such as sulfonation time and temperature as well as carbonisation duration and temperature can be conducted. Other than that, parameter studies on the interesterification such as methyl acetate to oleic acid molar ratio, reaction temperature and time can also be performed to find the optimum operating conditions for higher yield.

iv. Each parameter study must be carried out with more set of experimental runs so that the set values tested do not lie too far from each other.

v. Once the catalysts have been produced, they must be employed in the characterisation analysis and reaction as soon as possible to avoid degradation, oxidation or contamination to happen.

vi. Biodiesel product obtained must be analysed quickly to avoid any possible degradation or contamination.

vii. It is advisable to improve the catalyst specific surface area which has significant effect on catalytic activity. Different activating agents can be investigated. Low density biomass can be tested since it offers high porosity and surface area.

viii. Since the carbonisation process was done in the presence of air, oxidation of sulfuric acid might occur which rendered to blockage of pore and reduction in porosity and surface area of the catalyst support. Carbonisation in inert gas such as nitrogen is advisable to be carried out.

ix. Further literature review on the exact mechanism of interesterification reaction may find out ways to improve the biodiesel yield.

x. Since oleic acid gave a good biodiesel yield, other low cost feedstocks from biomass or waste which are rich in oleic acid are proposed to be used in the interesterification reaction.

REFERENCES

Abdullah, S., Hanapi, N., Azid, A., Umar, R., Juahir, H., Khatoon, H. and Endut, A., 2017. A review of biomass-derived heterogeneous catalyst for a sustainable biodiesel production. *Renewable and Sustainable Energy Reviews*, 70, pp.1040-1051.

Adewale, P., Dumont, M. and Ngadi, M., 2015. Enzyme-catalyzed synthesis and kinetics of ultrasonic-assisted biodiesel production from waste tallow. *Ultrasonics Sonochemistry*, 27, pp.1-9.

Aguilar-Garnica, E., Paredes-Casillas, M., Herrera-Larrasilla, T., Rodr ǵuez-Palomera, F. and Ram ŕez-Arreola, D., 2013. Analysis of recycled poly (styrene-co-butadiene) sulfonation: a new approach in solid catalysts for biodiesel production. *SpringerPlus*, 2(1), p.475.

Andrade, T., Errico, M. and Christensen, K., 2017. Influence of the reaction conditions on the enzyme catalyzed transesterification of castor oil: A possible step in biodiesel production. *Bioresource Technology*, 243, pp.366-374.

Ang, G., Tan, K. and Lee, K., 2014. Recent development and economic analysis of glycerol-free processes via supercritical fluid transesterification for biodiesel production. *Renewable and Sustainable Energy Reviews*, 31, pp.61-70.

Ashton Acton, Q., 2013. *Lanthanoid Series Elements—Advances in Research and Application: 2013 Edition*.

Asikainen, M., Munter, T. and Linnekoski, J., 2015. Conversion of polar and non-polar algae oil lipids to fatty acid methyl esters with solid acid catalysts – A model compound study. *Bioresource Technology*, 191, pp.300-305.

Atabani, A., Silitonga, A., Ong, H., Mahlia, T., Masjuki, H., Badruddin, I. and Fayaz, H., 2013. Non-edible vegetable oils: a critical evaluation of oil extraction, fatty acid compositions, biodiesel production, characteristics, engine performance and emissions production. *Renewable and Sustainable Energy Reviews*, 18, pp. 211-245.

Atadashi, I., Aroua, M., Abdul Aziz, A. and Sulaiman, N., 2013. The effects of catalysts in biodiesel production: A review. *Journal of Industrial and Engineering Chemistry*, 19(1), pp.14-26.

Ayodele, O. and Dawodu, F., 2014. Production of biodiesel from Calophyllum inophyllum oil using a cellulose-derived catalyst. *Biomass and Bioenergy*, 70, pp.239-248.

Bharathiraja, B., Chakravarthy, M., Kumar, R., Yuvaraj, D., Jayamuthunagai, J., Kumar, R. and Palani, S., 2014. Biodiesel production using chemical and biological methods – A review of process, catalyst, acyl acceptor, source and process variables. *Renewable and Sustainable Energy Reviews*, 38, pp.368-382.

Boon-anuwat, N., Kiatkittipong, W., Aiouache, F. and Assabumrungrat, S., 2015. Process design of continuous biodiesel production by reactive distillation: Comparison between homogeneous and heterogeneous catalysts. *Chemical Engineering and Processing: Process Intensification*, 92, pp.33-44.

Bora, A., Dhawane, S., Anupam, K. and Halder, G., 2018. Biodiesel synthesis from Mesua ferrea oil using waste shell derived carbon catalyst. *Renewable Energy*, 121, pp.195-204.

BP., 2017. *BP statistical review of world energy*. 66th ed. [pdf] British: BP Plc. Available at: <https://www.bp.com/content/dam/bp/en/corporate/pdf/energy-economics/statistical-review-2017/bp-statistical-review-of-world-energy-2017-full-report.pdf> [Accessed 26 Feb. 2018].

Buasri, A., Rochanakit, K., Wongvitvichot, W., Masa-ard, U. and Loryuenyong, V, 2015. The application of calcium oxide and magnesium oxide from natural dolomitic rock for biodiesel synthesis. *Energy Procedia*, 79, pp.562-566.

Calero, J., Luna, D., Sancho, E., Luna, C., Bautista, F., Romero, A., Posadillo, A., Berbel, J. and Verdugo-Escamilla, C., 2015. An overview on glycerol-free processes for the production of renewable liquid biofuels, applicable in diesel engines. *Renewable and Sustainable Energy Reviews*, 42, pp.1437-1452.

Casas, A., Ramos, M. and Pérez, Á., 2011a. Kinetics of chemical interesterification of sunflower oil with methyl acetate for biodiesel and triacetin production. *Chemical Engineering Journal*, 171(3), pp.1324-1332.

Casas, A., Ramos, M. and Pérez, Á., 2011b. New trends in biodiesel production: Chemical interesterification of sunflower oil with methyl acetate. *Biomass and Bioenergy*, 35(5), pp.1702-1709.

Casas, A., Ramos, M. and Pérez, Á., 2013. Methanol-enhanced chemical interesterification of sunflower oil with methyl acetate. *Fuel*, 106, pp.869-872.

Chakraborty, R., Chatterjee, S., Mukhopadhyay, P. and Barman, S., 2016. Progresses in waste biomass derived catalyst for production of biodiesel and bioethanol: s review. *Procedia Environmental Sciences*, 35, pp. 546-554.

Chellappan, S., Nair, V., V, S. and K, A., 2018a. Experimental validation of biochar based green Bronsted acid catalysts for simultaneous esterification and transesterification in biodiesel production. *Bioresource Technology Reports*, 2, pp.38-44.

Chellappan, S., Nair, V., V., S. and K., A., 2018b. Synthesis, optimization and characterization of biochar based catalyst from sawdust for simultaneous esterification and transesterification. *Chinese Journal of Chemical Engineering*.

Chen, H. and Cui, Z., 2016. A microwave-sensitive solid acid catalyst prepared from sweet potato via a simple method. *Catalysts*, 6(12), p.211.

Chen, S., Lao-ubol, S., Mochizuki, T., Abe, Y., Toba, M. and Yoshimura, Y., 2014. Production of Jatropha biodiesel fuel over sulfonic acid-based solid acids. *Bioresource Technology*, 157, pp.346-350.

Chisti, Y., 2013. Constraints to commercialization of algal fuels. *Journal of Biotechnology*, 167(3), pp. 201-214.

Coates, J., 2006. Interpretation of Infrared Spectra, A Practical Approach. *Encyclopedia of Analytical Chemistry*.

Colombo, K., Ender, L. and Barros, A., 2017. The study of biodiesel production using CaO as a heterogeneous catalytic reaction. *Egyptian Journal of Petroleum*, 26(2), pp.341-349.

Correia, L., Saboya, R., de Sousa Campelo, N., Cecilia, J., Rodríguez-Castellón, E., Cavalcante, C. and Vieira, R., 2014. Characterization of calcium oxide catalysts from natural sources and their application in the transesterification of sunflower oil. *Bioresource Technology*, 151, pp.207-213.

Dawodu, F., Ayodele, O., Xin, J., Zhang, S. and Yan, D., 2014. Effective conversion of non-edible oil with high free fatty acid into biodiesel by sulphonated carbon catalyst. *Applied Energy*, 114, pp.819-826.

Domingues, C., Correia, M., Carvalho, R., Henriques, C., Bordado, J. and Dias, A., 2013. Vanadium phosphate catalysts for biodiesel production from acid industrial by-products. *Journal of Biotechnology*, 164(3), pp. 433-440.

Dong, T., Gao, D., Miao, C., Yu, X., Degan, C., Garcia-Pérez, M., Rasco, B., Sablani, S. and Chen, S., 2015. Two-step microalgal biodiesel production using acidic catalyst generated from pyrolysis-derived bio-char. *Energy Conversion and Management*, 105, pp.1389-1396.

Ee, T., Lim, S., Ling, P., Huei, W. and Chyuan, O., 2017. Synthesis of seaweed based carbon acid catalyst by thermal decomposition of ammonium sulfate for biodiesel production. *AIP Conference Proceedings*, 1828(1).

Efavi, J., Kanbogtah, D., Apalangya, V., Nyankson, E., Tiburu, E., Dodoo-Arhin, D., Onwona-Agyeman, B. and Yaya, A., 2018. The effect of NaOH catalyst concentration and extraction time on the yield and properties of Citrullus vulgaris seed oil as a potential biodiesel feed stock. *South African Journal of Chemical Engineering*.

Ehsan, M. and Chowdhury, M., 2015. Production of biodiesel using alkaline based catalysts from waste cooking oil: a case study. *Procedia Engineering*, 105, pp.638-645.

Eliezer, A., Ramón, P., Leonardo, G., Roger, S. and Sebastian, V., 2015. Emulsification of animal fats and vegetable oils for their use as a diesel engine fuel: An overview. *Renewable and Sustainable Energy Reviews*, 47, pp.623-633.

Emrani, J. and Shahbazi, A., 2012. A single bio-based catalyst for bio-fuel and bio-diesel. *Journal of Biotechnology & Biomaterials*, 02(01).

Endut, A., Abdullah, S., Hanapi, N., Hamid, S., Lananan, F., Kamarudin, M., Umar, R., Juahir, H. and Khatoon, H., 2017. Optimization of biodiesel production by solid acid catalyst derived from coconut shell via response surface methodology. *International Biodeterioration & Biodegradation*, 124, pp.250-257.

Energy Commission., n.d.. *Malaysia Energy Information Hub-statistics, MEIH*. [online] Available at: <http://meih.st.gov.my/statistics> [Accessed 26 Feb. 2018].

Energy Commission, 2016. *Malaysia energy statistics handbook 2016*. [online] Available at: <http://meih.st.gov.my/documents/10620/57af5e2a-7695-4618-a111-4ba0a49ba992> [Accessed 12 Apr. 2018].

Ezebor, F., Khairuddean, M., Abdullah, A. and Boey, P., 2014. Oil palm trunk and sugarcane bagasse derived solid acid catalysts for rapid esterification of fatty acids and moisture-assisted transesterification of oils under pseudo-infinite methanol. *Bioresource Technology*, 157, pp. 254-262.

Fadoni, M. and Lucarelli, L., n.d.. *Temperature programmed desorption, reduction, oxidation and flow chemisorption for the characterisation of heterogeneous catalysts. Theoretical aspects, instrumentation and applications*. [ebook] Available at: <https://pdfs.semanticscholar.org/7962/dd7e7b0db6eccf86260794663881712ed1fc.pdf> [Accessed 29 Mar. 2018].

Fernandes, P., Borges, L., Carvalho, C. and Souza, R., 2014. Microwave assisted biodiesel production from trap grease. *Journal of the Brazilian Chemical Society*.

Ghoreishi, S. and Moein, P., 2013. Biodiesel synthesis from waste vegetable oil via transesterification reaction in supercritical methanol. *The Journal of Supercritical Fluids*, 76, pp.24-31.

Guldhe, A., Singh, P., Ansari, F., Singh, B. and Bux, F., 2017. Biodiesel synthesis from microalgal lipids using tungstated zirconia as a heterogeneous acid catalyst and its comparison with homogeneous acid and enzyme catalysts. *Fuel*, 187, pp.180-188.

Hu, Z., Chen, F., Xu, J., Nian, Q., Lin, D., Chen, C., Zhu, X., Chen, Y. and Zhang, M., 2018. 3D printing graphene-aluminum nanocomposites. *Journal of Alloys and Compounds*, 746, pp.269-276.

Johari, A., Nyakuma, B., Mohd Nor, S., Mat, R., Hashim, H., Ahmad, A., Yamani Zakaria, Z. and Tuan Abdullah, T., 2015. The challenges and prospects of palm oil based biodiesel in Malaysia. *Energy*, 81, pp. 255-261.

Kang, S., Ye, J. and Chang, J., 2013. Recent advances in carbon-based sulfonated catalyst: preparation and application. *International Review of Chemical Engineering*, 5(2), pp.133-144.

Kanicky, J. and Shah, D., 2002. Effect of Degree, Type, and Position of Unsaturation on the pKa of Long-Chain Fatty Acids. *Journal of Colloid and Interface Science*, 256(1), pp.201-207.

Kim, B., Im, H. and Lee, J., 2015. In situ transesterification of highly wet microalgae using hydrochloric acid. *Bioresource Technology*, 185, pp.421-425.

Kirubakaran, M. and Arul Mozhi Selvan, V., 2018. A comprehensive review of low cost biodiesel production from waste chicken fat. *Renewable and Sustainable Energy Reviews*, 82, pp.390-401.

Konwar, L., Boro, J. and Deka, D., 2014. Review on latest developments in biodiesel production using carbon-based catalysts. *Renewable and Sustainable Energy Reviews*, 29, pp. 546-564.

Konwar, L., Das, R., Thakur, A., Salminen, E., Mäki-Arvela, P., Kumar, N., Mikkola, J. and Deka, D., 2014. Biodiesel production from acid oils using sulfonated carbon catalyst derived from oil-cake waste. *Journal of Molecular Catalysis A: Chemical*, 388-389, pp.167-176.

Korkut, I. and Bayramoglu, M., 2018. Selection of catalyst and reaction conditions for ultrasound assisted biodiesel production from canola oil. *Renewable Energy*, 116, pp.543-551.

Ladenberger, A., Demetriades, A., Reimann, C., Birke, M., Sadeghi, M., Uhlbäck, J., Andersson, M. and Jonsson, E., 2015. GEMAS: Indium in agricultural and grazing land soil of Europe — Its source and geochemical distribution patterns. *Journal of Geochemical Exploration*, 154, pp.61-80.

Lee, J., Jung, J., Oh, J., Sik Ok, Y. and Kwon, E., 2017. Establishing a green platform for biodiesel synthesis via strategic utilization of biochar and dimethyl carbonate. *Bioresource Technology*, 241, pp.1178-1181.

Leggieri, P., Senra, M. and Soh, L., 2018. Cloud point and crystallization in fatty acid ethyl ester biodiesel mixtures with and without additives. *Fuel*, 222, pp.243-249.

Li, M., Zheng, Y., Chen, Y. and Zhu, X., 2014. Biodiesel production from waste cooking oil using a heterogeneous catalyst from pyrolyzed rice husk. *Bioresource Technology*, 154, pp.345-348.

Liu, T., Li, Z., Li, W., Shi, C. and Wang, Y., 2013. Preparation and characterization of biomass carbon-based solid acid catalyst for the esterification of oleic acid with methanol. *Bioresource Technology*, 133, pp.618-621.

Maddikeri, G., Pandit, A. and Gogate, P., 2013. Ultrasound assisted interesterification of waste cooking oil and methyl acetate for biodiesel and triacetin production. *Fuel Processing Technology*, 116, pp.241-249.

Mao, D., Zhang, X., Zhang, X., Jia, M. and Yao, J., 2018. Glucose-derived solid acids and their stability enhancement for upgrading biodiesel via esterification. *Chinese Journal of Chemical Engineering*.

Mardhiah, H., Ong, H., Masjuki, H., Lim, S. and Pang, Y., 2017. Investigation of carbon-based solid acid catalyst from Jatropha curcas biomass in biodiesel production. *Energy Conversion and Management*, 144, pp.10-17.

Marx, S., 2016. Glycerol-free biodiesel production through transesterification: a review. *Fuel Processing Technology*, 151, pp.139-147.

Meher, L., Churamani, C., Arif, M., Ahmed, Z. and Naik, S., 2013. Jatropha curcas as a renewable source for bio-fuels—A review. *Renewable and Sustainable Energy Reviews*, 26, pp.397-407.

Meng, Y., Wang, B., Li, S., Tian, S. and Zhang, M., 2013. Effect of calcination temperature on the activity of solid Ca/Al composite oxide-based alkaline catalyst for biodiesel production. *Bioresource Technology*, 128, pp.305-309.

Micic, R., Tomić, M., Kiss, F., Martinovic, F., Simikić, M. and Molnar, T., 2016. Comparative analysis of single-step and two-step biodiesel production using supercritical methanol on laboratory-scale. *Energy Conversion and Management*, 124, pp.377-388.

Mohamed, S., Md., M. and Mazlan, A., 2016. Power generation sources in Malaysia: status and prospects for sustainable development. *Journal of Advanced Review on Scientific Research*, 25(1), pp.11-28.

Mondal, S., 2011. Thermo-regulating textiles with phase-change materials. *Functional Textiles for Improved Performance, Protection and Health*, pp.163-183.

Negm, N., Sayed, G., Habib, O., Yehia, F. and Mohamed, E., 2017. Heterogeneous catalytic transformation of vegetable oils into biodiesel in one-step reaction using super acidic sulfonated modified mica catalyst. *Journal of Molecular Liquids*, 237, pp.38-45.

Ngaosuwan, K., Goodwin, J. and Prasertdham, P., 2016. A green sulfonated carbon-based catalyst derived from coffee residue for esterification. *Renewable Energy*, 86, pp.262-269.

Niu, S., Ning, Y., Lu, C., Han, K., Yu, H. and Zhou, Y., 2018. Esterification of oleic acid to produce biodiesel catalyzed by sulfonated activated carbon from bamboo. *Energy Conversion and Management*, 163, pp.59-65.

Nomanbhay, S. and Ong, M., 2017. A review of microwave-assisted reactions for biodiesel production. *Bioengineering*, 4(2), p.57.

Nordblad, M., Silva, V., Nielsen, P. and Woodley, J., 2014. Identification of critical parameters in liquid enzyme-catalyzed biodiesel production. *Biotechnology and Bioengineering*, 111(12), pp.2446-2453.

Oh, T., Hasanuzzaman, M., Selvaraj, J., Teo, S. and Chua, S., 2018. Energy policy and alternative energy in Malaysia: issues and challenges for sustainable growth – an update. *Renewable and Sustainable Energy Reviews*, 81, pp. 3021-3031.

Onukwuli, D., Emembolu, L., Ude, C., Aliozo, S. and Menkiti, M., 2017. Optimization of biodiesel production from refined cotton seed oil and its characterization. *Egyptian Journal of Petroleum*, 26(1), pp.103-110.

Ortiz-Martínez, V., Salar-García, M., Palacios-Nereo, F., Olivares-Carrillo, P., Quesada-Medina, J., Ríos, A. and Hernández-Fernández, F., 2016. In-depth study of the transesterification reaction of Pongamia pinnata oil for biodiesel production using catalyst-free supercritical methanol process. *The Journal of Supercritical Fluids*, 113, pp.23-30.

Ouda, O., Raza, S., Nizami, A., Rehan, M., Al-Waked, R. and Korres, N., 2016. Waste to energy potential: a case study of Saudi Arabia. *Renewable and Sustainable Energy Reviews*, 61, pp. 328-340.

Palma, C., Contreras, E., Urra, J. and Martínez, M., 2010. Eco-friendly technologies based on banana peel use for the decolourization of the dyeing process wastewater. *Waste and Biomass Valorization*, 2(1), pp.77-86.

Pereira, C., Portilho, M., Henriques, C. and Zotin, F., 2014. $SnSO_4$ as catalyst for simultaneous transesterification and esterification of acid soybean oil. *Journal of the Brazilian Chemical Society*, 25(12), pp.2409-2416.

Pourzolfaghar, H., Abnisa, F., Daud, W. and Aroua, M., 2016. A review of the enzymatic hydroesterification process for biodiesel production. *Renewable and Sustainable Energy Reviews*, 61, pp.245-257.

Prachpreecha, O., Pipatpanyanugoon, K. and Sawangwong, P., 2016. A study of characterizations and efficiency of activated carbon prepared from peel and bunch of banana for methyl orange dye adsorption. *IOSR Journal of Environmental Science, Toxicology and Food Technology (IOSR-JESTFT)*, 10(4), pp.17-26.

Rajalingam, A., Jani, S., Senthil Kumar, A. and Adam Khan, M., 2016. Production methods of biodiesel. *Journal of Chemical and Pharmaceutical Research*, 8(3), pp.170-173.

Sakdasri, W., Sawangkeaw, R. and Ngamprasertsith, S., 2015. Continuous production of biofuel from refined and used palm olein oil with supercritical methanol at a low molar ratio. *Energy Conversion and Management*, 103, pp.934-942.

Sakdasri, W., Sawangkeaw, R. and Ngamprasertsith, S., 2018. Techno-economic analysis of biodiesel production from palm oil with supercritical methanol at a low molar ratio. *Energy*.

Salar-García, M., Ortiz-Martínez, V., Olivares-Carrillo, P., Quesada-Medina, J., de los Ríos, A. and Hernández-Fernández, F., 2016. Analysis of optimal conditions for biodiesel production from Jatropha oil in supercritical methanol: Quantification of thermal decomposition degree and analysis of FAMEs. *The Journal of Supercritical Fluids*, 112, pp.1-6.

Samniang, A., Tipachan, C. and Kajorncheappun-ngam, S., 2014. Comparison of biodiesel production from crude Jatropha oil and Krating oil by supercritical methanol transesterification. *Renewable Energy*, 68, pp.351-355.

Sánchez, B., Mendow, G., Levrand, P. and Querini, C., 2013. Optimization of biodiesel production process using sunflower oil and tetramethyl ammonium hydroxide as catalyst. *Fuel*, 113, pp.323-330.

Sandouqa, A., Al-Hamamre, Z. and Asfar, J., 2018. Preparation and performance investigation of a lignin-based solid acid catalyst manufactured from olive cake for biodiesel production. *Renewable Energy*, 132, pp.667-682.

Santos Ribeiro, J., Celante, D., Simões, S., Bassaco, M., Silva, C. and Castilhos, F., 2017. Efficiency of heterogeneous catalysts in interesterification reaction from macaw oil (Acrocomia aculeata) and methyl acetate. *Fuel*, 200, pp.499-505.

Shuit, S., Ng, E. and Tan, S., 2015. A facile and acid-free approach towards the preparation of sulphonated multi-walled carbon nanotubes as a strong protonic acid catalyst for biodiesel production. *Journal of the Taiwan Institute of Chemical Engineers*, 52, pp.100-108.

Shuit, S. and Tan, S., 2014. Feasibility study of various sulphonation methods for transforming carbon nanotubes into catalysts for the esterification of palm fatty acid distillate. *Energy Conversion and Management*, 88, pp.1283-1289.

Su, F., Peng, C., Li, G., Xu, L. and Yan, Y., 2016. Biodiesel production from woody oil catalyzed by Candida rugosa lipase in ionic liquid. *Renewable Energy*, 90, pp.329-335.

Sustere, Z., Murnieks, R. and Kampars, V., 2016. Chemical interesterification of rapeseed oil with methyl, ethyl, propyl and isopropyl acetates and fuel properties of obtained mixtures. *Fuel Processing Technology*, 149, pp.320-325.

Talha, N. and Sulaiman, S., 2016. Overview of catalysts in Biodiesel Production. *ARPN Journal of Engineering and Applied Sciences*, 11(1), pp.439-448.

Tamborini, L., Militello, M., Balach, J., Moyano, J., Barbero, C. and Acevedo, D., 2015. Application of sulfonated nanoporous carbons as acid catalysts for Fischer esterification reactions. *Arabian Journal of Chemistry*.

Tang, Z., Lim, S., Pang, Y., Wong, K. and Ong, H., 2017. Synthesis of seaweed based carbon acid catalyst by thermal decomposition of ammonium sulfate for biodiesel production.

The United States Pharmacopeial Convention, 2016. *Stearic acid*. Stage 6 Harmonization. [online] Available at: <https://www.uspnf.com/sites/default/files/usp_pdf/EN/USPNF/usp-nf-notices/m78200.pdf> [Accessed 22 Aug. 2018].

Thushari, I. and Babel, S., 2018. Sustainable utilization of waste palm oil and sulfonated carbon catalyst derived from coconut meal residue for biodiesel production. *Bioresource Technology*, 248, pp.199-203.

Tian, Y., Xiang, J., Verni, C. and Soh, L., 2018. Fatty acid methyl ester production via ferric sulfate catalyzed interesterification. *Biomass and Bioenergy*, 115, pp.82-87.

Tiwari, A., Rajesh, V. and Yadav, S., 2018. Biodiesel production in micro-reactors: A review. *Energy for Sustainable Development*, 43, pp.143-161.

Touhami, D., Zhu, Z., Balan, W., Janaun, J., Haywood, S. and Zein, S., 2017. Characterization of rice husk-based catalyst prepared via conventional and microwave carbonisation. *Journal of Environmental Chemical Engineering*, 5(3), pp.2388-2394.

United Nations, 2017. *World population 2017.* [pdf] Available at: <https://esa.un.org/unpd/wpp/Publications/Files/WPP2017_Wallchart.pdf> [Accessed 25 Feb. 2018].

U.S. Energy Information Administration, 2017. *International energy outlook 2017*. [pdf] Available at: <https://www.eia.gov/outlooks/ieo/pdf/0484(2017).pdf> [Accessed 26 Feb. 2018].

Viena, V., Elvitriana and Wardani, S., 2018. Application of banana peels waste as adsorbents for the removal of CO2, NO, NOx, and SO2 gases from motorcycle emissions. *IOP Conference Series: Materials Science and Engineering*, 334, p.012037.

Wu, H., Liu, Y., Zhang, J. and Li, G., 2014. In situ reactive extraction of cottonseeds with methyl acetate for biodiesel production using magnetic solid acid catalysts. *Bioresource Technology*, 174, pp.182-189.

Wu, L., Kobayashi, T., Li, Y., Xu, K. and Lv, Y., 2017. Determination and abatement of methanogenic inhibition from oleic and palmitic acids. *International Biodeterioration & Biodegradation*, 123, pp.10-16.

Yu, H., Niu, S., Lu, C., Li, J. and Yang, Y., 2017. Sulfonated coal-based solid acid catalyst synthesis and esterification intensification under ultrasound irradiation. *Fuel*, 208, pp.101-110.

Zhang, M., Sun, A., Meng, Y., Wang, L., Jiang, H. and Li, G., 2014. Catalytic performance of biomass carbon-based solid acid catalyst for esterification of free fatty acids in waste cooking oil. *Catalysis Surveys from Asia*, 19(2), pp.61-67.

Zhao, C., Lv, P., Yang, L., Xing, S., Luo, W. and Wang, Z., 2018. Biodiesel synthesis over biochar-based catalyst from biomass waste pomelo peel. *Energy Conversion and Management*, 160, pp.477-485.

Zhao, S., Li, P., Adkins, J., Zhu, L., Du, F., Zhou, Q. and Zheng, J., 2018. Carboxyl grafted sulfur-expanded graphite composites as cathodes for lithium-sulfur batteries. *Journal of Electroanalytical Chemistry*, 823, pp.422-428.

APPENDICES

APPENDIX A: Experimental Progress

Figure A-1: Waste Banana Peels Before Drying

Figure A-2: Waste Banana Peels After Drying

Figure A-3: Powder of Dried Waste Banana Peels

Figure A-4: Chemical Activation of Waste Banana Peels Powder

Figure A-5: Chemically Activated Banana Peels

Figure A-6: Carbonisation of Chemically Activated Banana Peels

Figure A-7: Size Reduction of WBPAC Using Mortar and Pestle

Figure A-8: Sieving of WBPAC under 300 Micron

Figure A-9: Apparatus Set Up of Sulfonation and Interesterification Reactions

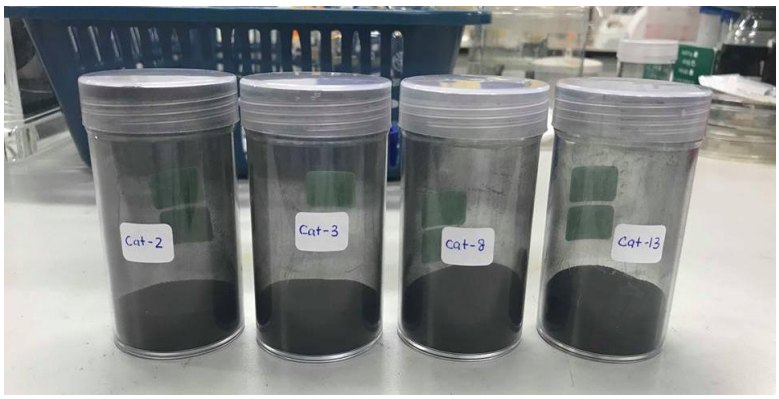

Figure A-10: Synthesised Catalysts

Figure A-11: Biodiesel Product

APPENDIX B: EDX Reports

Element	Wt%	At%
CK	42.95	59.37
OK	35.46	36.80
SiK	00.67	00.39
PK	00.62	00.33
SK	00.44	00.23
InL	19.86	02.87
Matrix	Correction	ZAF

Element	Wt%	At%
CK	36.73	57.58
OK	30.27	35.62
SiK	01.23	00.82
PK	01.13	00.69
SK	00.65	00.38
InL	30.00	04.92
Matrix	Correction	ZAF

Element	Wt%	At%
CK	37.15	53.93
OK	38.50	41.97
SiK	00.41	00.26
PK	00.33	00.18
SK	00.19	00.10
InL	23.43	03.56
Matrix	Correction	ZAF

Element	Wt%	At%
CK	41.64	58.19
OK	35.51	37.26
SiK	01.69	01.01
PK	00.67	00.36
SK	00.49	00.26
InL	20.00	02.92
Matrix	Correction	ZAF

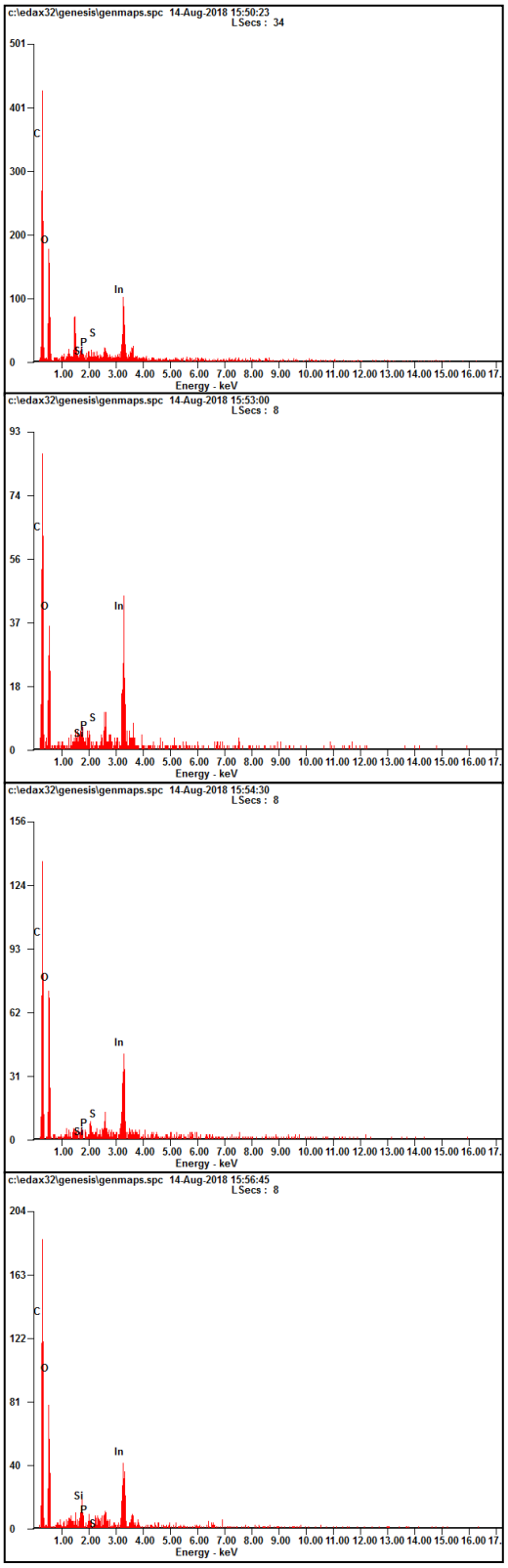

Figure B-1: EDX Analysis at Different Locations of Biomass Waste Banana Peels

Element	Wt%	At%
CK	57.46	65.51
OK	38.58	33.02
SiK	00.48	00.23
PK	01.86	00.82
SK	00.72	00.31
InL	00.89	00.11
Matrix	Correction	ZAF

Element	Wt%	At%
CK	59.96	67.57
OK	37.14	31.42
SiK	00.41	00.20
PK	01.24	00.54
SK	00.40	00.17
InL	00.85	00.10
Matrix	Correction	ZAF

Element	Wt%	At%
CK	60.96	68.75
OK	34.87	29.52
SiK	00.85	00.41
PK	02.52	01.10
SK	00.39	00.16
InL	00.40	00.05
Matrix	Correction	ZAF

Element	Wt%	At%
CK	61.23	69.58
OK	32.86	28.03
SiK	00.86	00.42
PK	03.42	01.51
SK	00.88	00.38
InL	00.75	00.09
Matrix	Correction	ZAF

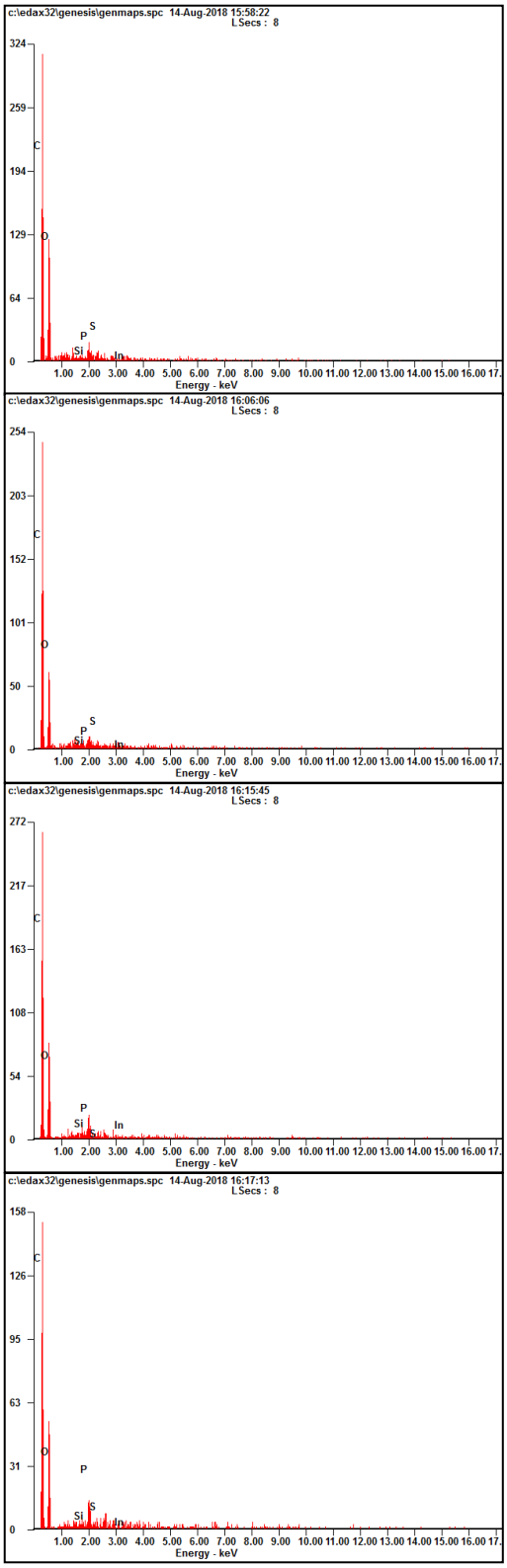

Figure B-2: EDX Analysis at Different Locations of Chemically Activated Banana Peels

Element	Wt%	At%
CK	77.16	84.55
OK	15.30	12.59
SiK	01.22	00.57
PK	05.06	02.15
SK	00.00	00.00
InL	01.26	00.14
Matrix	Correction	ZAF

Element	Wt%	At%
CK	76.40	84.73
OK	13.87	11.55
SiK	02.46	01.17
PK	05.10	02.19
SK	00.37	00.15
InL	01.79	00.21
Matrix	Correction	ZAF

Element	Wt%	At%
CK	75.19	82.90
OK	17.12	14.17
SiK	00.46	00.22
PK	06.01	02.57
SK	00.00	00.00
InL	01.21	00.14
Matrix	Correction	ZAF

Element	Wt%	At%
CK	66.29	76.51
OK	20.03	17.35
SiK	06.93	03.42
PK	05.37	02.41
SK	00.49	00.21
InL	00.89	00.11
Matrix	Correction	ZAF

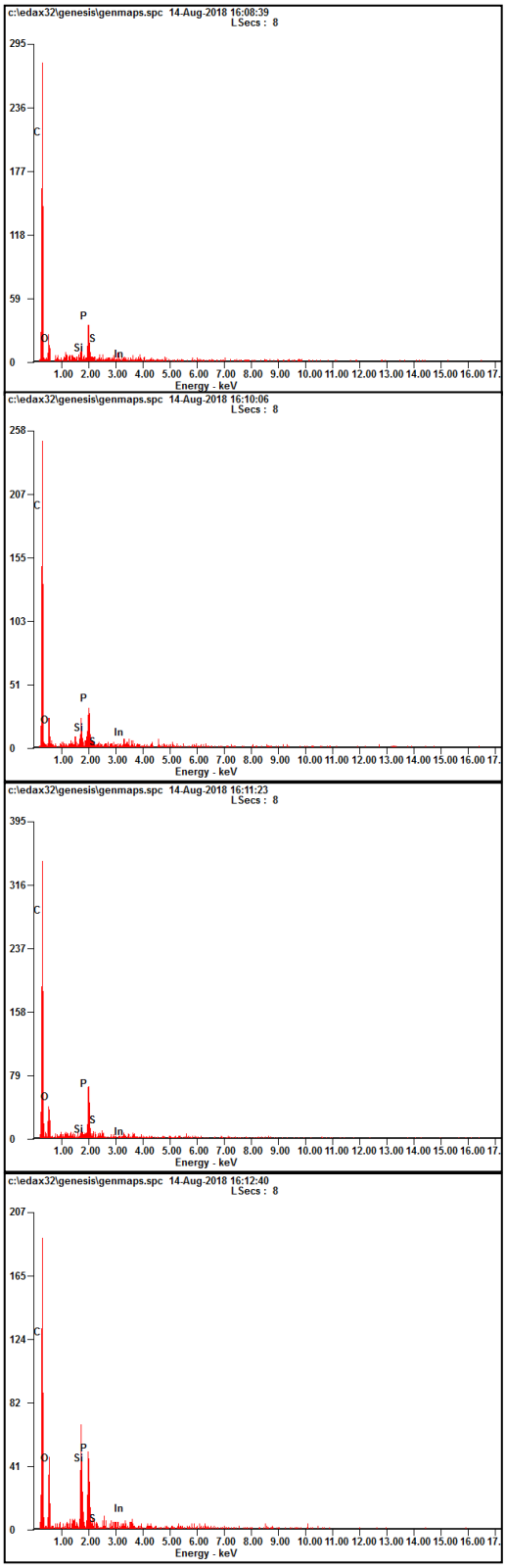

Figure B-3: EDX Analysis at Different Locations of WBPAC

Element	Wt%	At%
CK	82.26	88.24
OK	10.92	08.79
SiK	03.69	01.69
PK	01.70	00.71
SK	01.42	00.57
InL	00.00	00.00
Matrix	Correction	ZAF

Element	Wt%	At%
CK	82.12	89.10
OK	08.88	07.23
SiK	02.55	01.18
PK	04.10	01.72
SK	01.69	00.69
InL	00.65	00.07
Matrix	Correction	ZAF

Element	Wt%	At%
CK	79.79	85.81
OK	15.26	12.32
SiK	01.38	00.63
PK	01.47	00.61
SK	01.34	00.54
InL	00.76	00.09
Matrix	Correction	ZAF

Element	Wt%	At%
CK	83.99	89.05
OK	11.38	09.06
SiK	00.32	00.14
PK	02.52	01.04
SK	01.79	00.71
InL	00.00	00.00
Matrix	Correction	ZAF

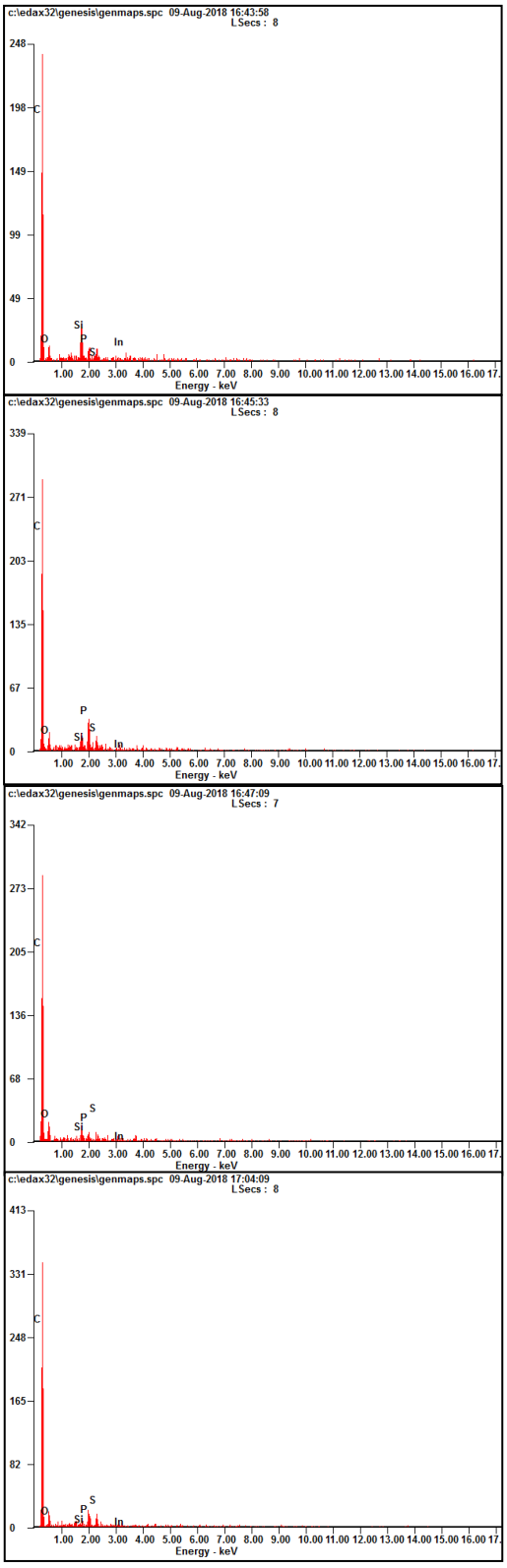

Figure B-4: EDX Analysis at Different Locations of Cat-2

Element	Wt%	At%
CK	79.90	85.51
OK	15.79	12.69
SiK	00.86	00.40
PK	02.01	00.83
SK	01.43	00.57
InL	00.00	00.00
Matrix	Correction	ZAF

Element	Wt%	At%
CK	75.02	83.62
OK	14.01	11.72
SiK	05.58	02.66
PK	02.76	01.19
SK	01.64	00.68
InL	00.99	00.12
Matrix	Correction	ZAF

Element	Wt%	At%
CK	81.64	87.89
OK	11.11	08.98
SiK	03.03	01.40
PK	01.99	00.83
SK	02.23	00.90
InL	00.00	00.00
Matrix	Correction	ZAF

Element	Wt%	At%
CK	80.80	87.54
OK	11.44	09.31
SiK	02.38	01.10
PK	02.43	01.02
SK	02.37	00.96
InL	00.59	00.07
Matrix	Correction	ZAF

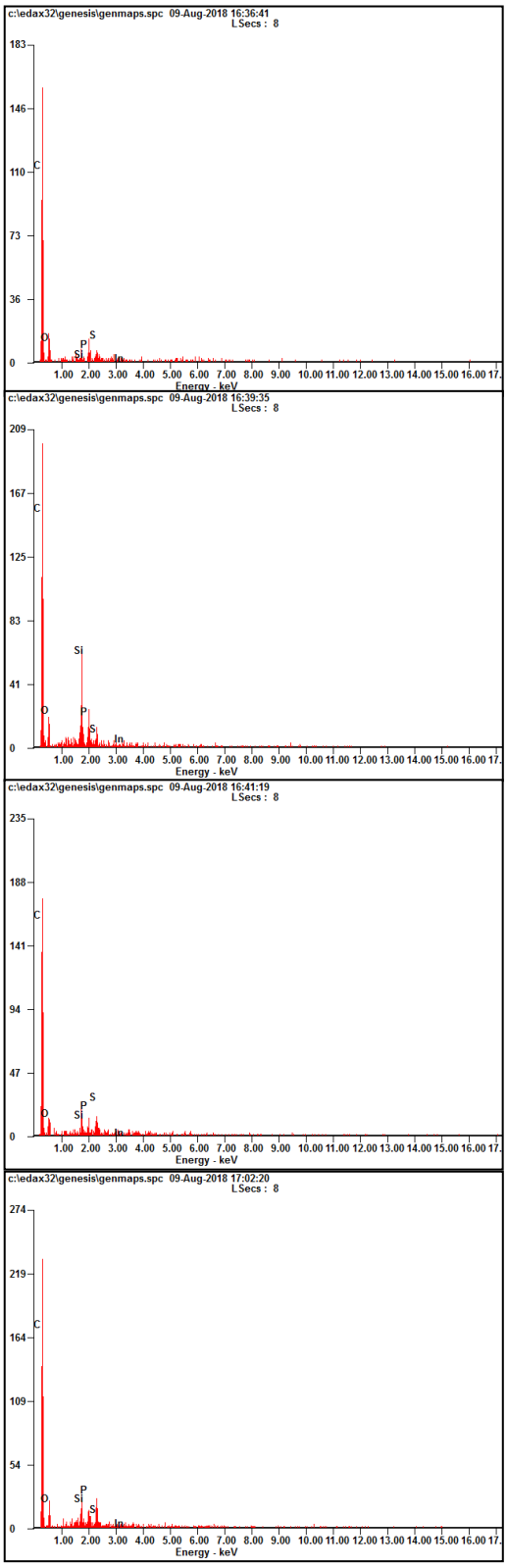

Figure B-5: EDX Analysis at Different Locations of Cat-3

Element	Wt%	At%
CK	75.73	83.67
OK	15.16	12.57
SiK	01.91	00.90
PK	03.45	01.48
SK	03.16	01.31
InL	00.59	00.07
Matrix	Correction	ZAF

Element	Wt%	At%
CK	80.32	87.21
OK	12.05	09.82
SiK	01.78	00.83
PK	02.10	00.88
SK	02.83	01.15
InL	00.92	00.10
Matrix	Correction	ZAF

Element	Wt%	At%
CK	75.65	84.17
OK	14.09	11.77
SiK	01.24	00.59
PK	04.84	02.09
SK	02.98	01.24
InL	01.20	00.14
Matrix	Correction	ZAF

Element	Wt%	At%
CK	77.11	84.81
OK	13.99	11.55
SiK	02.18	01.03
PK	02.60	01.11
SK	03.46	01.42
InL	00.66	00.08
Matrix	Correction	ZAF

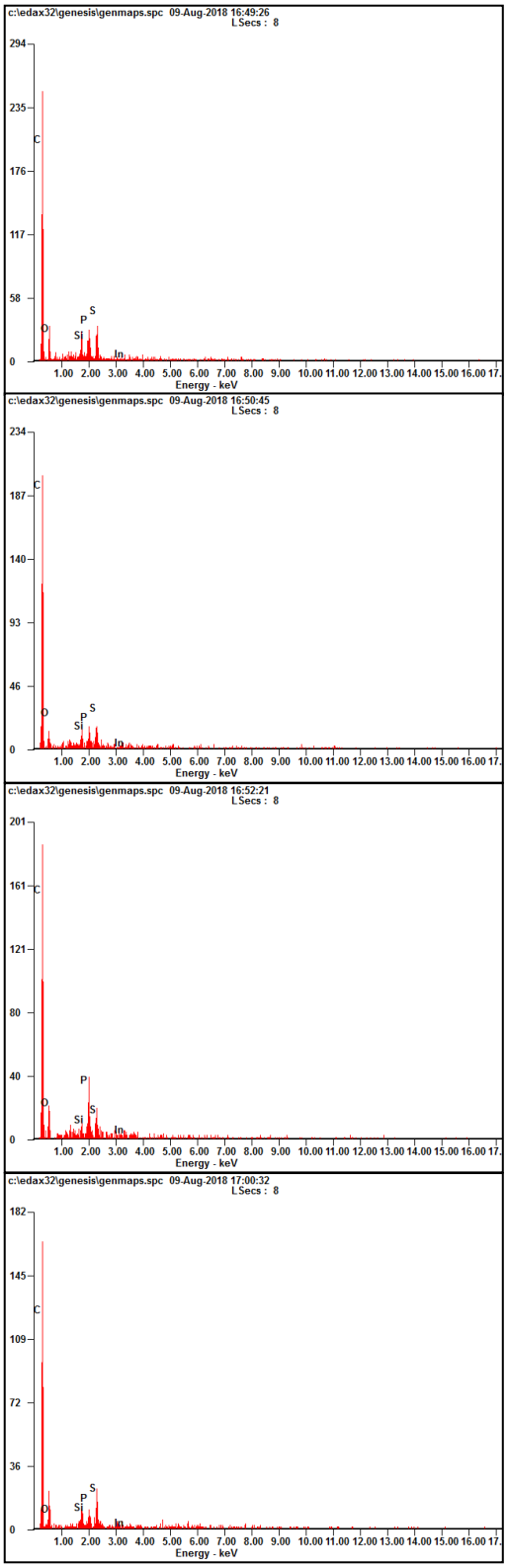

Figure B-6: EDX Analysis at Different Locations of Cat-8

Element	*Wt%*	*At%*
CK	72.38	79.89
OK	21.19	17.55
SiK	01.43	00.67
PK	01.16	00.50
SK	03.17	01.31
InL	00.67	00.08
Matrix	Correction	ZAF

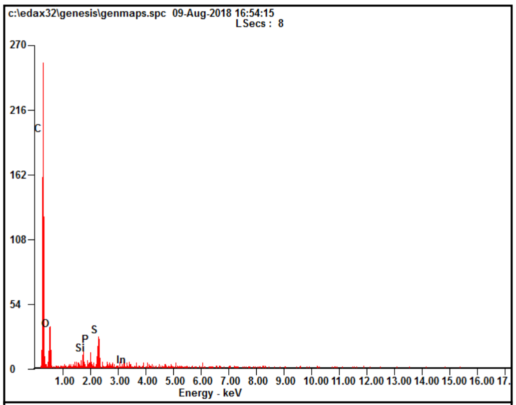

Element	*Wt%*	*At%*
CK	72.38	79.89
OK	21.19	17.55
SiK	01.43	00.67
PK	01.16	00.50
SK	03.17	01.31
InL	00.67	00.08
Matrix	Correction	ZAF

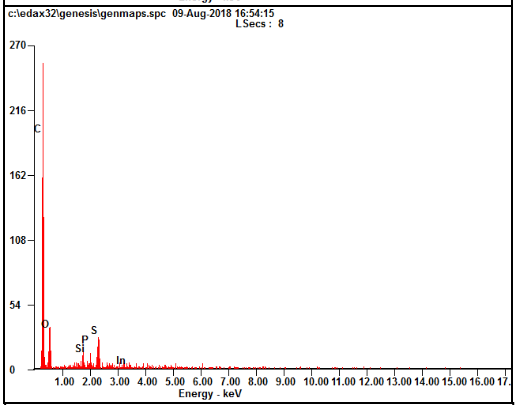

Element	*Wt%*	*At%*
CK	72.38	79.89
OK	21.19	17.55
SiK	01.43	00.67
PK	01.16	00.50
SK	03.17	01.31
InL	00.67	00.08
Matrix	Correction	ZAF

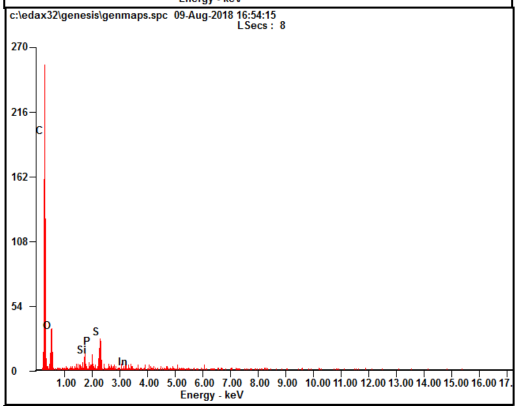

Element	*Wt%*	*At%*
CK	76.75	84.85
OK	14.19	11.78
SiK	01.45	00.69
PK	02.02	00.87
SK	03.92	01.62
InL	01.66	00.19
Matrix	Correction	ZAF

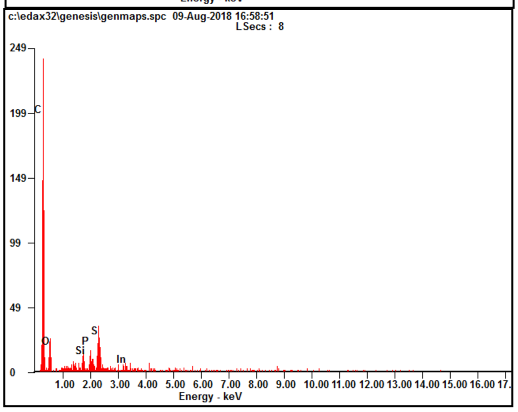

Figure B-7: EDX Analysis at Different Locations of Cat-13

APPENDIX C: FTIR Reports

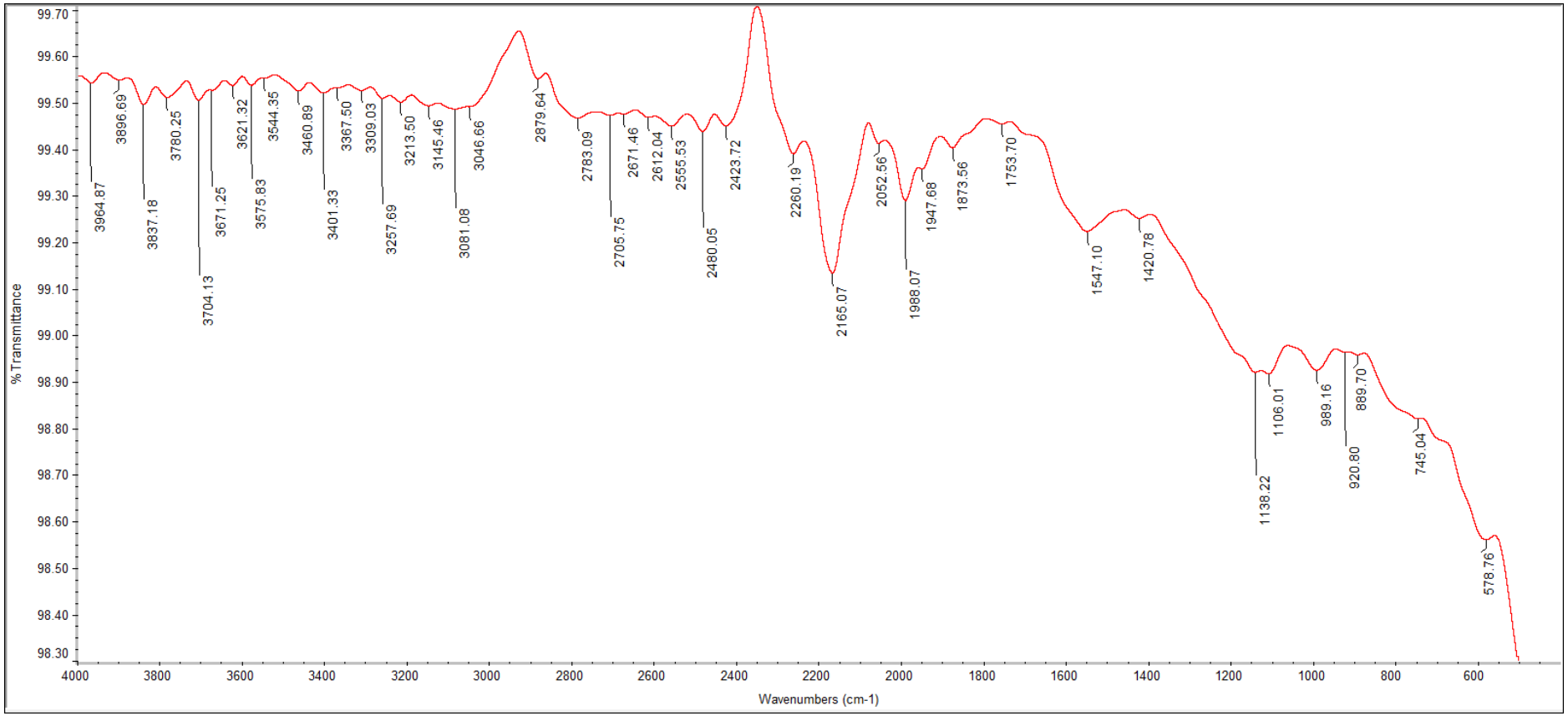

Figure C-1: FTIR Spectrum of WBPAC

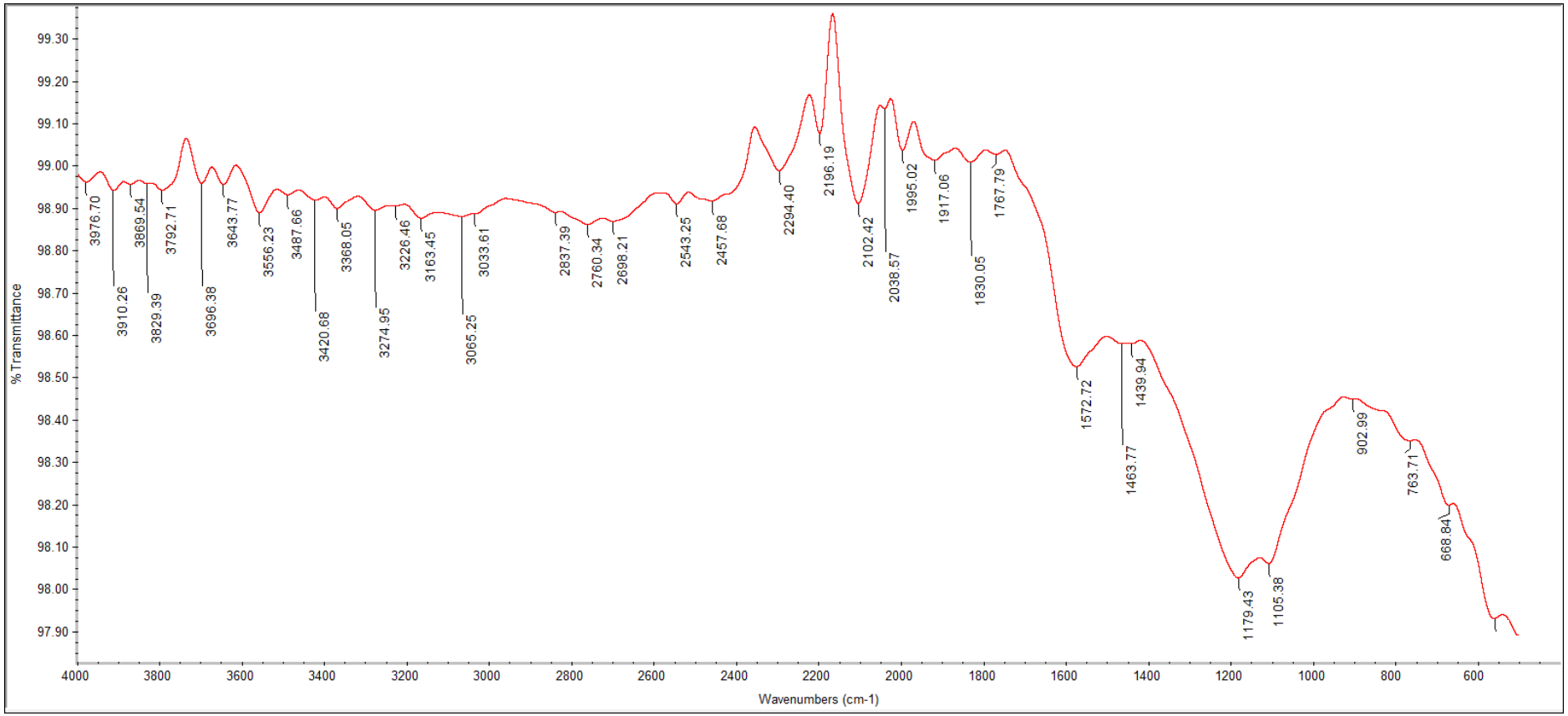

Figure C-2: FTIR Spectrum of Cat-2

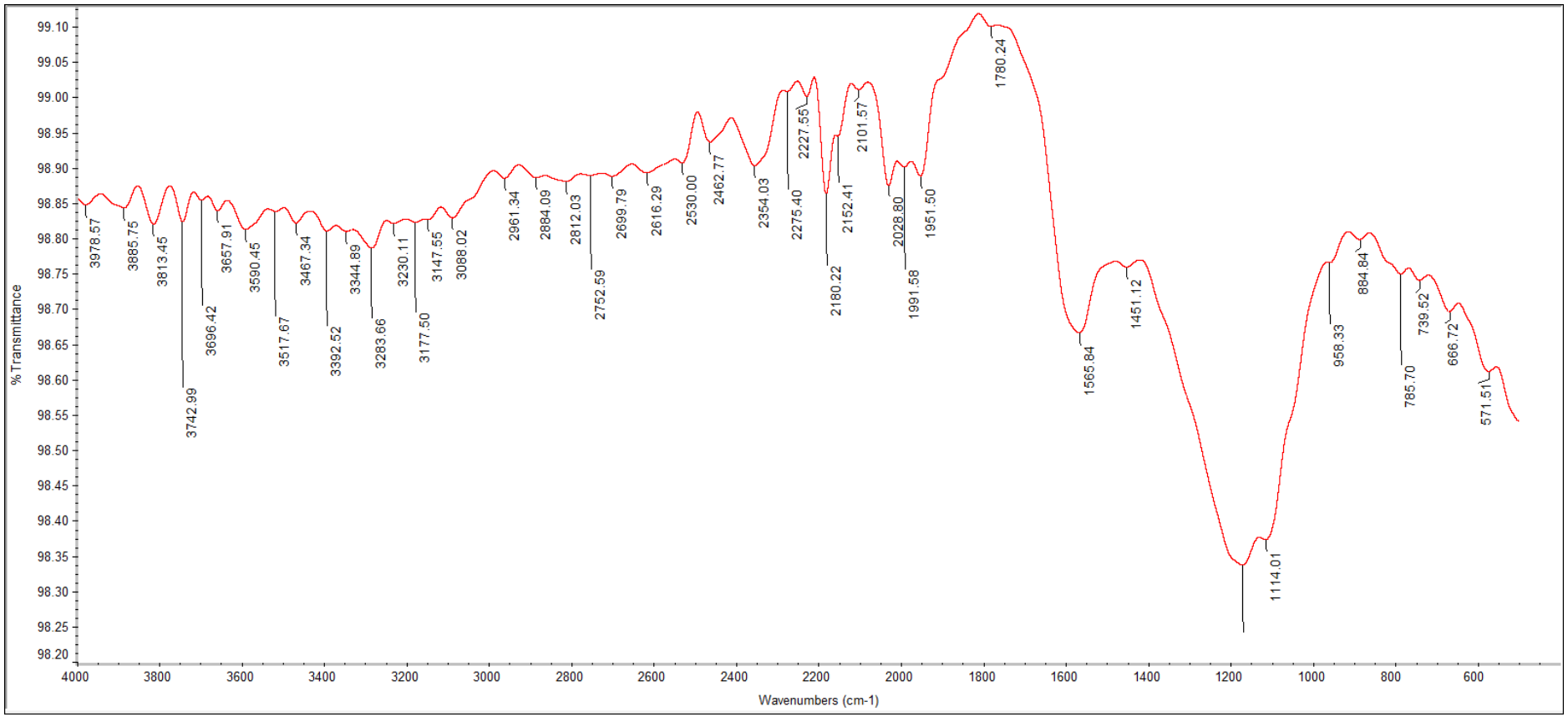

Figure C-3: FTIR Spectrum of Cat-3

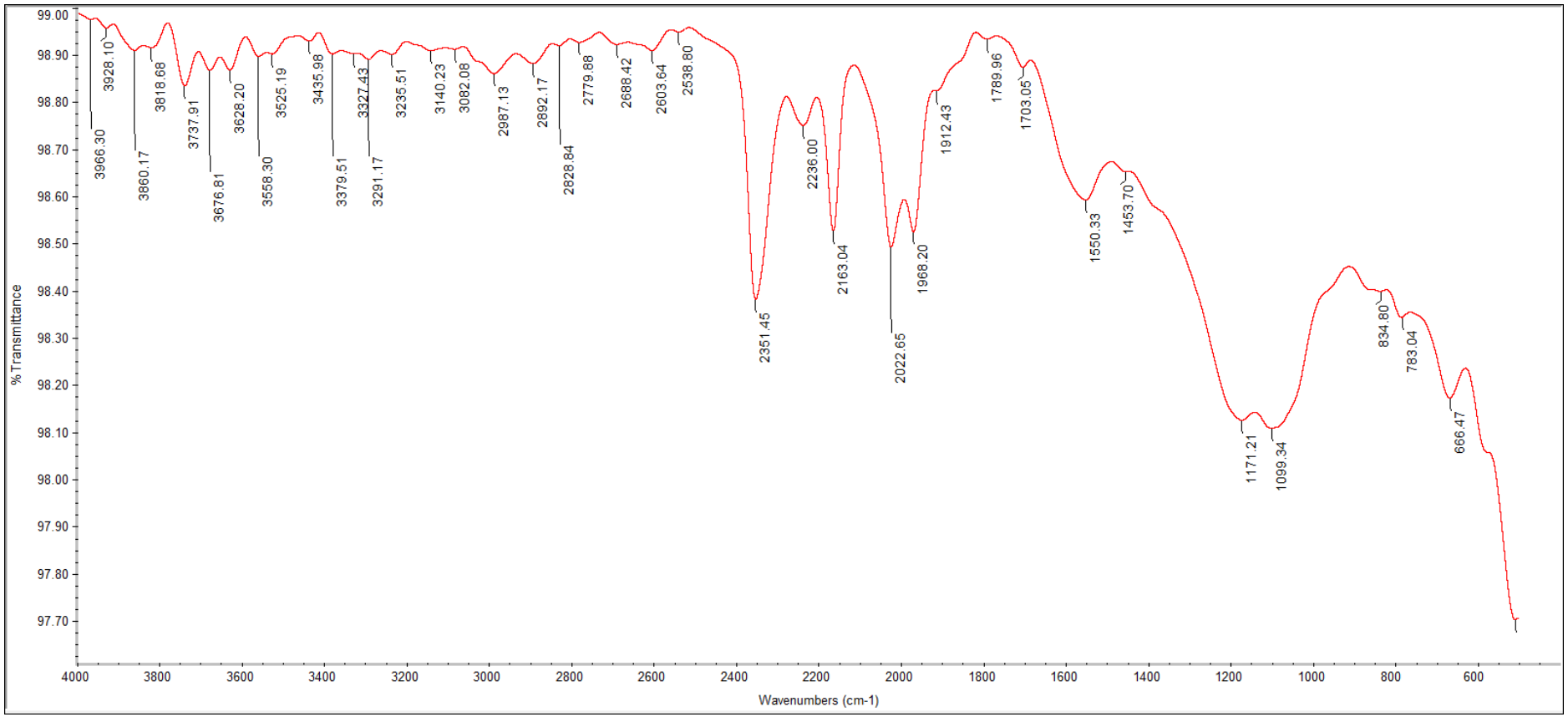

Figure C-4: FTIR Spectrum of Cat-8

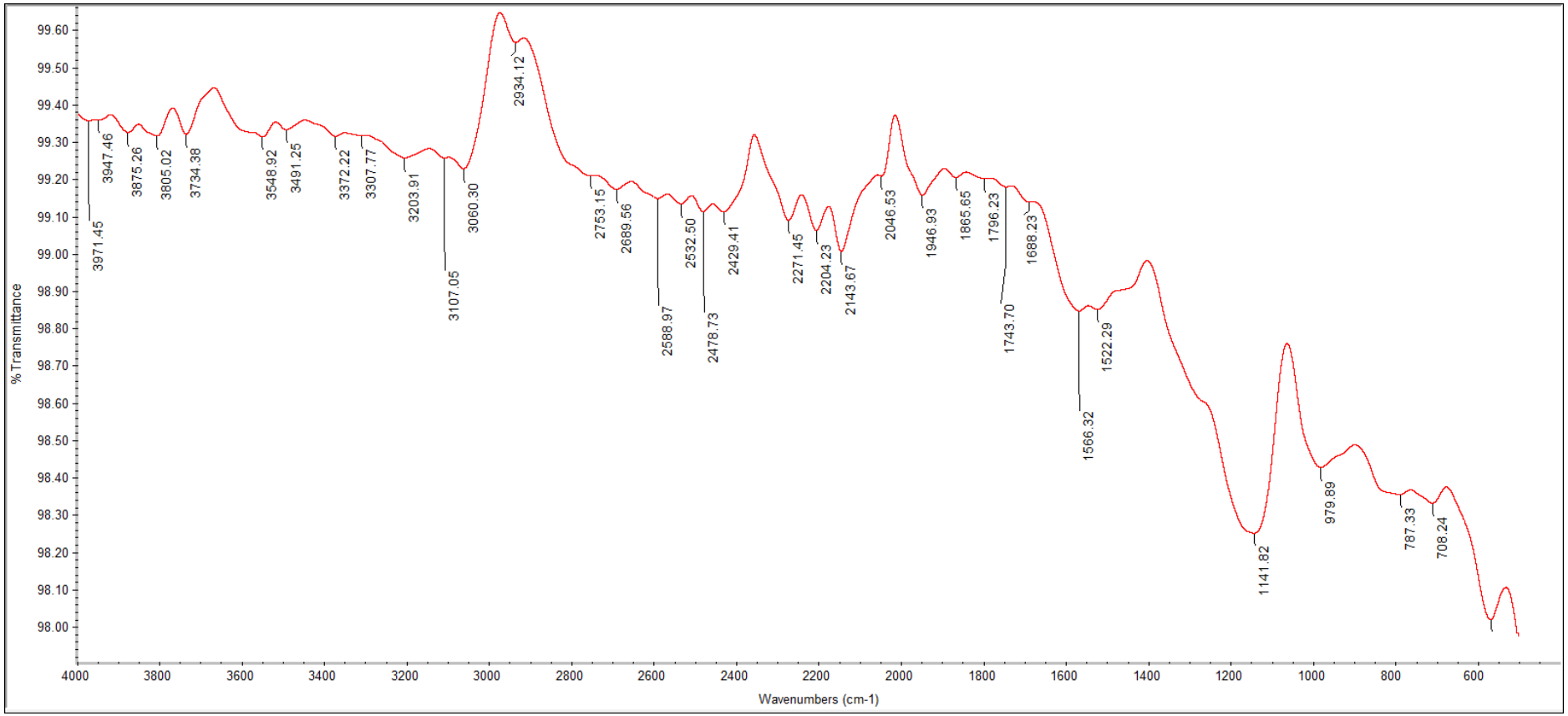

Figure C-5: FTIR Spectrum of Cat-13

APPENDIX D: GC Reports

Peak #	Time [min]	Area [µV·s]	Height [µV]	Area [%]	Norm. Area [%]	BL	Area/Height [s]
1	1.914	1269451.54	961929.21	99.80	99.80	BV	1.3197
2	2.059	341.88	214.72	0.03	0.03	VB	1.5923
3	4.847	277.43	128.90	0.02	0.02	BB	2.1523
4	13.413	1976.32	541.70	0.16	0.16	BB	3.6483
		1272047.17	962814.53	100.00	100.00		

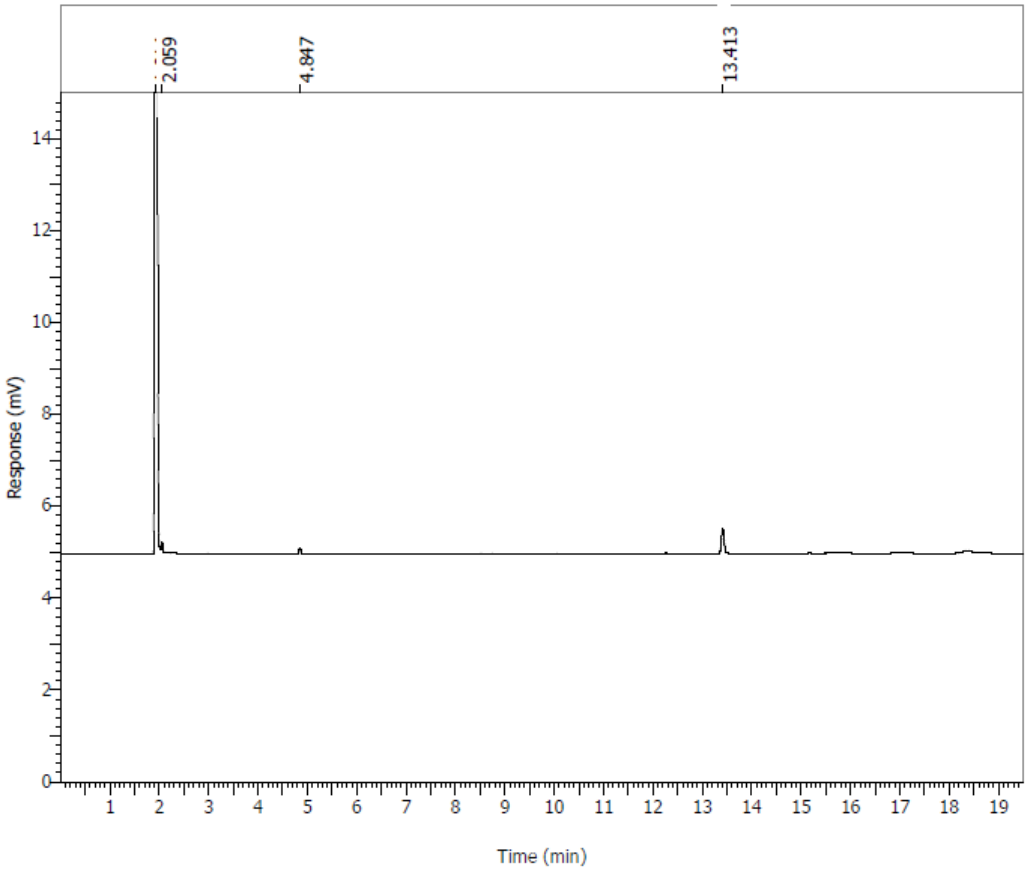

Figure D-1: Peak Report and Chromatogram of Cat-2

Peak #	Time [min]	Area [µV·s]	Height [µV]	Area [%]	Norm. Area [%]	BL	Area/Height [s]
1	1.915	1356033.64	982689.75	99.81	99.81	BB	1.3799
2	13.150	2106.58	644.01	0.16	0.16	BB	3.2710
3	14.814	499.47	79.75	0.04	0.04	BB	6.2628
		1358639.68	983413.51	100.00	100.00		

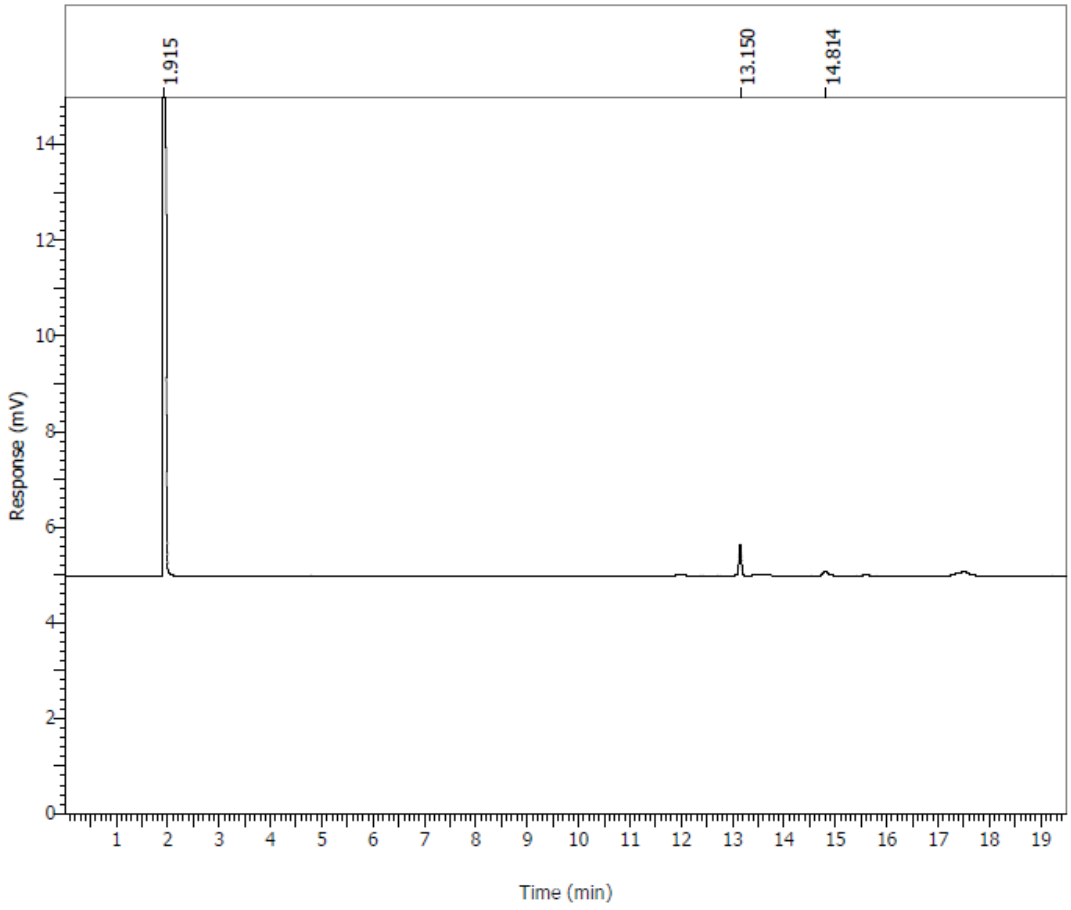

Figure D-2: Peak Report and Chromatogram of Cat-3

Peak #	Time [min]	Area [µV·s]	Height [µV]	Area [%]	Norm. Area [%]	BL	Area/Height [s]
1	1.915	1281291.42	978112.86	98.98	98.98	BE	1.3100
2	1.964	7597.60	7727.99	0.59	0.59	EB	0.9831
3	4.830	958.61	435.11	0.07	0.07	BB	2.2032
4	12.194	274.60	98.86	0.02	0.02	BB	2.7776
5	13.327	1944.89	539.73	0.15	0.15	BB	3.6034
6	15.064	2248.55	493.72	0.17	0.17	BB	4.5544
7	15.878	199.08	47.29	0.02	0.02	BB	4.2098
		1294514.76	987455.55	100.00	100.00		

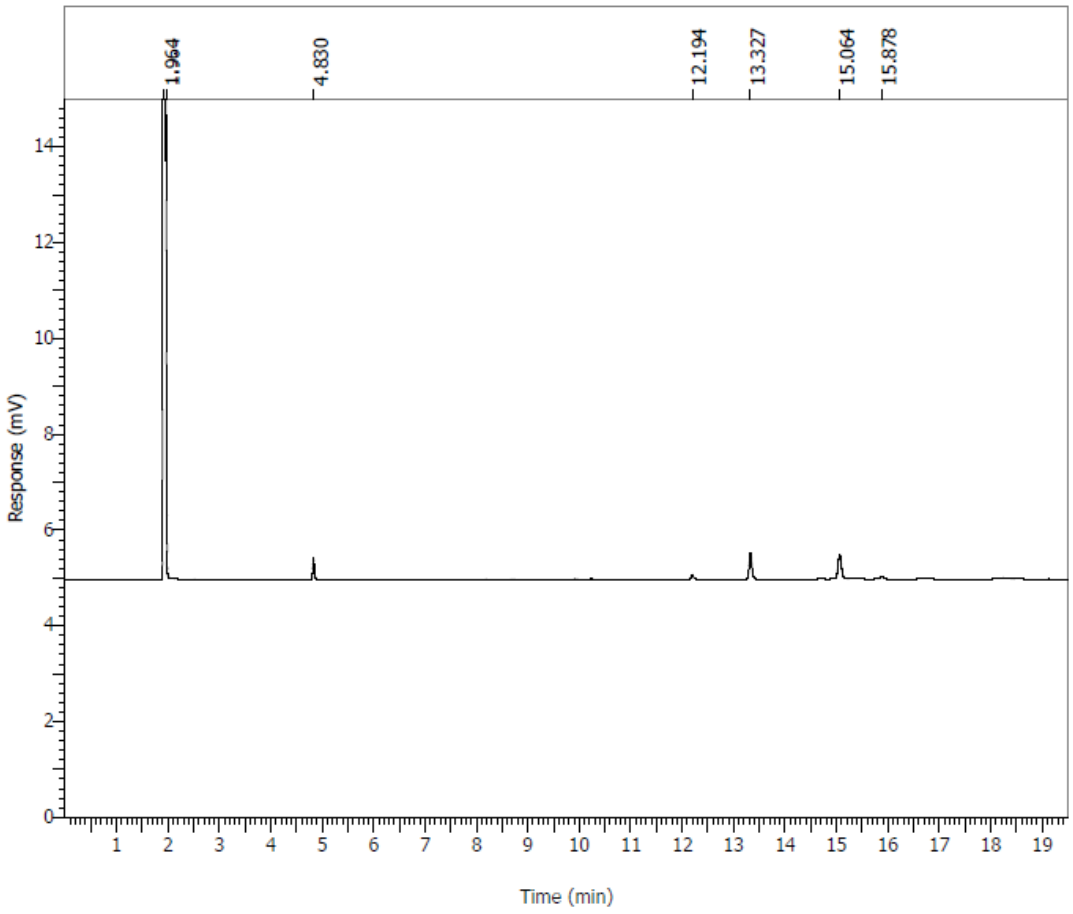

Figure D-3: Peak Report and Chromatogram of Cat-8

Peak #	Time [min]	Area [µV·s]	Height [µV]	Area [%]	Norm. Area [%]	BL	Area/Height [s]
1	1.910	1332849.61	979783.46	99.01	99.01	BB	1.3604
2	4.828	435.42	201.01	0.03	0.03	BB	2.1662
3	10.249	66.73	30.89	0.00	0.00	BB	2.1602
4	12.219	593.86	211.42	0.04	0.04	BB	2.8089
5	13.366	1990.54	553.64	0.15	0.15	BB	3.5954
6	14.747	81.30	24.17	0.01	0.01	BB	3.3635
7	15.137	9302.15	1873.07	0.69	0.69	BB	4.9662
8	15.940	905.98	189.29	0.07	0.07	BB	4.7862
		1346225.60	982866.96	100.00	100.00		

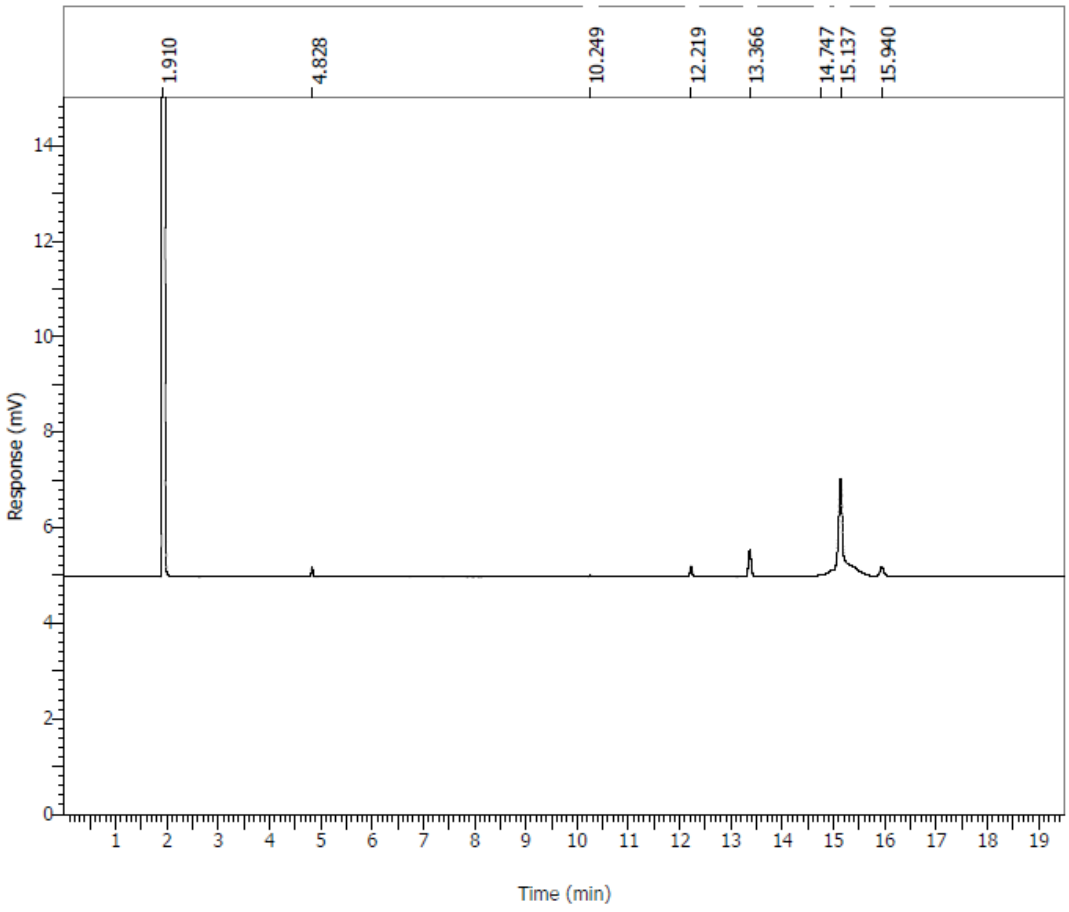

Figure D-4: Peak Report and Chromatogram of Cat-13

Peak #	Time [min]	Area [µV·s]	Height [µV]	Area [%]	Norm. Area [%]	BL	Area/Height [s]
1	1.931	1105837.26	895307.21	99.26	99.26	BE	1.2351
2	1.979	6289.46	6320.33	0.56	0.56	EB	0.9951
3	4.863	85.56	41.51	0.01	0.01	BB	2.0611
4	13.341	1855.53	547.67	0.17	0.17	BB	3.3880
		1114067.80	902216.72	100.00	100.00		

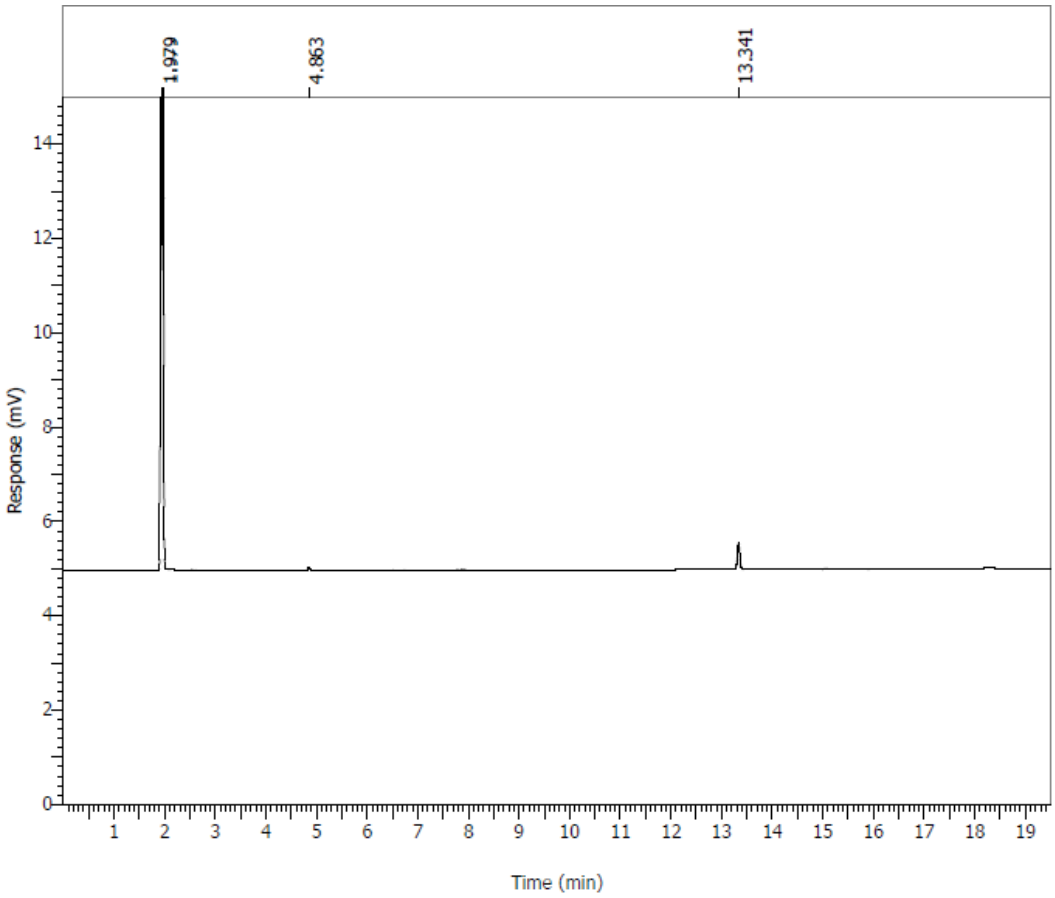

Figure D-5: Peak Report and Chromatogram of Biodiesel Product from Interesterification Using Solid Catalyst Synthesised with Concentrated Sulfuric Acid

Peak #	Time [min]	Area [µV·s]	Height [µV]	Area [%]	Norm. Area [%]	BL	Area/Height [s]
1	1.926	1222511.51	977754.09	97.43	97.43	BE	1.2503
2	1.975	10277.73	9809.03	0.82	0.82	EB	1.0478
3	10.187	96.13	43.71	0.01	0.01	BB	2.1994
4	12.133	919.91	345.23	0.07	0.07	BB	2.6647
5	13.254	2045.64	620.47	0.16	0.16	BB	3.2969
6	14.600	305.27	68.73	0.02	0.02	BB	4.4419
7	15.019	16350.70	3443.88	1.30	1.30	BB	4.7477
8	15.783	2291.96	491.46	0.18	0.18	BB	4.6636
		1254798.86	992576.60	100.00	100.00		

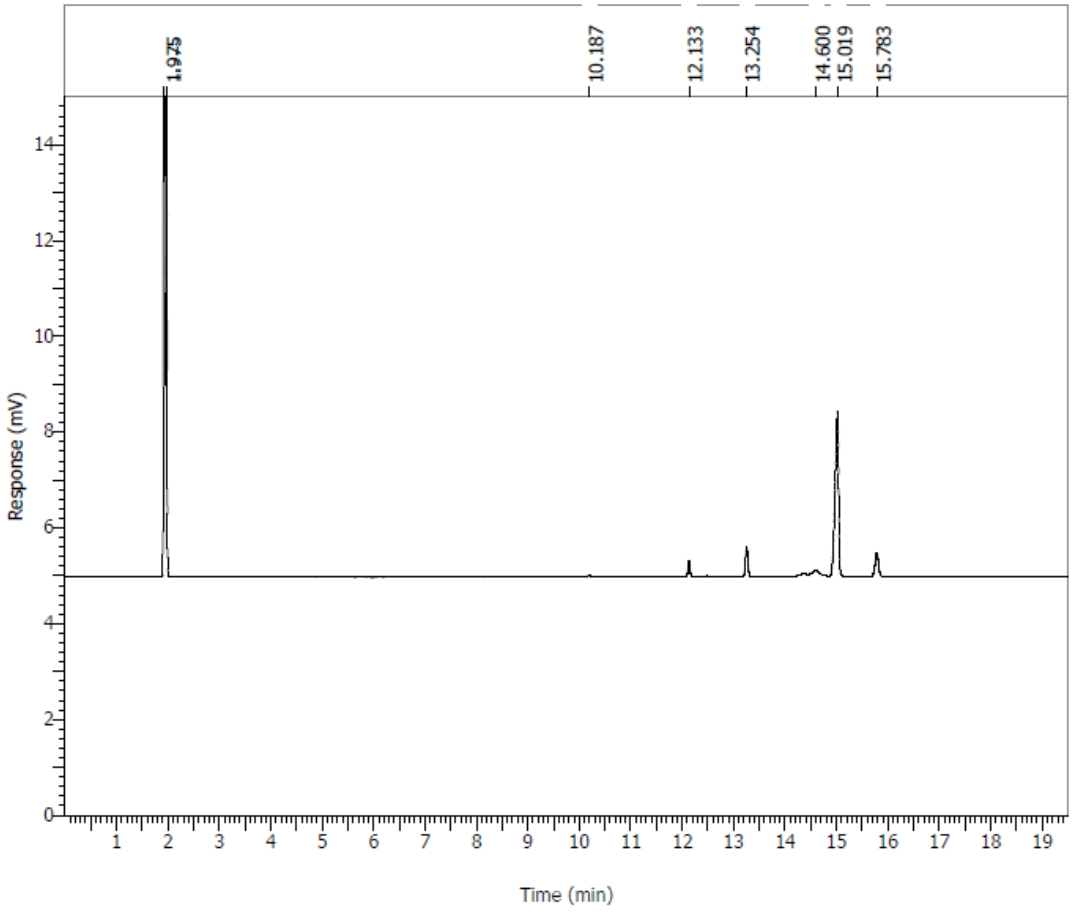

Figure D-6: Peak Report and Chromatogram of Biodiesel Product from Transesterification Using Cat-13

Peak #	Time [min]	Area [µV·s]	Height [µV]	Area [%]	Norm. Area [%]	BL	Area/Height [s]
1	1.914	1337561.74	982376.29	98.16	98.16	BE	1.3616
2	1.962	6022.98	5489.51	0.44	0.44	EV	1.0972
3	2.060	177.36	116.84	0.01	0.01	VB	1.5179
4	10.230	120.29	52.89	0.01	0.01	BB	2.2745
5	12.188	976.68	338.16	0.07	0.07	BB	2.8882
6	13.323	2298.95	624.35	0.17	0.17	BB	3.6821
7	14.689	259.19	58.93	0.02	0.02	BB	4.3982
8	15.093	13589.14	2794.11	1.00	1.00	BB	4.8635
9	15.873	1589.49	323.59	0.12	0.12	BB	4.9120
		1362595.82	992174.67	100.00	100.00		

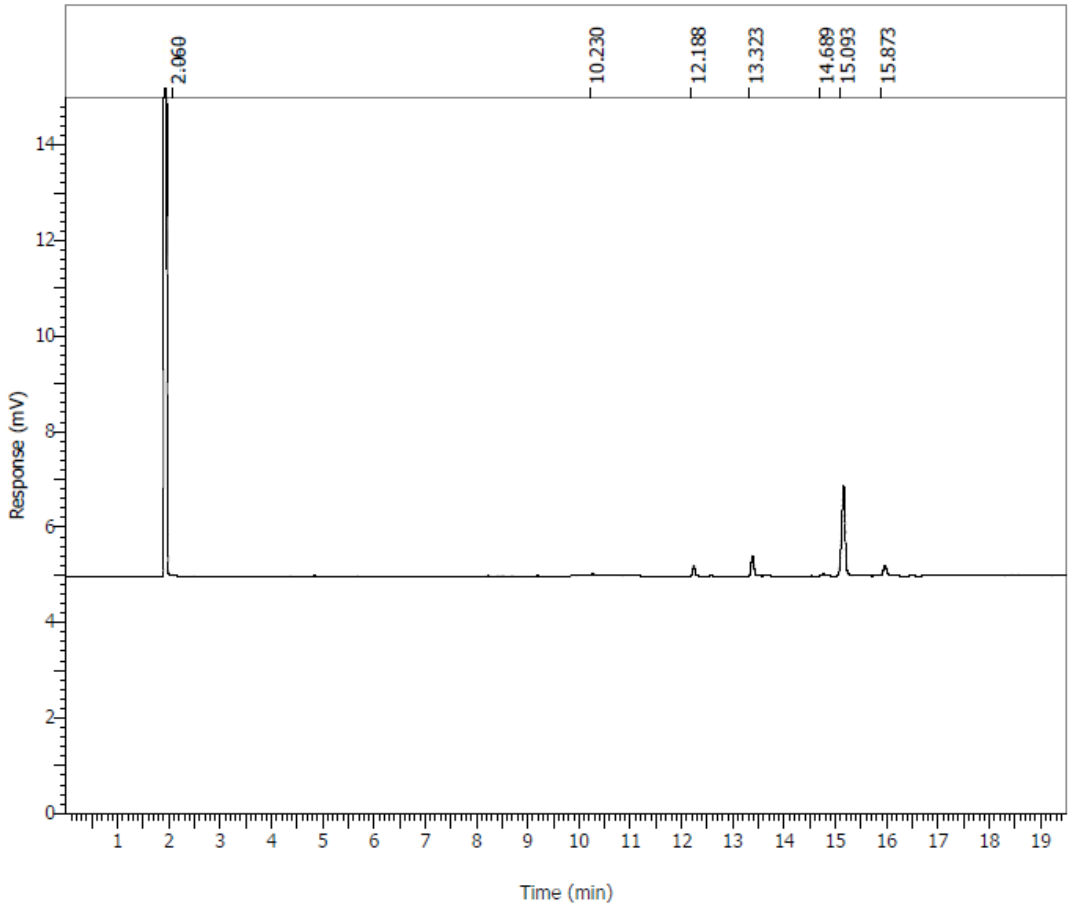

Figure D-7: Peak Report and Chromatogram of Biodiesel Product from Interesterification of Oleic Acid Catalysed by Concentrated Sulfuric Acid

Peak #	Time [min]	Area [µV·s]	Height [µV]	Area [%]	Norm. Area [%]	BL	Area/Height [s]
1	1.913	1350693.82	985494.73	98.17	98.17	BE	1.3706
2	1.962	10975.98	10432.83	0.80	0.80	EV	1.0521
3	2.057	1121.46	886.81	0.08	0.08	VB	1.2646
4	4.831	68.30	34.10	0.00	0.00	BB	2.0028
5	12.217	11409.76	3843.54	0.83	0.83	BB	2.9686
6	13.325	1534.17	428.82	0.11	0.11	BB	3.5777
		1375803.50	1.00e+06	100.00	100.00		

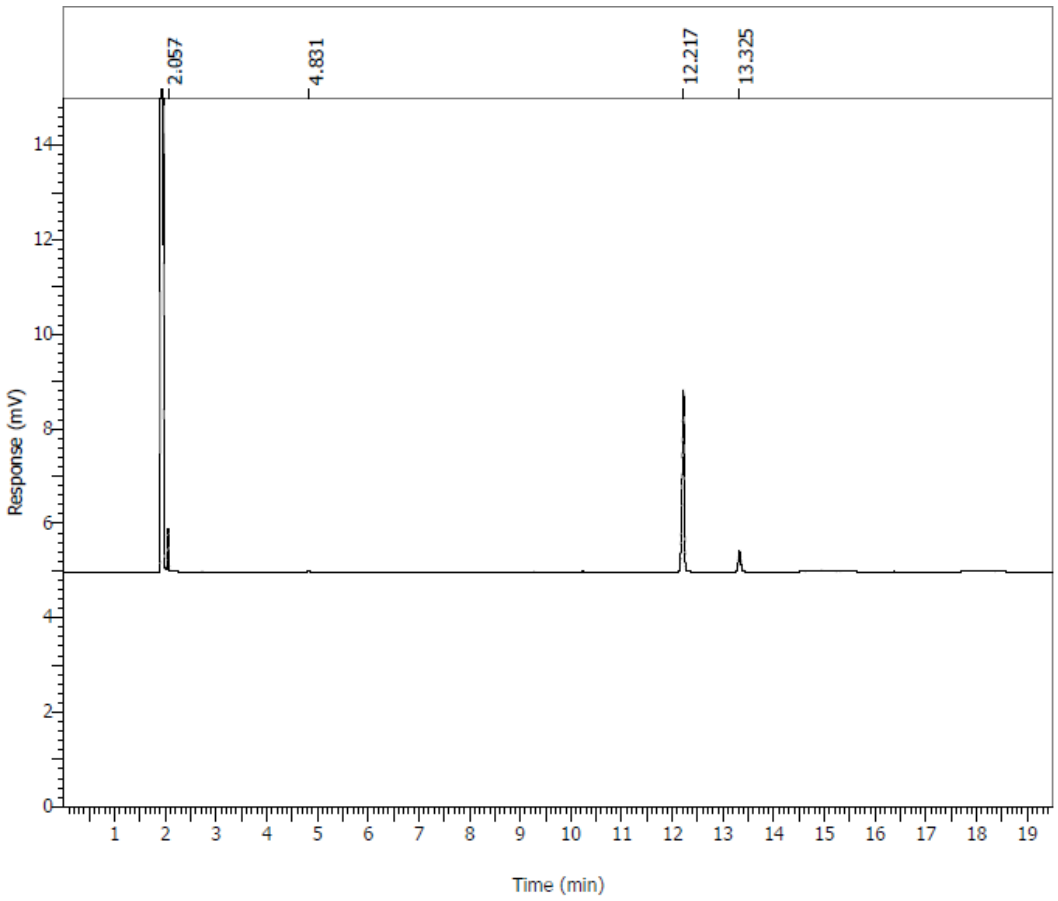

Figure D-8: Peak Report and Chromatogram of Biodiesel Product from Interesterification of Palmitic Acid Catalysed by Concentrated Sulfuric Acid

Peak #	Time [min]	Area [µV·s]	Height [µV]	Area [%]	Norm. Area [%]	BL	Area/Height [s]
1	1.913	1474021.76	988905.22	97.99	97.99	BE	1.4906
2	1.964	13786.83	13024.99	0.92	0.92	EV	1.0585
3	2.060	1127.79	902.37	0.07	0.07	VB	1.2498
4	4.835	109.88	53.55	0.01	0.01	BB	2.0519
5	12.179	151.71	57.04	0.01	0.01	BB	2.6597
6	13.312	1851.61	517.47	0.12	0.12	BB	3.5782
7	14.713	12284.67	2654.86	0.82	0.82	BB	4.6272
8	15.206	524.00	38.59	0.03	0.03	BB	13.5802
9	18.186	330.69	54.54	0.02	0.02	BB	6.0628
		1504188.93	1.01e+06	100.00	100.00		

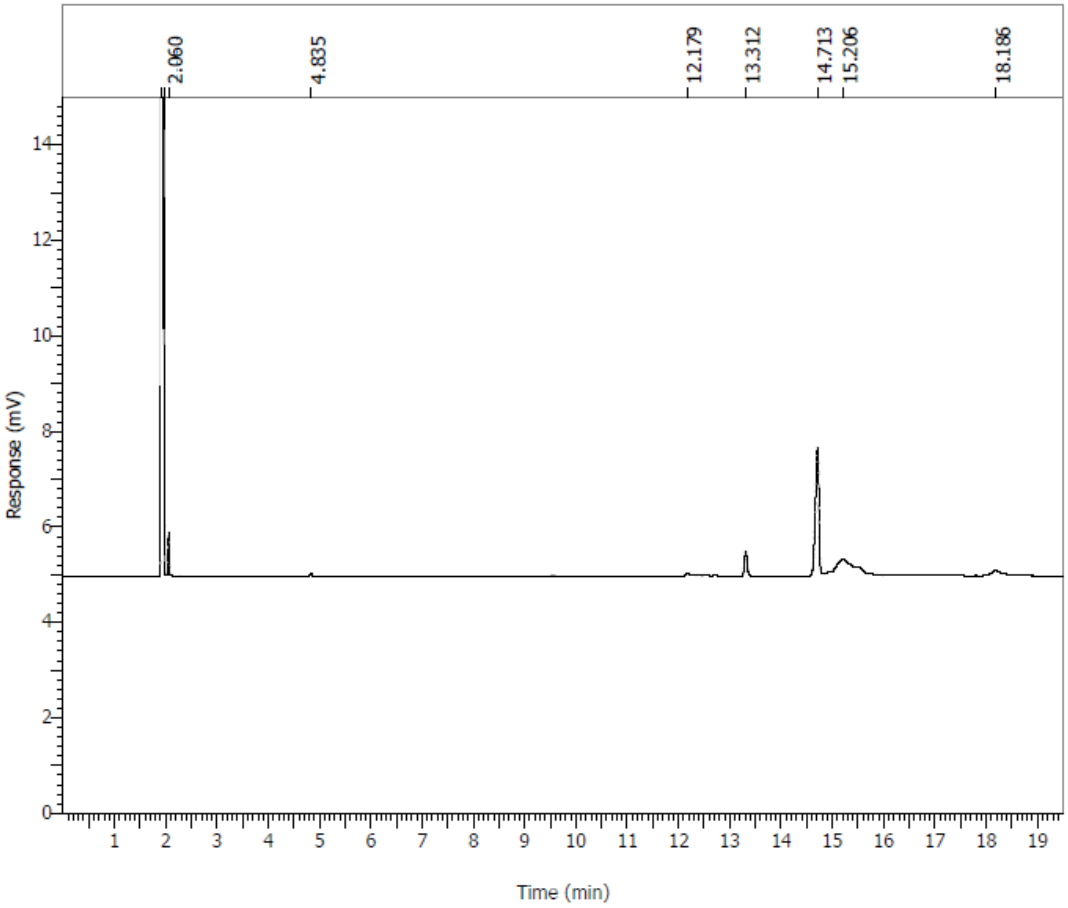

Figure D-9: Peak Report and Chromatogram of Biodiesel Product from Interesterification of Stearic Acid Catalysed by Concentrated Sulfuric Acid

Peak #	Time [min]	Area [µV·s]	Height [µV]	Area [%]	Norm. Area [%]	BL	Area/Height [s]
1	1.923	1150560.83	903383.34	98.68	98.68	BE	1.2736
2	1.972	8689.43	8531.60	0.75	0.75	EV	1.0185
3	2.068	213.51	143.22	0.02	0.02	VB	1.4908
4	4.853	124.26	59.07	0.01	0.01	BB	2.1035
5	12.206	669.36	202.17	0.06	0.06	BB	3.3109
6	13.342	2151.44	612.57	0.18	0.18	BB	3.5122
7	14.707	144.20	38.84	0.01	0.01	BB	3.7126
8	15.093	3298.60	537.27	0.28	0.28	BB	6.1395
9	15.895	150.08	38.81	0.01	0.01	BB	3.8673
		1166001.72	913546.89	100.00	100.00		

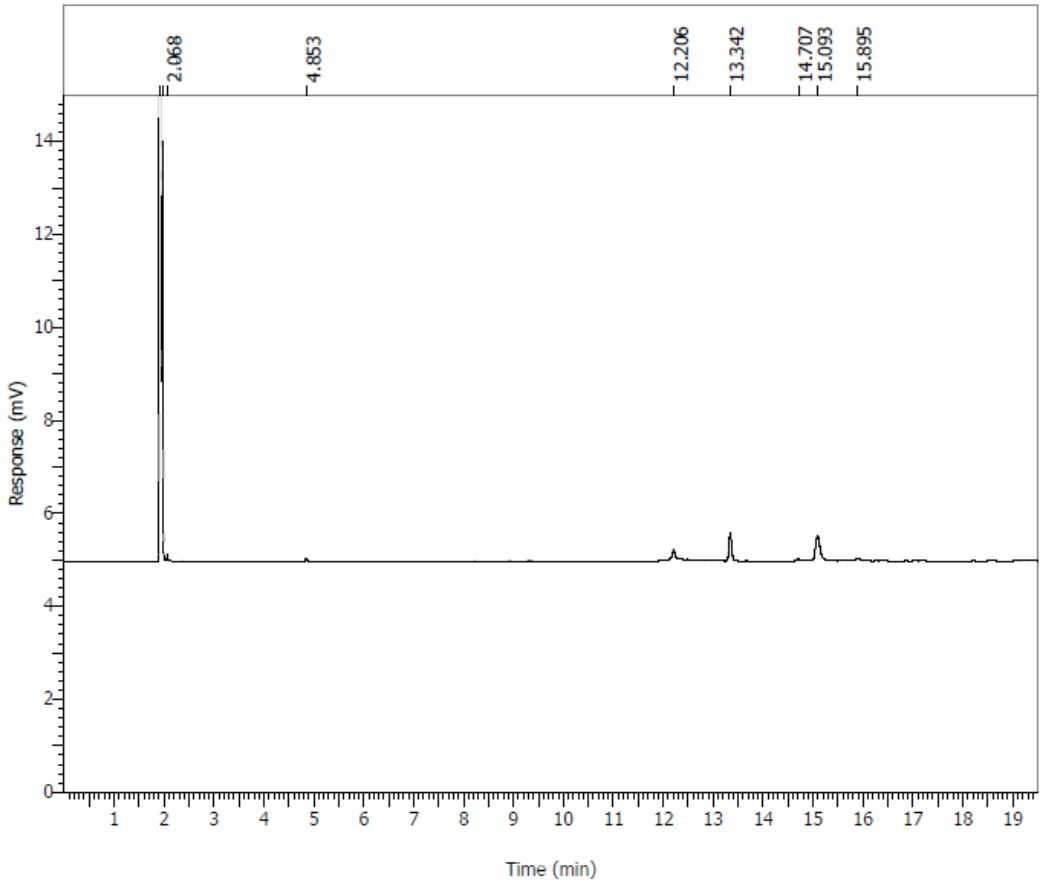

Figure D-10: Peak Report and Chromatogram of Biodiesel Product from Interesterification of Cooking Oil Catalysed by Concentrated Sulfuric Acid

APPENDIX E: Sample Calculations

Biodiesel Yield

Taking data of Cat-13 from Figure D-4,

$$Methyl\ oleate\ peak\ area\ =\ 9302.15$$

$$Internal\ standard\ peak\ area\ =\ 1990.54$$

$$\frac{Methyl\ oleate\ peak\ area}{Internal\ standard\ peak\ area} = \frac{9302.15}{1990.54} = 4.673179$$

From the line equation of calibration curve,

$$\frac{Methyl\ oleate\ peak\ area}{Internal\ standard\ peak\ area}$$

$$= 0.2472\ \times Concentration\ of\ methyl\ oleate\ (\frac{g}{L})$$

$$4.673179 = 0.2472\ \times Concentration\ of\ methyl\ oleate\ (\frac{g}{L})$$

$$Concentration\ of\ methyl\ oleate = 18.904446\,\frac{g}{L}$$

$$Yield(\%) = \frac{\frac{Concentration\ of\ methyl\ oleate\ (\frac{g}{L})}{Dilution\ factor} \times Volume(L)}{10\ mL\ oleic\ acid \times Density\ of\ oleic\ acid\ (\frac{g}{mL})} \times 100\%$$

$$= \frac{\frac{18.904446\,\frac{g}{L}}{40} \times 8.25\ mL\ \times \frac{1\ L}{1000\ mL}}{10\ mL \times 0.00089\,\frac{g}{mL}} \times 100\%$$

$$= 43.81\ \%$$

Acid Value Conversion

Taking data of initial acid value of oleic acid from Table 4.5 and final acid value for the case of Cat-13 from Table 4.7,

$$Acid\ Value\ Conversion\ (\%) = \frac{a^i - a^f}{a^i} \times 100\%$$

$$= \frac{239.59 - 40.40}{239.59} \times 100\%$$

$$= 83.14\ \%$$